

**Dissertation zur Erlangung des Doktorgrades  
der Fakultät für Chemie und Pharmazie  
der Ludwig-Maximilians-Universität München**

**Functional characterization of Pura *in vivo* and *in vitro*  
- Pura knock-out mice and Pura DNA unwinding activity**

**von**

**Haiyan Ding**

**aus**

**Hangzhou**

**V.R. China**

**2001**

### Erklärung

Diese Dissertation wurde im Sinne von §13 Abs. 3 bzw. 4 der Promotionsordnung vom 29. Januar 1998 von Prof. Dr. E.-L. Winnacker betreut.

### Ehrenwörtliche Versicherung

Diese Dissertation wurde selbständig, ohne unerlaubte Hilfe angefertigt.

München, am 26.11.2001

Dissertation eingereicht am 26.11.2001

1. Berichterstatter: Prof. Dr. E.-L. Winnacker

2. Berichterstatter: PD. Dr. Michael Meisterernst

Tag der mündlichen Prüfung: 14.12.2001

## Acknowledgements

At first, I would like to deeply thank Prof. Dr. E-L. Winnacker for giving me the opportunity to pursue the doctoral degree of Biochemistry in his laboratory and challenge myself in this completely new field of molecular biology. I would also like to thank him for his trust and encouragement throughout the entire period of my study.

Uncountable thanks go to my two supervisors: Dr. Marion Jurk, who led me into the door of molecular biotechnology and has been always paying her great attention to the project; Dr. Heidi Feldmann, who has supervised my work and given me many advice and suggestions. Their devotion to science and the hard-working impressed me very much and their broad knowledge was very helpful for my work.

I would like to thank Prof. Dr. E. Wolf for a fruitful cooperation and the many interesting, intensive and helpful discussions. Thanks go also to the friendly and efficient colleagues in his lab: to Dr. Nicola Zink for her excellent work on the ES cell electroporation; to Petra Renner and Ingrid Renner-Müller for carefully looking after my hundreds of mice.

I would like to thank the scientists of the Aurigon company for their cooperation. Much thanks go to Dr. Marina Karaphiosoff for many scientific discussions. Also many thanks to Dr. Elisabeth Kremmer for the monoclonal anti-Pur $\alpha$  antibody obtained after hundreds of tests.

A lot of thanks go to all members in our laboratory: Sigrun Jaklin, Bettina Meier, Lucia Driller, Kasten Beck, Renate Dombi, Karin Marbach, Andreas Uldschmid and Sabine Gauczynski, for their many comprehensive scientific discussions, useful suggestions, and a lot of private moments we shared together, which made my daily life in Germany colorful and plentiful. They also helped me by “Deutsch” writing and speaking, especially “Bayerisch”!

Special thanks to Siegi Kastenmüller for her great help during my stay at the Gene Center. Thanks a lot for her fighting against bureaucracy and solving all of the problems together with me. All what she did permit me to concentrate myself on research.

I also would like to thank Dr. Heidi Feldmann, Dr. Horst Ibelgauf, Dr. Nicola Zink and Dr. Harald Lahm for their intensive review and helpful feedback on my manuscript.

The deepest thanks go to my husband, Jiadong Shen, who always has been giving me much-not only support and patience, but also big help with computer problems. The same deep thanks belong to my parents and my young brother in China for their understanding and support.

The data presented in this work are in preparation for publications:

1. “Knock-out of the highly conserved Pur $\alpha$  mouse paralogue leads to severe tremors and obesity. ”
2. “Characterization of the DNA unwinding activity of single-stranded DNA-binding protein Pur $\alpha$ .”

# Content

<b>CONTENT</b>	<b>I</b>
<b>ABBREVIATIONS</b>	<b>VII</b>
<b>1 INTRODUCTION</b>	<b>1</b>
<b>1.1 Helicase-catalyzed DNA unwinding</b>	<b>1</b>
1.1.1 Properties of helicases	1
1.1.1.1 “Polarity” and processivity of duplex DNA unwinding	2
1.1.1.2 Oligomeric nature of helicases	3
1.1.1.3 Modulation of DNA binding affinity by nucleotide cofactors	3
1.1.2 Mechanisms of DNA unwinding and translocation by helicases	4
1.1.3 The role of helicases in aging	6
<b>1.2 Helix-destabilizing proteins catalyze DNA unwinding</b>	<b>7</b>
1.2.1 Properties of helix-destabilizing proteins differing from helicase	8
1.2.2 Mechanism of DNA unwinding by helix-destabilizing proteins	8
<b>1.3 Pura, a multifunctional single-stranded DNA- and RNA-binding protein</b>	<b>9</b>
1.3.1 Structural characteristics Pur $\alpha$	10
1.3.2 Pur $\alpha$ and gene transcription and replication	11
1.3.3 Pur $\alpha$ and control of cell growth	13
1.3.4 Pur family and possibly related diseases	13
<b>1.4 The aim of this study</b>	<b>14</b>
<b>2 MATERIAL</b>	<b>16</b>
<b>2.1 Cell lines</b>	<b>16</b>
<b>2.2 Bacterial strains</b>	<b>16</b>
<b>2.3 Genomic DNA libraries</b>	<b>16</b>
<b>2.4 Phages</b>	<b>16</b>
<b>2.5 Plasmids</b>	<b>16</b>
<b>2.6 Cell-culture</b>	<b>17</b>
<b>2.7 Enzyme</b>	<b>17</b>
<b>2.8 Antibodies</b>	<b>17</b>
<b>2.9 Chemical reagents</b>	<b>18</b>
<b>2.10 Synthetic oligonucleotides</b>	<b>20</b>

<b>3</b>	<b>METHODS</b>	<b>21</b>
<b>3.1</b>	<b>Cloning and propagation of DNA in E. coli</b>	<b>21</b>
3.1.1	Bacterial culture	21
3.1.1.1	Liquid culture	21
3.1.1.2	Plate culture	21
3.1.1.3	Glycerol stocks	21
3.1.2	Preparation of competent cells	22
3.1.3	Transformation of competent E. coli	22
<b>3.2</b>	<b>Mammalian cell culture</b>	<b>23</b>
3.2.1	Cell culture of NIH3T3 and 293	23
3.2.2	Freezing cells	23
3.2.3	Transfection of mammalian cells	23
3.2.3.1	Transfection of adherent cells	23
3.2.3.2	DNA transfection for stable expression	24
3.2.4	ES cell culture	24
3.2.4.1	General condition and ES cell culture media	24
3.2.4.2	Passaging of ES cells	25
3.2.4.3	Thawing and expanding of ES cells	25
3.2.4.4	Freezing of ES cells	26
3.2.4.5	Electroporation of ES cells, antibiotic selection, picking, expansion and freezing of resistant ES cell clones	26
3.2.4.6	Expansion of positive clones	29
<b>3.3</b>	<b>Plasmid isolation from E. coli.</b>	<b>29</b>
3.3.1	Mini-prep DNA isolation	29
3.3.2	Maxi-prep DNA with Qiagen Plasmid Maxi Kits	30
<b>3.4</b>	<b>Analysis and enzymatic digestion of DNA</b>	<b>30</b>
3.4.1	DNA purification through phenol extraction and ethanol precipitation	30
3.4.2	Measurement of DNA concentration	31
3.4.3	Agarose gel electrophoresis of DNA	31
3.4.4	Elution of DNA from agarose gel	31
3.4.4.1	Electro-elution of DNA	31
3.4.4.2	Elution of DNA with QIAquick Gel Extraction Kit	32
3.4.5	Sequencing double-stranded DNA	32
3.4.6	Polyacrylamid sequence gel electrophoresis	33
3.4.6.1	Gel preparation	33
3.4.6.2	Electrophoresis	34
3.4.7	Restriction endonuclease digestion	34

---

3.4.8	Fill in of 5' overhanging ends with Klenow DNA-polymerase	34
3.4.9	Generation of blunt ends with T4 DNA-polymerase	34
3.4.10	Dephosphorylation of DNA with alkaline phosphatase	35
<b>3.5</b>	<b>Isolation of genomic DNA and enzymatic digestion</b>	<b>35</b>
3.5.1	Preparation of genomic DNA from 48-well plates and enzymatic digestion	35
3.5.2	Isolation of genomic DNA from a 10 cm-dish	36
3.5.3	Isolation of genomic DNA from mice tails	36
3.5.4	A quick method for the isolation of unpurified genomic DNA from ES cells for PCR	37
<b>3.6</b>	<b>Amplification of DNA-fragments by Polymerase chain reaction (PCR)</b>	<b>37</b>
3.6.1	Screening positive homologous recombined ES cell clones by PCR	37
3.6.2	Amplification of Pur $\alpha$ cDNA fragments of different length by PCR	38
3.6.3	Amplification of homologous arms for the target vector	39
<b>3.7</b>	<b>Radioactive labeling of DNA</b>	<b>39</b>
3.7.1	5' end labeling with T4-polynucleotide kinase	39
3.7.2	DNA labeling with Random prime kit	40
3.7.3	Removal of unincorporated dNTPs with a Sephadex G- 50 column	40
<b>3.8</b>	<b>Southern-blot analysis</b>	<b>40</b>
3.8.1	Transfer of DNA on Nylon- or Nitrocellulose membrane	40
3.8.2	Hybridization of oligonucleotides	41
3.8.3	Hybridization with Church solution	42
3.8.4	Hybridization with ExpressHyb <sup>TM</sup> Hybridization Solution	43
3.8.5	Removing the radiolabeled DNA probe from the blot	43
<b>3.9</b>	<b>Screening recombinant DNA libraries</b>	<b>44</b>
3.9.1	Preparation of phage competent bacteria	44
3.9.2	Titration of recombinant $\lambda$ -phage	44
3.9.3	Absorption of phages into host bacteria	45
3.9.4	Phage blotting and identification of positive phages	45
3.9.5	Screening phage library for Pur $\alpha$ genomic DNA	46
3.9.6	Purification of $\lambda$ -phage DNA	46
3.9.6.1	Liquid lysate of $\lambda$ -phage	46
3.9.6.2	Isolation of $\lambda$ -phage DNA	46
<b>3.10</b>	<b>Analysis of proteins</b>	<b>47</b>
3.10.1	Preparation of cellular protein extracts from mammalian cells	47
3.10.2	Measurement of Protein concentration by Bradford assay	47
3.10.3	Preparation of protein extracts from mice tissues and measurement of protein concentration	48

3.10.4	SDS-polyacrylamid gel eletrophoresis (SDS-Page)	48
3.10.5	In gel staining of proteins	50
3.10.5.1	Coomassie blue staining	50
3.10.5.2	Rapid Coomassie blue staining	50
3.10.6	Western-blot	51
3.10.7	Eletro mobility shift assay – EMSA	51
3.10.8	Antibody supershift assay	52
3.10.9	Immunprecipitation	53
3.10.10	In vitro transcription and translation	53
3.10.11	Pull-down assay	54
3.10.12	Expression and purification of GST- fusion proteins	54
3.10.12.1	Induction of expression of GST-fusion proteins	54
3.10.12.2	Purification of GST-fusion proteins	55
3.10.12.3	Regeneration of glutathione-sepharose beads	55
3.10.12.4	Dialysis of GST-fusion protein	56
3.10.13	Unwinding assay	56
3.10.13.1	Generation of different substrates	56
3.10.13.1.1	Preparation of 5'-labeled unwinding substrate	56
3.10.13.1.2	Preparation of blunt ended duplex and small linear DNA unwinding substrate	57
3.10.13.2	DNA Unwinding assay	57
3.10.13.3	Generation of point-mutations in a Pur $\alpha$ deletion mutant	58
<b>4</b>	<b>RESULTS</b>	<b>59</b>
<b>4.1</b>	<b>The generation of Pura knock-out mice</b>	<b>59</b>
4.1.1	Structure of Pur $\alpha$ genomic DNA	59
4.1.1.1	Isolation of Pur $\alpha$ genomic DNA	59
4.1.1.2	Analysis of phage p5/1	60
4.1.1.3	Analysis of phage p14/2	63
4.1.1.4	Genomic structure of the Pur $\alpha$ locus	65
4.1.1.5	The exon/intron junction of the Pur $\alpha$ gene	66
4.1.2	The targeting constructs for the generation of Pur $\alpha$ knock-out mice	68
4.1.2.1	Design of the targeting vector for deleting Pur $\alpha$ locus	69
4.1.2.2	Generation of the targeting vector for deletion of the Pur $\alpha$ locus	70
4.1.3	Generation of Pur $\alpha$ knock-out mice	72
4.1.3.1	Screening of positive ES clones by PCR	72
4.1.3.2	Screening of positive ES clones by Southern-blot	74
4.1.3.3	Generation of chimeras and germ line transmission	76



---

4.1.3.4	Generation and detection of Pur $\alpha$ heterozygous knock-out mice	76
4.1.3.5	Generation and detection of Pur $\alpha$ homozygous knock-out mice	77
4.1.3.6	Pur $\alpha$ Western-blot	78
4.1.4	Primary phenotypic analysis of Pur $\alpha$ knock-out mice	79
4.1.5	Dissection of Pur $\alpha$ knock-out mice	82
4.1.6	Clinical investigations	83
4.1.7	Shorter life span of Pur $\alpha$ knock-out mice	84
4.1.8	Histological staining	85
4.1.9	Detection of MBP levels in Pur $\alpha$ knock-out mice	85
<b>4.2</b>	<b>Biochemical characterization of Pura</b>	<b>87</b>
4.2.1	DNA unwinding activity of Pur $\alpha$ purified from calf thymus	87
4.2.2	Cloning Pur $\alpha$ cDNA in the expression vector pGEX4T1	88
4.2.3	Expression of GST-Pur $\alpha$ fusion protein in E. coli and its purification	89
4.2.4	DNA-binding activity of GST-Pur $\alpha$	90
4.2.5	dsDNA unwinding activity of GST-Pur $\alpha$	90
4.2.6	Titration of amount of GST-Pur $\alpha$ for maximal unwinding activity	91
4.2.7	dsDNA unwinding activity with various substrates	92
4.2.8	Pur $\alpha$ DNA Unwinding activity is not influenced by ATP or Mg <sup>2+</sup> concentration	93
4.2.9	Pur $\alpha$ unwinding activity can be inhibited by specific oligonucleotides	95
4.2.10	Generation of different GST-Pur $\alpha$ deletion mutants	96
4.2.11	DNA binding activity with different deletion mutants	99
4.2.12	dsDNA unwinding activity with different deletion mutants	100
4.2.13	Self-Association of Pur $\alpha$	101
<b>5</b>	<b>DISCUSSION</b>	<b>104</b>
<b>5.1</b>	<b>The generation of Pura knock-out mice</b>	<b>104</b>
<b>5.2</b>	<b>Analysis of the phenotypes of Pura knock-out mice</b>	<b>107</b>
5.2.1	Decreased MBP levels in 16-day-old Pur $\alpha$ KO mice - The explanation of tremor phenotype?	107
5.2.2	Brain development of Pur $\alpha$ knock-out mice	111
5.2.3	Weight development of Pur $\alpha$ KO mice	113
<b>5.3</b>	<b>Helix destabilizing activity of Pura</b>	<b>114</b>
<b>5.4</b>	<b>Cellular Pura function</b>	<b>117</b>
<b>6</b>	<b>SUMMARY</b>	<b>120</b>
<b>7</b>	<b>LITERATURE</b>	<b>122</b>

<b>8</b>	<b>APPENDIX</b>	<b>132</b>
<b>8.1</b>	<b>Southern-blots of p5/1 and p14/2</b>	<b>132</b>
<b>8.2</b>	<b>The oligonucleotides used in this study</b>	<b>133</b>
8.2.1	Oligonucleotides used for generation of Pur $\alpha$ knock-out mice	133
8.2.2	Oligonucleotides used for the generation of truncated Pur $\alpha$ mutants	134
8.2.3	Oligonucleotids used for the DNA binding assay	135
<b>9</b>	<b>APPENDIX OF COLOR FIGURES</b>	<b>136</b>

## Abbreviations

Amp	ampicillin	mM	millimolar
APS	ammonium persulfate	µg	microgram
ATP	adenosine triphosphate	µl	microliter
aa	amino acid	ng	nanogram
bp	base pair	nm	nanometer
BPB	bromophenol blue	MOPS	3-(N-morpholino)propan sulfonic acid
BCIP	5-bromo-4-chloro-3-indolyl- 1-phosphat	NBT	nitroblue tetrazolium
BSA	bovine serum albumin	NP 40	Nonidet P-40
Ci	Curie (1 Ci = 3,7 x 10 <sup>10</sup> Bequerel)	<i>Neo</i>	neomycin gene
CIA	chloroform/isoamyl alcohol	OD	optical density
cpm	counts per minute	oligo	oligonucleotide
DNA	deoxyribonucleic acid	ORF	open reading frame
DMSO	dimethyl sulfoxide	PCR	polymerase chain reaction
ds	double stranded	pfu	"Plaque forming unit"
dNTP	desoxynucleoside triphosphate	PIPES	Piperazine-N,N'-bis (2-ethansulfonic acid)
DTT	dithiothreitol	pmol	Picomol
EDTA	ethylene diamintetraacetic acid	PMSF	phenylmethylsulfonyl fluoride
ELISA	Enzyme-linked immunoabsorbent assay	RT	room temperature
ES cells	embryonic stem cells	SDS	sodium dodecyl sulfate
fmol	femtomol	ss	single strand
g	gram	SSC	sodium chloride/ sodium citrate
hr	hour	Tris	tris(hydroxymethyl)- aminomethane
HEPES	N-2-hydroxyethylpiperazine- N'-2-ethansulfonic acid	TEMED	N,N,N',N'-tetramethyl- ethylendiamine
kb	kilobase	U	unit
kDa	kiloDalton	UV	ultraviolet
KO	knock-out	V	volt
MES	2-(N-morpholino)ethanesulfonic acid	w/v	weight/vol
mA	milliampere		
mg	milligram		
ml	milliliter		



# 1 Introduction

## 1.1 Helicase-catalyzed DNA unwinding

Double helical DNA is the stable form of most DNAs *in vivo*; This DNA duplex must be unwound transiently to separate the two complementary strands, at least partially, in order to form single-stranded (ss) DNA intermediates required for DNA replication, repair and recombination (Lohman, 1993). In each of these processes, duplex DNA unwinding is catalyzed by enzymes known as helicases, which function to destabilize hydrogen bonds between the complementary base pairs (bp) in duplex DNA in reactions that are coupled to the binding and hydrolysis of nucleoside 5'-triphosphates (NTP). Intimately linked to the DNA unwinding reaction is the requirement for helicases to translocate along the DNA filament in order to unwind the DNA duplex processively at rates that can be as fast as 500-1000 bp s<sup>-1</sup>.

DNA helicases appear to be ubiquitous, having been identified in various prokaryotes and eukaryotes as well as in bacteriophages and viruses (Egelman, 1998; Lohman, 1992; Thommes and Hubscher, 1990; Thommes and Hubscher, 1992). Most organisms encode multiple helicases; for example, *E. coli* encodes at least 12 different helicases (Matson *et al.*, 1994). An analysis of the yeast genome suggests that there may be as many as 50 different helicases (Li *et al.*, 1992; Mewes *et al.*, 1998). Till now, 60 DNA helicases have been demonstrated *in vitro* since their discovery in 1976, although this number is increasing rapidly (Abdel-Monem *et al.*, 1976). In addition to functioning in DNA replication, recombination and repair, enzymes with DNA helicase activity are components of eukaryotic transcription complexes and are important in coupling transcription to DNA repair (Hanawalt, 1994; Sancar, 1994). A number of enzymes with demonstrated RNA and RNA/DNA helicase activity have been proposed to function during transcription (Steinmetz *et al.*, 1990), translation (Ray *et al.*, 1985) and RNA splicing (Company *et al.*, 1991). An increasing number of putative helicases have been identified also on the basis of comparisons of their primary structures (Hodgman, 1988); however, the extent to which such sequence comparisons can identify true helicases is unknown.

### 1.1.1 Properties of helicases

All helicases share common biochemical properties, including nucleic acid binding, NTP binding and hydrolysis, and NTP hydrolysis-dependent unwinding of duplex nucleic acids.

### 1.1.1.1 “Polarity” and processivity of duplex DNA unwinding

Most DNA helicases display a preference for unwinding DNA containing a ssDNA region flanking the duplex. Some helicases require ssDNA attached to the 3' end of the duplex, whereas others require ssDNA attached to the 5' end of the duplex. Determination of this preference has generally been made using a partially duplex DNA substrate consisting of a linear ssDNA with complementary oligonucleotides annealed to each end as shown in Figure 1-1 (Yarranton and Gefter, 1979). The “polarity” of unwinding is defined operationally by the backbone polarity of the flanking ssDNA that facilitates initiation of DNA unwinding *in vitro*. For example, if a helicase preferentially unwinds duplex A in Figure 1-1, it unwinds with 5'- to -3' polarity (a 5'- to -3' helicase). If duplex B is unwound preferentially, the helicase is a 3'- to 5' helicase. Such studies indicate that the polarity of the ssDNA backbone flanking the duplex is an important determinant for the initiation of unwinding, and the polarity can differ for different helicases. The polarity of unwinding is undefined for helicases that initiate unwinding only on blunt-ended duplex DNA or “forked” duplex DNA. For example, *E. coli* RecBCD, *E. coli* UvrD (Helicase II), and *E. coli* RecQ, can initiate DNA unwinding at the ends of fully duplex DNA; in fact, initiation of DNA unwinding by RecBCD is inhibited if the DNA duplex has ssDNA flanking regions (Lohman and Bjornson, 1996).

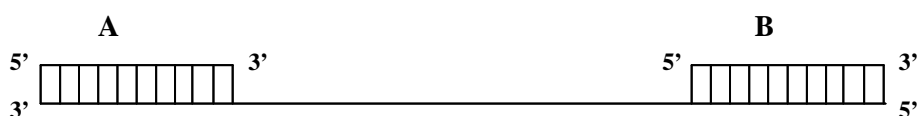


Figure 1-1: Diagram of a DNA substrate used to investigate the “polarity” of DNA unwinding by a helicase. Modified from Lohman (1996).

The processivity of DNA unwinding by a helicase is a measure of the number of base pairs unwound for each DNA binding event. At the molecular level this is related to the relative probabilities for unwinding a base pair versus dissociation of the helicase (Lohman, 1992). A number of helicases, e.g. Rec, helicase I, DnaB and Rep unwind DNA with high processivity. The maximum processivity of RecBCD corresponds to the unwinding of an average of about 25000 bp per binding event. A DNA helicase involved in DNA replication is expected to have high processivity, whereas a helicase involved in repair of short patches of DNA may not require high processivity. On the other hand, high processivity does not appear to be a property of all helicases *in vitro*. For example, unwinding of duplex DNA by *E. coli* Helicase II appears to be distributive and requires protein in quantities proportional to the extent of unwinding (Matson and George, 1987; Runyon *et al.*, 1990). Whether the *in vitro* processivity of a helicase correlates with *in vivo* activity is difficult to assess, since processivity may be

modulated by accessory proteins and is may dependent also upon solution conditions *in vitro* (Lohman, 1992).

### 1.1.1.2 Oligomeric nature of helicases

Most proposed mechanisms for helicase-catalyzed DNA unwinding, such as rolling or inch-worm mechanisms, require the functional helicase to possess at least two DNA binding sites (Lohman, 1992; Lohman, 1993). Although multiple DNA binding sites can potentially exist within a single polypeptide, all helicases for which the assembly state has been examined in detail form an oligomeric structure, usually dimers or hexamers (Chao and Lohman, 1991) (Lohman, 1992; Lohman, 1993). The immediate consequence of such oligomeric structures is that they provide a simple mechanism for helicases to acquire multiple DNA binding sites.

Table 1-1 lists DNA helicases for which the assembly state has been characterized in some detail, as well as those for which oligomerization has been demonstrated, but the form that is active in DNA unwinding is not yet known. With the apparent exception of the RecBCD enzyme, these helicases form either homodimers or homo-hexamers (Daniele *et al.*, 1999). Under some conditions, these helicases exist as a mixture of oligomeric states. Oligomerization of several helicases is modulated by interaction with other ligands. *E. coli* Rep helicase is monomeric in solution in the absence of DNA, but can dimerize upon binding either ssDNA or dsDNA (Chao and Lohman, 1991).

Helicase	Assembly state	Unwinding polarity
<i>E. coli</i> DnaB	hexamer (Bujalowski <i>et al.</i> , 1994; Donate <i>et al.</i> , 2000)	5' to 3'
SV40 large T antigen	hexamer (Mastrangelo <i>et al.</i> , 1989)	3' to 5'
T4 phage gene 41	hexamer (requires GTP) (Dong, 1995)	5' to 3'
<i>E. coli</i> Tral	oligomer (Lahue and Matson, 1988)	5' to 3'
<i>E. coli</i> RecBCD	hetero-trimer (Daniele <i>et al.</i> , 1999)	undefined
<i>E. coli</i> RecB	oligomer (dimer-tetramer) (Boehmer, 1992)	3' to 5'
<i>E. coli</i> Rep	dimer (DNA-induced) (Wong and Lohman, 1992)	3' to 5'
HSV-1	helicase/primase hetero-dimer (Bruckner <i>et al.</i> , 1991)	5' to 3'

Table 1-1: Oligomeric nature and the unwinding polarity of helicases.

### 1.1.1.3 Modulation of DNA binding affinity by nucleotide cofactors

Helicases, by definition, require ATP (or another nucleoside triphosphate) for function. The proposal has been made that binding of ATP, its hydrolysis, and the subsequent release of products (ADP and  $\text{PO}_4^{2-}$ ) cycles the helicase through specific conformational (energetic) states, thus effecting the unwinding reaction (Hill and Tsuchiya, 1981). All DNA helicases appear to possess a consensus NTP binding site, as indicated by the presence of the conserved

Walker A and B consensus motifs (motifs I and II) (Gorbalenya AE, 1993). Therefore, homooligomeric helicases possess at least one potential NTP binding site per subunit.

The relative affinity of these helicases for ss and ds DNA is influenced by the type of nucleotide cofactor (ATP or ADP) that is bound to the helicase (Wong *et al.*, 1992; Wong and Lohman, 1992). The NTP-free protein binds well to both ss and dsDNA; however, upon binding ATP, the affinity of helicase for dsDNA increases significantly, whereas ADP increases its affinity for ssDNA. Figure 1-2 depicts the five states that Rep dimer can form in the presence of both ss and ds oligonucleotides. Each subunit of Rep dimer can bind either ssDNA (S) or dsDNA (D) to form Rep dimers that are either half saturated ( $P_2S$  and  $P_2D$ ) or fully saturated ( $P_2S_2$ ,  $P_2D_2$ , and  $P_2SD$ ). As shown in Figure 1-2, both the binding of ADP and AMPP(NH)P, a non-hydrolyzable ATP analogue, influence the ability of a Rep dimer to form the different species. ADP stabilizes the Rep dimer species with ssDNA bound to both subunits ( $P_2S_2$ ), whereas AMPP(NH)P stabilizes the hybrid dimer species,  $P_2SD$ , in which ss and dsDNA are bound to a Rep dimer. This allosteric influence of nucleotide cofactors suggests a cycling scheme (“rolling model”) that might be used by Rep dimers to unwind duplex DNA (Wong *et al.*, 1992).

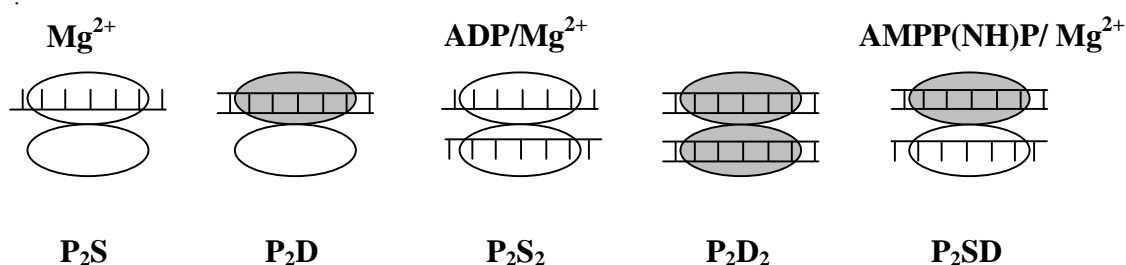


Figure 1-2: Representation of five different states that the Rep dimer can form in the presence of ss- and ds-oligonucleotides short enough to allow only one Rep monomer to bind per oligonucleotide. At equimolar concentrations of ssDNA, duplex DNA, and Rep monomers, the  $P_2S$  dimer is favored in the presence of  $Mg^{2+}$ , the  $P_2S_2$  dimer is favored in the presence of  $ADP/Mg^{2+}$  and the  $P_2SD$  dimer is favored in the presence of  $AMPP(NH)P/Mg^{2+}$ . Modified from Lohman (1993).

### 1.1.2 Mechanisms of DNA unwinding and translocation by helicases

Although all DNA helicases do not appear to unwind DNA by precisely the same mechanism, certain features of DNA unwinding and translocation are likely to be common to all helicases. In theory, mechanisms of helicase-catalyzed DNA unwinding can be classified as either ‘passive’ or ‘active’. In an active mechanism, the helicase plays a direct role in destabilizing the duplex DNA by breaking the hydrogen bonds between the base pairs. However, in passive models, the helicase would facilitate unwinding indirectly by binding to the ssDNA that becomes available through transient local internal melting or fraying of the end of the DNA



duplex. Direct evidence does not support a passive mechanism indicates that *E. coli* Rep unwinds DNA by an active mechanism, the “rolling” model (Amaratunga and Lohman, 1993).

The best-studied DNA helicase with regard to its mechanism of DNA unwinding is the *E. coli* Rep helicase (Lohman, 1992; Lohman, 1993; Wong and Lohman, 1992). In solution in the absence of DNA, *E. coli* Rep helicase exists as a monomer, and binding of either ssDNA or dsDNA induces the protein to dimerize. New study showed that Rep monomers are unable to initiate DNA unwinding *in vitro*, and that oligomerization is required for helicase activity (Cheng *et al.*, 2001). These data support the “active, rolling” model for DNA unwinding and translocation by Rep dimer, which was proposed by Wong and Lohman in 1992 (Figure 1-3). A rolling mechanism requires at least two identical DNA binding sites, both of which must be able to bind ssDNA as well as dsDNA. This model is based on the observed allosteric effects of nucleotide cofactors on the ss and dsDNA binding properties of the *E. coli* Rep dimer and may apply to homo-oligomeric helicases. It is assumed that each subunit of the dimer binds ssDNA with defined polarity and the Rep dimer possesses C2 symmetry (Wong and Lohman, 1992). In the rolling model, one subunit of the Rep dimer is bound always to the 3' ssDNA at the fork, while the other subunit is bound either to the same single strand or to the adjacent duplex region ahead of the fork. Figure 1-3 starts with intermediate I in which both subunits of the Rep dimer are bound to the 3' single strand in a P<sub>2</sub>S<sub>2</sub> complex. Due to the binding of ATP, the affinity for ssDNA of one subunit of the dimer decreases, forming intermediate II (P<sub>2</sub>S complex). In the meantime, the affinity for dsDNA increases, resulting in the formation of intermediate III (P<sub>2</sub>SD) in which the Rep dimer is bound simultaneously to the duplex ahead of the fork as well as to the 3' ssDNA. In the next step, hydrolysis of ATP induces protein conformational changes that destabilize the base pairs within the region to duplex DNA bound to one Rep subunit. Therefore, the 5' single strand is displaced while the Rep subunit bound to the 3' strand resulting a P<sub>2</sub>S<sub>2</sub> complex. The subsequent release of the ADP and inorganic phosphate completes the cycle by forming intermediate I', which is functionally equivalent to intermediate I because Rep is a homodimer.

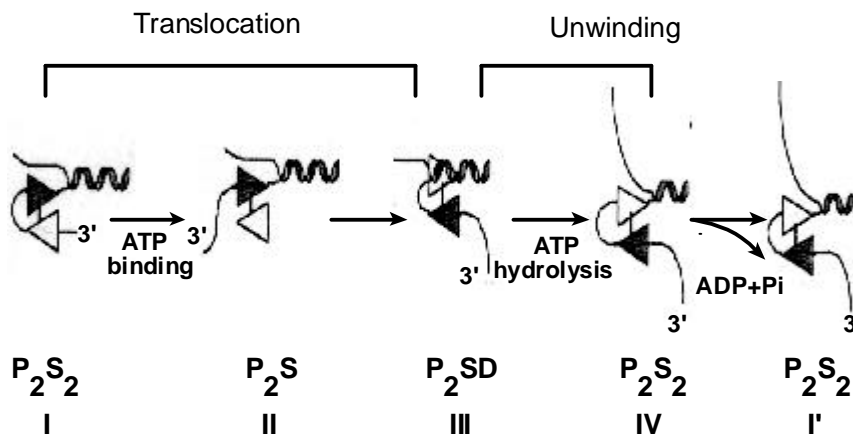


Figure 1-3: “Active, rolling” mechanism for dimeric Rep-catalyzed DNA unwinding. The dimeric Rep helicase is shown with triangular subunits assumed to be related by C2 symmetry. The two Rep subunits are distinguished (open vs stoppled) in order to indicate how the positioning of each subunit changes during the unwinding cycle. Modified from Wond and Lohman (1992).

In the rolling model, the Rep dimer translocates by rolling along the DNA, with translocation (step I to III) coupled to ATP binding, whereas DNA unwinding (step III to I') is coupled to ATP hydrolysis. In principle, any oligomeric helicase could operate by a rolling mechanism if this helicase possesses at least 2 DNA binding sites that could switch between binding of ssDNA and dsDNA (Ganesan and Smith, 1993).

The dimeric “inch-worm” model suggests a second mechanism how helicases can unwind actively dsDNA. In the “inch-worm” model, the same subunit of the dimer acts as the lead subunit interacting transiently with the duplex DNA, while the trailing subunit interacts only with ssDNA during unwinding and translocation. This is in contrast to the “active, rolling” model, where the two subunits alternate in their binding to the duplex DNA at the ss-ds-DNA junction to unwind the duplex. All existing data are equally consistent with a dimeric inch-worm model in which the two Rep dimer subunits do not alternate in their binding to the duplex DNA, but rather the same subunit remains as the leading subunit (Yarranton and Geftter, 1979). Therefore, both a dimeric inch-worm and a dimeric rolling model need to be considered equally as possible mechanisms (Cheng *et al.*, 2001).

### 1.1.3 The role of helicases in aging

More than 30 human proteins have been described to be putative helicases since they contain the seven-helicase motifs (I, II, III, IV, V, and VI) (Hall and Matson, 1999). They function in fundamental processes of life, including DNA replication, DNA repair, recombination, transcription, RNA splicing, and translation. To date, seven human disorders that manifest age-related phenotypes have been found to be caused by alterations in five proteins, all

containing the seven conserved helicase motifs. These disorders are Xeroderma pigmentosum, Cockayne syndrome, trichothiodystrophy, Bloom syndrome, Werner syndrome, X-linked  $\alpha$ -thalassemia/mental retardation syndrome, and Juberg-Marsisi syndrome (Nakura *et al.*, 2000). A decline of probably multiple and fundamental functions of helicases in these disorders is, therefore, implied to underlie not only the various age-related phenotypes but also the multiple and universal nature of ordinary aging.

Werner syndrome (WS) has the most similarities to premature aging. WS is a high-ranked autosomal recessive segmental progeroid syndrome. The clinical phenotypes of WS patients include the early appearance of senility, loss or graying of hairs, increase in irregular pigmentation, beaked nose, small mouth and atrophic scleroderma-skin. The WS gene (WRN) has been cloned by Yu (1996). It encodes a 1432-amino-acid peptide with homology to RecQ related helicases. The WRN protein functions as a 3' to 5' DNA helicase (Gray *et al.*, 1997). To date, at least 19 mutations have been found in WS patients, all of which truncate the WRN protein. The truncated WRN protein fails to translocate into the nucleus due to the absence of the nuclear localization signal at the C-terminus of the protein, which results in loss of protein function. In WS patients, death occurs at an average age of 47 years, and the major causes of death are malignant tumors and myocardial infarction (Nakura *et al.*, 2000).

It is very interesting to clarify the pathways through which each helicase disorder will generate age-related phenotypes. This would lead also to an improved understanding of the relationship between the disorders and ordinary aging.

## **1.2 Helix-destabilizing proteins catalyze DNA unwinding**

Helix-destabilizing protein (HDP) are essential components in a variety of DNA metabolic processes. HDP also has the name “DNA-unwinding protein” or “DNA-melting protein”. The more general term “single-stranded DNA binding protein” (SSB) is now used (Chase and Williams, 1986). Helix-destabilizing protein is used in this dissertation because this name implies a function, i.e. unwinding of partial duplexes of DNA.

There are many helix-destabilizing proteins *in vivo* and they are found in eukaryotes, prokaryotes and dsDNA viruses (Chase and Williams, 1986; McDougal and Guarino, 1999). They bind with high affinity to single-stranded nucleic acids as compared to double-stranded nucleic acids. Most of these proteins bind sequence unspecifically and usually cooperatively to ssDNA or ssRNA (Lohman *et al.*, 1988). Research to date has shown that helix-destabilizing proteins serve as accessory factors required for efficient action of replicative enzymes, DNA polymerases, and DNA helicases. Helix-destabilizing proteins also participate in DNA repair and recombination (Lohman *et al.*, 1988).

### 1.2.1 Properties of helix-destabilizing proteins differing from helicase

Although helix-destabilizing proteins are capable of unwinding DNA duplexes, these proteins do not play an active role in DNA unwinding during replication as seen for DNA helicases, which catalyze the unwinding of dsDNA. However, one role of helix-destabilizing proteins is to stabilize single-stranded regions generated by DNA helicases (Mikhailov, 2000). The properties of helix-destabilizing proteins differ from DNA helicases mainly in three points:

Firstly, helicases unwind DNA duplex with hydrolysis of ATP or another nucleoside triphosphat. Helix-destabilizing proteins unwind DNA duplex in an NTP-independent manner (Boehmer and Lehman, 1993; Chase and Williams, 1986).

“Polarity” in the unwinding of DNA duplex is the second difference between DNA helicases and helix-destabilizing proteins. Most known DNA helicases are capable of unwinding DNA duplexes in one direction only, from 3' to 5' on the leading strand or 5' to 3' on the lagging strand (Lohman, 1993). Unlike DNA helicases, which translocate unidirectionally on DNA, there does not appear to be a strict directionality to the unwinding caused by known helix-destabilizing proteins (Boehmer and Lehman, 1993; Mikhailov, 2000). For example, the *E. coli* SSB melts both 3'-tailed and 5'-tailed partial duplexes. The DNA unwinding promoted by adenovirus DNA-binding protein, DBP, does not proceed with a specific directionality (Monaghan, 1994). However, the baculoviral protein LEF-3 produces the polar melting effect on duplex DNA only with a 5'-ss tail (Mikhailov, 2000).

Thirdly, cooperative binding to ssDNA is a common feature of helix-destabilizing proteins (Lohman *et al.*, 1988). Cooperativity is the result of protein-protein interactions between monomers. In contrast, the oligomeric nature is one characteristic of helicases. Helicases can bind ssDNA generally as dimers or hexamers. If cooperativity between DNA-bound proteins is sufficiently high, these proteins can saturate a stretch of single-stranded nucleic acid at low concentrations. The ability to saturate a long stretch of ssDNA, which is not possible for proteins that bind noncooperatively, is thought to be necessary to protect DNA from the action of nucleases and to hold the DNA in a conformation that facilitates the function of other replication, recombination or repair enzymes. This property may be necessary for the biological function of helix-destabilizing proteins (Mikhailov, 2000; Zijdeveld and van der Vliet, 1994).

### 1.2.2 Mechanism of DNA unwinding by helix-destabilizing proteins

Multimerization and cooperative DNA binding of helix-destabilizing proteins may be a general mechanism of unwinding dsDNA (Dekker *et al.*, 1997). As described above,

cooperative binding to ssDNA is a common feature of helix-destabilizing proteins and is required to fully saturate the ssDNA and to protect it against nuclease activities.

The known helix-destabilizing protein bacteriophage T4 gene 32 (gp32) forms oligomers in solution (Carroll *et al.*, 1975) and forms protein chains on ssDNA (Kowalczykowski *et al.*, 1981). ICP8, the single-stranded binding protein of herpes simplex virus, forms long filaments in solution (Boehmer and Lehman, 1993; O'Donnell *et al.*, 1987). It binds ssDNA in a highly cooperative fashion and unwinds duplex DNA. Not all helix-destabilizing proteins form oligomers in the absence of DNA. Bacteriophage P5 and eukaryotic heterotrimeric RP-A are monomeric in solution (Kim and Wold, 1995; Soengas *et al.*, 1995). DNA binding is cooperative, however, and continuous arrays of proteins are formed on the ssDNA. These proteins unwind DNA and it has been suggested that this is driven by cooperativity. Therefore, other helix-destabilizing proteins may employ a similar mechanism by which the energy required to unwind DNA is provided by strong protein-protein interactions instead of ATP hydrolysis as in the case of true DNA helicases.

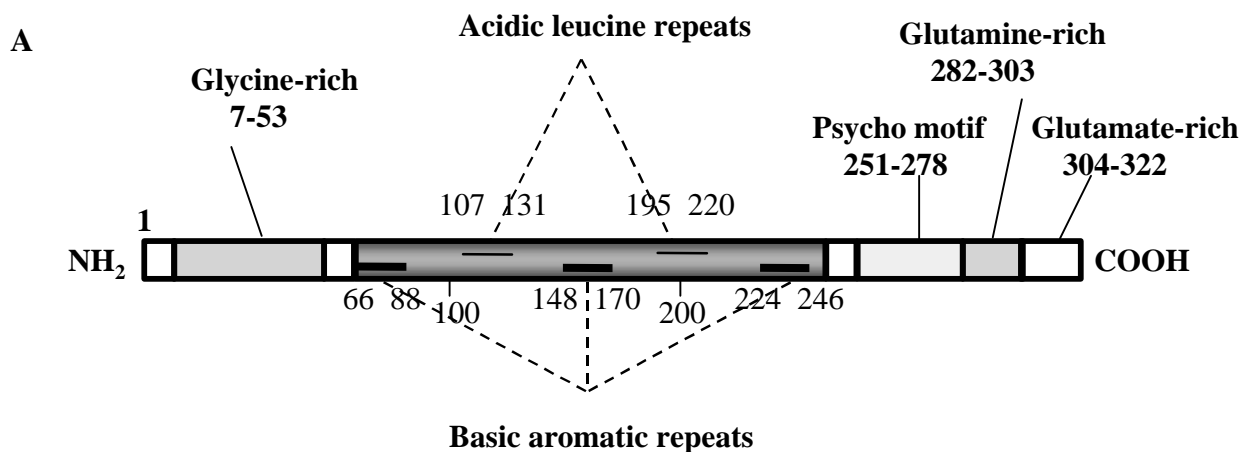
### **1.3 *Pur* $\alpha$ , a multifunctional single-stranded DNA- and RNA-binding protein**

Pur $\alpha$  is a ubiquitous, sequence-specific DNA- and RNA-binding protein that is highly conserved in eukaryotic cells. The Pur factor was identified originally as a HeLa cell nuclear protein which binds a sequence element adjacent to a region of stably-bent DNA upstream of the human c-myc gene (Bergemann *et al.*, 1992). This element is near the center of a region implicated as an initiation zone for chromosomal replication and is found at several eukaryotic origins of DNA replication. Pur $\alpha$  binds preferentially to purine-rich single-stranded DNA. In addition to mammalian cells, the Pur $\alpha$  gene has been cloned also from *Drosophila melanogaster*, *Caenorhabditis elegans*, *Schistosoma mansoni* and *Arabidopsis thaliana* (Gallia *et al.*, 2000). The sequence of Pur $\alpha$  is highly conserved among species. Between human and mouse Pur $\alpha$ , an extraordinary degree of conservation has been reported: there are only two single-amino-acid changes between human and mouse Pur $\alpha$ . The mouse protein lacks Gly49 and includes an Ala306-Thr substitution (Ma *et al.*, 1994). To date, three members of the Pur family (Pur $\alpha$ , Pur $\beta$  and Pur $\gamma$ ) are known, however the Pur $\alpha$  protein is the best-studied one. Research on Pur $\alpha$  protein is getting more and more interesting in the last years because Pur $\alpha$  has been implicated in diverse cellular functions, including transcriptional activation and repression, translation, and cell growth (Gallia *et al.*, 2000).

### 1.3.1 Structural characteristics Pura

The deduced amino acid sequence of Pur $\alpha$  reveals a modular repeat structure unique among known DNA-binding proteins. There are three repeats of 23-amino-acid motif (class I repeats) interspersed with two repeats of 26-amino-acid motif (class II repeats), which composes the central region of Pur $\alpha$  (Figure 1-4 A). While the sequence between these repeats is not conserved, each repeat preserves several identical and conservative substitution of amino acid residues (Figure 1-4 B).

Pur $\alpha$  contains structural features of potential importance in addition to the repeat modules, denoted in Figure 1-4 A. Near the amino-terminal end of Pur $\alpha$  there is a prominent stretch of 18 glycine residues broken only by a single serine residue. Similar glycine stretches are present in proteins serving a wide variety of functions, including helix-destabilizing proteins (Haynes *et al.*, 1987). Carboxy terminal to the repeat modules there is a potential  $\alpha$ -helical region which confers a strongly amphipathic character. This motif is present also in transforming proteins of several DNA tumor viruses, as well as in proteins of yeast and human cells. The consensus of this motif contains PSY and C, and has been termed the 'psycho' motif. It is necessary for Pur $\alpha$  binding to hypophosphorylated Rb protein (pRb). The carboxy-terminus of Pur $\alpha$  consists of a glutamine-glutamate-rich domain. The entire sequence from aa 276 through aa 321 consists of 50% glutamine and glutamate residues. Glutamine-rich domains have been implicated as transcriptional activation regions in several DNA-binding proteins (Courey *et al.*, 1989).



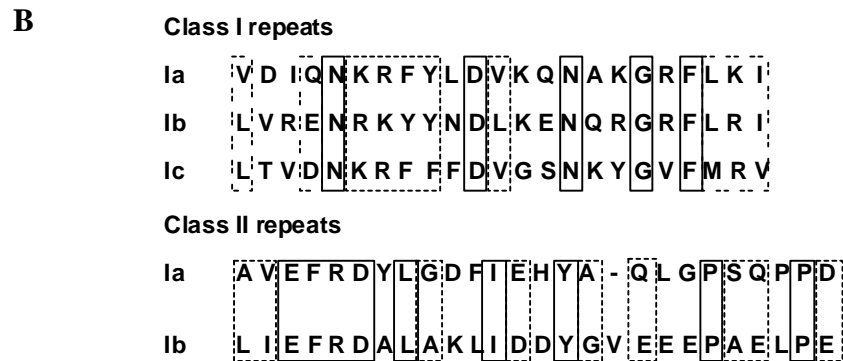


Figure 1-4: Structural organization of the human Pur $\alpha$  protein. (A) Graphic representation of the domains and motifs of Pur $\alpha$ . The three basic aromatic class I repeats are indicated by heavy horizontal lower lines in the central repeat region and the two acidic leucine-rich regions are indicated by light horizontal upper lines in the central repeat region. (B) Class I motifs are aligned at the top and class II repeat motifs are aligned at the bottom. Solid boxes indicate identical amino acid residues and dotted boxed indicate conservative changes. Modified from Bergemann (1992).

It is interesting that there are three members of the PUR family identified in mammals to date. Pur $\alpha$ , Pur $\beta$ , and Pur $\gamma$  display a high degree of homology. Murine Pur $\alpha$  and Pur $\beta$  possess 71% sequence identity while human Pur $\alpha$  and Pur $\gamma$  possess 54% sequence identity. It is unclear if these proteins are expressed differentially and whether they are functionally redundant or biologically unique. Several structural features suggest that they may possess different functions (Gallia *et al.*, 2000).

### 1.3.2 Pura and gene transcription and replication

Pur $\alpha$  has been implicated in the transcriptional control of many cellular genes. Myelin basic protein (MBP) represents the first cellular gene that was shown to be transcriptionally regulated by Pur $\alpha$  (Haas *et al.*, 1995).

Myelin basic proteins (MBPs) are major protein components of myelin, comprising more than 30% of the central nervous system (CNS) myelin protein and about 18% of the peripheral nervous system (PNS) myelin protein. MBPs are a class of proteins consisting of multiple polypeptides varying in molecular weight from 14 to 21.5kDa. In mice, six isoforms of MBPs (14kDa, 17.2kDa, 17.3kDa, 18.5kDa, 20.2kDa and 21.5kDa) have been identified (Campagnoni and Skoff, 2001). All isoforms are coded by alternative splicing of a single major transcript (Campagnoni and Skoff, 2001; de Ferra *et al.*, 1985; Kamholz *et al.*, 1986; Newman *et al.*, 1987; Roth *et al.*, 1986; Roth *et al.*, 1987; Takahashi *et al.*, 1985). The expression of MBP is regulated at the transcriptional level (Monuki *et al.*, 1990). A proximal element, termed MB1, which contains the Pur $\alpha$  binding motif, dictates cell type-specific expression of MBP (Mukherjee and Chambon, 1990). In mice, Pur $\alpha$  is more abundant in

brain during and after the period of active myelination. Functionally, Pur $\alpha$  stimulates transcription of the MBP promoter in glial cells through binding to the MB1 sequence (Haas *et al.*, 1995; Tretiakova *et al.*, 1999). Pur $\alpha$  also interacts with other cellular regulatory proteins, including MyEF-2 and Sp1, further two factors regulating MBP gene transcription. The repressor protein MyEF-2 decreases transcription of the MBP gene. It has been suggested that Pur $\alpha$  and MyEF-2 exert a negative effect on each other's DNA binding activity. Moreover, Pur $\alpha$  also associates with the ubiquitous transcription factor Sp1 that interacts with the MB1 DNA motif at a region that partially overlaps with the Pur $\alpha$  binding site. Functionally, the overexpression of Pur $\alpha$  and Sp1 in the CNS cells results in a synergistic stimulation of the MBP promoter (Tretiakova *et al.*, 1999).

Pur $\alpha$  has been suggested to play a role in the transcriptional regulation of the FE65 gene (Zambrano *et al.*, 1997). FE65 is a 90 kDa adapter protein that interacts with the Alzheimer  $\beta$ -amyloid precursor protein. In Chinese hamster ovary cells, where the activity of the FE65 promoter is very low, transient overexpression of Pur $\alpha$  increases expression from the FE65 minimal promoter (Zambrano *et al.*, 1997).

Pur $\alpha$  has been implicated also in the transcription of other cellular genes, including murine vascular smooth muscle (VSM)  $\alpha$ -actin (Becker *et al.*, 2000), neuronal nicotinic acetylcholine (nAch) receptor (Du *et al.*, 1997). Moreover, Pur $\alpha$  is involved also in regulating several human viruses which replicate in the CNS, including JC virus (JCV) (Chen *et al.*, 1995; Chen and Khalili, 1995) and HIV-1 (Krachmarov *et al.*, 1996). Pur $\alpha$  is capable of stimulating viral promoters, including JCV early gene promoter and the HIV-1 long terminal repeat. Interestingly, there is a high incidence (4-8%) of the JCV-induced demyelinating disease "progressive multifocal leucoencephalopathy" (PML) among individuals with acquired immunodeficiency syndrome (AIDS) (Krachmarov *et al.*, 1996), suggesting that the presence of HIV in the brains of infected individuals may induce JCV gene transcription and replication. In fact, the Tat protein, the transregulatory protein of HIV-1, is capable to activate the JCV late gene promoter (Chowdhury *et al.*, 1993; Chowdhury *et al.*, 1992). Tat is a transcription activator that can stimulate transcription of the HIV genome (Jones, 1997). It has been shown that the Tat responsive sequence of JCV contains a PUR element and Pur $\alpha$  and Tat activate the JCV late gene promoter synergistically (Krachmarov *et al.*, 1996).

Pur elements are present at eukaryotic origins of DNA replication. Pur $\alpha$  has been shown to interact with viral origins of DNA replication, including the JCV and bovine papillomavirus (Chang *et al.*, 1996; Jurk *et al.*, 1996). Pur $\alpha$  suppresses JC viral DNA replication in human glial cells (Chang *et al.*, 1996). It has been suggested that endogenous Pur $\alpha$  may exerts a negative effect on DNA replication.



### 1.3.3 Pura and control of cell growth

Pur $\alpha$  seems to play a role in the control of cellular growth and proliferation. This conclusion is based on the following observations: (i) The level of Pur $\alpha$  fluctuates during the cell cycle. (ii) The intracellular localization of Pur $\alpha$  alters during the cell cycle. (iii) Pur $\alpha$  associates with some key cell cycle regulatory proteins and viral oncoproteins (Darbinian *et al.*, 1999; Itoh *et al.*, 1998; Johnson *et al.*, 1995; Ma *et al.*, 1995; Stacey *et al.*, 1999).

Levels of Pur $\alpha$  are altered during cells cycle of the CV-1 cells. Just prior to the onset of S phase, Pur $\alpha$  level drops dramatically and then increases slowly to nearly 8-fold throughout S and G2 phase and peaks just after mitosis (Itoh *et al.*, 1998). As observed previously, Pur $\alpha$  binds the hypophosphorylated retinoblastoma protein, pRb (Johnson *et al.*, 1995), which functions as a tumor suppressor and is an integral protein involved in cell cycle progression. The pRb interacts with a variety of proteins in the G0 and G1 phase of the cell cycle, including transcription factors such as E2F. Hyperphosphorylation of Rb protein results in the release of these factors from Rb. The release allows E2F to activate genes necessary for progression through G1 and entry into the S phase. The association of Pur $\alpha$  and Rb is restricted in G1 phase while Pur $\alpha$  was coimmunoprecipitated and co-localized with cyclin A in S and G2 phase of the cell cycle in the nucleus (Itoh *et al.*, 1998).

Interestingly, Pur $\alpha$  also has been shown to associate directly with E2F-1. E2F-1 is a DNA binding transcription factor which, upon interaction with its target DNA sequence, induces expression of several S phase specific genes allowing progression of the cell cycle. Its activity is modulated by its cellular partner, hypophosphorylated Rb protein (pRb), which binds to E2F-1 and inactivate its transcriptional activity. The association of Pur $\alpha$  and E2F-1 proteins suppresses transcriptional activity of E2F-1 (Darbinian *et al.*, 1999). Pur $\alpha$  suppresses the transcriptional activity of E2F-1 by inhibiting the interaction of E2F-1 with its target sequence. Interestingly, Pur $\alpha$  and E2F-1 bind to the same region of Rb, suggesting that the association of Pur $\alpha$  with Rb may liberate E2F-1. The associations of Pur $\alpha$  with Rb, E2F-1 and cyclin A coupled with its fluctuating levels throughout the cell cycle, position Pur $\alpha$  as a crucial factor in the cell cycle (Darbinian *et al.*, 1999).

### 1.3.4 Pur family and possibly related diseases

Pur $\alpha$  and Pur $\beta$  proteins belong together to the PUR protein family and possess high sequence identity (71% homology in mice). Recently, PURA and PURB gene deletions have been shown to occur in many cases of myeloid leukemia and myelodysplastic syndrome (Lezon-Geyda, 1997; Lezon-Geyda *et al.*, 2001).

PURA and PURB, encoding functionally cooperative proteins in the Pur family, are localized to chromosome bands 5q31 and 7p13, respectively (Ma *et al.*, 1995). Deletions or monosomy of chromosomes 5 and 7 are frequently associated with hematological malignancies, particularly myelodysplastic syndromes (MDS) and acute myelogenous leukemia (AML) (Le Beau *et al.*, 1993; Pedersen, 1993). One or both of these loci are shown to be hemizygotously deleted in 60 MDS or AML patients using fluorescence in situ hybridization (FISH). High-resolution mapping of PURA localizes it approximately 1.1 Mb telomeric to the EGR-1 gene. The frequency of PURA deletion and segregation with EGR-1 indicate that PURA is within the most commonly deleted segment in myeloid disorders characterized by del(5)(q31). No mutations have been detected within the coding sequence of PURA. Concurrent deletions of PURA and PURB occur in MDS at a rate nearly 1.5-fold higher than statistically expected and in AML at a rate > 5-fold higher (Le Beau *et al.*, 1993; Pedersen, 1993). This novel simultaneous deletion of two closely related gene family members may thus have consequences related to progression to AML. Pur $\alpha$ , an Rb-binding protein, has been implicated in cell cycle control and differentiation. Alterations in these genes could affect a delicate balance critical in myeloid development.

#### **1.4 The aim of this study**

Since its initial cloning in 1992 an impressive range of biochemical functions have been attributed to the predicted 322 amino acid human Pur $\alpha$  protein. Pur $\alpha$  binds both single-stranded and double-stranded DNA in a sequence-specific fashion, showing preference for the purine-rich ssDNA repeats (GGN) found in its recognition sequence. Pur $\alpha$  activity also partly involves interactions with a number of cellular and viral proteins including hypophosphorylated pRb, E2F, cyclin A, Sp1, members of the Y-box family of proteins, polyomavirus T antigens and HIV-1 Tat. As a result, Pur $\alpha$  may be involved in diverse cellular functions, including DNA replication, transcription, translation and cell growth control, however, many of the underlying molecular mechanisms governing these multiple functions remain unclear.

Although Pur $\alpha$  has been the subject of many studies, the exact mechanism of how Pur $\alpha$  accomplishes its different functions has remained elusive. Recently, a fortuitous observation in our laboratory demonstrated that Pur $\alpha$  purified from calf thymus is capable of unwinding short DNA duplexes in a helicase assay. One aim of this study was to perform helicase assays with Pur $\alpha$ , from which we hoped to establish a mechanism of how Pur $\alpha$  functions in different cellular processes like replication and transcription. Helicase assays should be carried out with different substrates and with nucleoside triphosphates. In addition, Pur $\alpha$  deletion mutants were planned to be generated for mapping of the Pur $\alpha$  unwinding and DNA binding domains.

The diverse functions of Pur $\alpha$  coupled to its highly conserved protein sequence between organisms, particularly mouse and man, makes it an ideal candidate paralogue for proteomics and Rosetta Stone mouse models. We therefore decided to bypass further biochemical analyses and to concentrate on whole animal models by constructing Pur $\alpha$  knock-out mice.

The second and the main aim of my study was to generate Pur $\alpha$  knock-out mice with homologous recombination techniques in ES cells to unravel the diverse functions of this protein through the phenotype analysis of Pur $\alpha$  knock-out (KO) mice.

## 2 Material

### 2.1 Cell lines

NIH3T3	Fibroblast of mouse
Hela	Human epithelial cell of
E14	Embryonic stem cell of 129/Ola mouse

### 2.2 Bacterial strains

Bacterial strains XLI Blue, K803, LE392, TOP10F' and XL1 Blue/MRA/P2 belong to the strain collections of the group of Prof. E.-L. Winnacker.

XLI Blue: *recA1, endA1, gyrA96, thi-1, hsdR17, supE44, relA1, lac, [F' traD36, proAB, lacI<sup>q</sup>ZΔM15, Tn10(*tet*<sup>r</sup>)]*

LE392: *e14-(mcrA), hsdR514, supE44, supF58, lacY1* or *Δ(lacIZY)6, galK2, galT22, metB1, trpR55*

K803: *F<sup>-</sup>e14<sup>-</sup> (mcrA), lacY1* or *Δ(lac)6, supE44, galK2, galT22, rfbD1, metB1, mcb1, hsdR2(r<sub>k</sub><sup>-</sup> m<sub>k</sub><sup>-</sup>)*

TOP10F': *F<sup>-</sup> (tet<sup>r</sup>lacI<sup>q</sup>), mcrA, Δ(mrr-hdsPMS-mcrBC), Φ80lacZΔM15, ΔlacX74deoR, recA1, araD139, Δ(ara-leu)7679, galU galK, rpsL, endA1, nupG*

XL1 Blue/MRA/P2: *Δ(mcrA)183, Δ(mcrCB-hsdSMR-mrr)173, endA1, supE44, thi-I gryA96, relA1, lac (P2 lysogen)*

### 2.3 Genomic DNA libraries

Stratagene:

129/SvJ Mouse Genomic Library, Lambda FIX II Vector

### 2.4 Phages

Lambda phage is from group of Prof. E.-L. Winnacker.

### 2.5 Plasmids

Promega, Biotec, Madison, Wi., USA

Vector **pGEM4Z** and **pcDNA3**

Invitrogen BV, Netherlands

Vector **pZERO**

Pharmacia Fine Chemicals, Freiburg

**pGEX4T1**

**pGEMMUT** was provided by Dr. Wolfgang Wendler; PKO Scrambler V920, pKO SelectTK and pKO SelectNeo V800 were kindly provided by Prof. Mathias Müller, Vienna.

## **2.6 Cell-culture**

Gibco BRL, Germany:

Geneticin; Dulbecco's MEM with Glutamax-I (with Sodium Pyruvate, 1000 mg/l Glucose, and Pyrodoxine); Glucose; L-glutamate; Sodium-pyruvate; MEM nonessential amino acids; Antibiotics (penicillin, streptomycin); Fetal Bovine Serum (FCS); Murine Leukemia Inhibitory Factor (ESGRO™); PBS (without Ca<sup>2+</sup> and Mg<sup>2+</sup>)

SIGMA, Munich:

DMSO (Dimethyl Sulfoxide); β-mercaptoethanol

## **2.7 Enzyme**

Roche Diagnostics GmbH, Mannheim:

Calf intestinal alkaline phosphatase (CIP); DNase I; Restriktion enzymes; RNase A; Expand™ Long Template PCR System; Complete™ Mini EDTA-free Protease-Inhibitor-Cocktail (Tablets)

New Englands Biolabs, Schwalbach:

T4 DNA-ligase; T4 polynucleotide kinase; Klenow DNA-polymerase; Restriction enzymes

Promega Biotec, Madison, Wi., USA:

RNasin, RNase-free DNase

## **2.8 Antibodies**

Purα monoclonal antibody 3C12-1-1 was kindly generated by Dr. Elisabeth Kremmer, GSF, Munich.

Chemicon International, Inc., USA

Rat anti-myelin basic protein (MBP) (82-87 Region) monoclonal antibody

Dianova, Hamburg

Peroxidase-conjugated AffiniPure Goat anti-Rat anti-IgG+M (H+L)

## **2.9 Chemical reagents**

### Amersham Pharmacia Biotech, USA

[ $\gamma$ -<sup>32</sup>P] ATP (3000 Ci/mmol); [ $\alpha$ -<sup>32</sup>P]-dATP, [ $\alpha$ -<sup>32</sup>P]-dGTP, [ $\alpha$ -<sup>32</sup>P]-dTTP, [ $\alpha$ -<sup>32</sup>P]-dCTP (3000 Ci/mmol); <sup>35</sup>S-Methionine, Hybond N<sup>+</sup>-Membrane und Hybond N-round filter, Hybond-N<sup>+</sup>

### Bethesda Research Laboratories GmbH, Neu-Isenburg

Agarose; Ammonium sulfate; bovine serum albumin (BSA); DNA-marker: 123 bp-marker, 1 Kb-marker; Electrophoresis Sequencing System, Model S2

### Biomol Feinchemikalien, GmbH, Hamburg

Calcium chloride (CaCl<sub>2</sub>); Dialyze membrane; 3-(N-morpholino)propan sulfonic acid (MOPS)

### BIO-RAD Lab, Richmond, Calif., USA

BIO-RAD-Protein assay, Protein standard, prestained Protein standard, MiniProtean II

### Boehringer Mannheim GmbH, Mannheim

Adenosine triphosphate (ATP); Isopropyl-1-thio- $\beta$ -D-galactoside (IPTG); Random primed DNA Labeling Kit; PEG 1500, Tris(hydroxymethyl)- aminomethane (Tris)

### Clontech, USA

ExpressHyb Hybridization Solution

### Qiagen GmbH, Düsseldorf

Qiagen Plasmid Kit

### Difco Laboratories, Detroit, Michigan, USA

Bacto-agar; Bacto-tryptone; Casamino acid; Difco-Minimal-Agar, Fetal calf serum (FCS); Yeast Extract

### Eppendorf Gerätebau, Hamburg

Table centrifuge 5415; Reaction tubes 1.5 and 2.2 ml

### Fermentas, Lithuania

$\lambda$ -DNA

Fluka Feinchemikalien, Neu-Ulm

Chloroform; Formamid; Nonidet<sup>®</sup>-P40 (NP40); Silicon solution

Greiner GmbH, Nürtingen

Plastic test tubes 10 and 50 ml; Monolayer flasks for cell culture; Plastic Petri-dishes, ø 9 cm and 14 cm

Hybaid Limited, Teddington, UK

Horizontal gel electrophoresis system

Eastman Kodak Company, Rochester, N.Y., USA

X-ray film XAR5, Biomax<sup>™</sup>MR

Invitrogen, USA

Easy-DNA<sup>™</sup> Kit

E. Merck AG, Darmstadt

Ammonia; Ammonium sulfate; Ammonium persulfate (APS); boric acid; Bromophenol blue; Chloroform; Dimethylformamid; Dimethyl sulfoxide (DMSO); Acetic acid; Ethylene diamintetraacetic acid (EDTA); Ethanol p.A.; Ethidiumbromid; Formamid; Formaldehyd; Glucose; Glycin; Urea; Isoamyl alkohol; Isopropanol; Calcium acetate; calcium chloride; calcium hydroxide; Magnesium acetate; Magnesium chloride; Magnesium sulfate; Methanol p.A.; Sodium acetate; Sodium chloride; Sodium dihydrogenphosphate; Sodium hydroxide; Sodium dodecyl sulfate (SDS); Phenol; hydrochloric acid ; Saccharose; N,N,N',N'-tetramethyl-ethylendiamine (TEMED); Triton X-100; Xylencyanol

Nunc-GmbH, Wiesbaden

Cryo-Tubes 2 ml; Inoculation loops; Plastic petri-dishes; Flasks for cell culture and cell culture dishes

NEN<sup>™</sup> Science Products, Inc., Boston

PolyScreen PVDF Transfer Membrane

Pharmacia Fine Chemicals, Freiburg

Deoxyribonucleoside triphosphate (dATP, dGTP, dCTP, dTTP); DEAE-Sepharose CL6B; Ficoll 400; Sequencing Kit; Sephadex G50; Glutathione sepharose

Promega, Biotec, Madison, WI, USA

5-bromo-4-chloro-3-indolyl-1-phosphat (BCIP); TNT<sup>®</sup> Quick Coupled Transcription/Translation Systems; Nitroblue tetrazolium (NBT); Ribonucleoside triphosphate (ATP, CTP, GTP, UTP)

Raytest Isotopenmeßgeräte GmbH

Fuji BAS 1000 Bio imaging analyzer, Fuji BAS imaging plate UR

Roth, Karlsruhe

Dithiothreitol (DTT); Glycerol, N-2-hydroxyethylpiperazine-N'-2-ethansulfonic acid (HEPES); Polyethyleneglycol (PEG) 6000; Phenol/TE

Sartorius GmbH, Göttingen

Mini art NML Sterile filter with the pore size 0,2 and 0,45 µm

Schleicher und Schüll, Dassel

Nitrocellulose filter BA 85, pore size 0,45 µm

Serva, Heidelberg

Acrylamide; β-Mercaptoethanol; Urea; Silicon solution

Sigma Chemie, Munich

Ampicillin; Diethylpyrocarbonate (DEPC); Sodium pyrophosphate; Piperazine-N,N'-bis(2-ethansulfonic acid) (PIPES); Phenylmethylsulfonyl fluoride (PMSF); poly-[d(A-T)]; poly-[d(I-C)]; Spermidine; Tetracycline; tRNA from yeast; L-amino acid; Trypan blue; Trysin Inhibitor from soybean; Leupeptin hemisulfate salt

Tetanal Photowerk, Norderstedt

Tetanal for film development

Whatman Limited, Springfield Mill, Maidstone, Kentucky, USA

3MM-Papier

## **2.10 Synthetic oligonucleotides**

The oligonucleotides used were synthesized by the group of Dr. G. Arnold in gene center or by Metabion, Munich.



## 3 Methods

### 3.1 Cloning and propagation of DNA in *E. coli*

#### 3.1.1 Bacterial culture

##### 3.1.1.1 Liquid culture

*E. coli* cultures were grown in LB medium supplemented, if necessary, with antibiotics. The cultures were grown at 37°C for 12-16 hrs, with shaking at 200 rpm.

##### LB medium:

10.0 g Bacto Tryptone  
5.0 g Yeast extract  
5.0 g NaCl  
add 1000 ml H<sub>2</sub>O bidest.

##### Addition of antibiotics:

Ampicillin	50 µg/ml	stock solution 50 mg/ml in H <sub>2</sub> O
Kanamycin	25 µg/ml	stock solution 50 mg/ml in H <sub>2</sub> O

##### 3.1.1.2 Plate culture

Autoclaved LB-Agar was cooled to 50°C, antibiotics were added and the agar solution was poured into sterile petri dishes. These agar plates were stored at 4°C.

##### LB-Agar:

15.0 g Agar  
10.0 g Bacto Tryptone  
5.0 g Yeast extract  
5.0 g NaCl  
add 1000 ml H<sub>2</sub>O bidest.

The bacteria were plated on LB-plates and incubated at 37°C for 12-16 hrs.

##### 3.1.1.3 Glycerol stocks

For long-term storage of bacterial strains, bacterial pellet was resuspended in 50% sterile glycerol/50% LB and kept at -80°C.

### 3.1.2 Preparation of competent cells

XL1 Blue and Top10F' competent cells were prepared as follows:

A single colony of bacteria was inoculated into 20 ml TYM, grown at 37°C with moderate shaking (200 rpm) to an OD<sub>600</sub> = 0.2 to 0.8. The culture was inoculated into 100 ml TYM and grown to an OD<sub>600</sub> = 0.6. 100 ml of the culture was then inoculated into a sterile 2-liter flask containing 400 ml TYM. As soon as the bacteria reached an OD<sub>600</sub> = 0.6, the flask was put on ice to cool the bacteria quickly. The bacteria suspension was centrifuged in a GSA-Rotor for 15 min at 4000 rpm (4°C). The supernatant was discarded, the bacteria pellet was resuspended carefully in 100 ml Tfb I and kept on ice for 15 min. After the bacteria were centrifuged once more at the same speed, the bacteria pellet was resuspended in Tfb II and aliquoted (200 µl aliquots) into ice-cold Eppendorf tubes. The bacteria were frozen in liquid nitrogen and stored at -80°C.

The competency of the cells was assessed by using 10 ng pGEM4Z to transform 100 µl of competent cells. Aliquots (1, 10, 25 µl) of the transformation culture were plated on LB/ampicillin plates and incubated at 37°C overnight. Afterwards the transformation efficiency (number of transformants per µg DNA) was assessed.

#### TYM:

2%	Bacto Tryptone
0.5%	Yeast extract
0.1 M	NaCl
10 mM	MgSO <sub>4</sub>

#### Tfb I:

30 mM	KOAc
50 mM	MnCl <sub>2</sub>
100 mM	CaCl <sub>2</sub>
15%	glycerol

#### Tfb II:

10 mM	MOPS, pH 7.0
75 mM	CaCl <sub>2</sub>
10 mM	KCl
15%	glycerol

### 3.1.3 Transformation of competent *E. coli*

An aliquot of 100 µl of chemical competent *E. coli* was thawed on ice, 10-20 µl of ligated DNA was added to the cells, mixed and kept on ice for 30 min. The cells were exported to a heat shock by placing the tubes into a 42°C water bath for 2 min and left on ice for 5 min. 0.9 ml LB-medium was added to each tube. The tubes were placed on a roller drum at 200 rpm for 1 hr at 37°C. Aliquots of transformed cultures were placed on LB/ampicillin or other appropriate antibiotic-containing plates, which were incubated at 37°C for 12-16 hrs.

## **3.2 Mammalian cell culture**

All tissue culture procedures described must be carried out under sterile conditions using sterile plastic ware and detergent-free glassware.

### **3.2.1 Cell culture of NIH3T3 and 293**

NIH3T3 and 293 were cultured in DMEM (Gibco) supplemented with 10% FCS and incubated at 37°C in a 5% CO<sub>2</sub> incubator. Cell cultures were splitted every 2-4 days, whenever they have reached subconfluence or confluence. When splitting, the cells were disaggregated by using trypsin. A cell pellet was obtained by centrifuging (1000 rpm), which could be used for extraction for genomic DNA or protein extraction.

### **3.2.2 Freezing cells**

The cells were trypsinized and a cell pellet was obtained by centrifugation. The cells were resuspended in pre-cooled freezing medium and transferred into freezing vials. The freezing tubes were quickly placed in a -80°C freezer or the air phase compartment of a liquid nitrogen storage vessel. For longer storage, the cells should be kept under liquid nitrogen, where they can survive almost indefinitely.

#### Freezing medium:

FCS + 15% DMSO (Dimethyl Sulfoxide)

### **3.2.3 Transfection of mammalian cells**

#### **3.2.3.1 Transfection of adherent cells**

NIH3T3 and 293 cells were transfected as follows:

About  $1-3 \times 10^5$  cells per well were seeded into each well of a 6-well or 35-mm culture plate containing 2 ml of complete growth medium. The cells were incubated at 37°C for about 18-24 hrs until they reached 50-80% confluence. LIPORECTAMINE™ Reagent (Gibco BRL) was used for transfection of mammalian cells. The following solutions were prepared for each transfection: Solution A: 1-2 µg DNA was pipetted into in 100 µl serum-free medium; Solution B: 25 µl LIPOFECTAMINE Reagent was diluted in 100 µl serum-free medium. The two solutions were combined, mixed well and incubated at room temperature for 15-45 min to allow DNA-liposome complexes to form. For each transfection, 0.8 ml of serum-free medium was added to the tube containing the complexes. The diluted complex solution was mixed gently and overlaid onto the rinsed cells. The cells were incubated with the complexes for 2-24 hrs at 37°C in a CO<sub>2</sub> incubator. Following incubation, 1 ml of growth medium containing

twice the normal concentration of serum was added without removing the transfection mixture. The medium was replaced with fresh, complete medium 18-24 hrs following the beginning of transfection. Finally, cell extracts were assayed for gene activity 24-72 hrs after the start of transfection.

### **3.2.3.2 DNA transfection for stable expression**

About 72 hrs after transfection, the cells were diluted 1:10 into the selective medium for the reporter gene used. In case of PCI Neo transfection, medium should contain Geneticin (Gibco). The cells that didn't containing the reporter gene could not survive in medium containing geneticin and died slowly after 3 days. The medium was replaced every two days. The cell colonies, which could be identified with the natural eyes, were picked into a 48-well culture plate containing 600  $\mu$ l of selective medium per well. After about 2 days, the colonies were trypsinized to a single cell suspension for further improved growth. After the cells reached confluence, they were trypsinized and transferred to a 24-well culture plate, thereafter to a 6-well plate and finally to a mini-dish to gain enough cells for a protein assay.

## **3.2.4 ES cell culture**

### **3.2.4.1 General condition and ES cell culture media**

For long-term culture and maintenance, ES cells should be grown on monolayers of mitotically inactivated feeder cells. Primary embryonic fibroblasts (EMFIS) or STO fibroblast cell lines are the most commonly used feeder layers. ES cell lines can also be cultured on gelatinized tissue culture plates for single passages in the presence of LIF or media conditioned by specific cell lines (i.e. BRL cells). The total substitution of feeder cells by LIF alone appears to work reasonable well for some ES cells, but other cell lines differentiate excessively without feeder cells. Under certain circumstances, i.e. to obtain genomic DNA from the cells, it is not necessary to provide either feeder layers, or LIF, since the differentiation of the cells does not impair the growth of the cells.

ES cell lines were cultured in Dulbecco's modified Eagle's medium (DMEM) with high glucose (4500 mg/l) (Gibco), supplemented with L-glutamin (Gibco), sodium-pyruvate (Gibco), MEM nonessential amino acids (Gibco),  $\beta$ -mercaptoethanol (Sigma), antibiotics (penicillin, streptomycin, Gibco), 10-15% of fetal calf serum (FCS) (batch tested and heat inactivated), and LIF (200 U/ml -1000 U/ml).

Basic medium (500 ml):

495 ml Dulbecco's MEM with Glutamax-I (with Sodium Pyruvate, 1000 mg/l Glucose, and Pyrodoxine)  
 5 ml MEM Non-essential amino acids (100 x stock)  
 5 µl 2-Mercaptoethanol

Growth medium for embryonic fibroblasts (EMFI medium):

For 100 ml:

90 ml Basic medium  
 10 ml FCS (10%) Fetal Bovine Serum

Growth medium for ES cells (ES cell medium):

For 100 ml:

84 ml Basic medium  
 15 ml FCS (15%), Fetal Bovine Serum (batch tested)  
 1 ml Murine Leukemia Inhibitory Factor (ESGRO™)  
 Dissolved in DMEM, 10<sup>5</sup> units

**3.2.4.2 Passaging of ES cells**

Trypsinization was performed as follows: ES cells that were grown on plates were washed twice with 1 x PBS (without Ca<sup>2+</sup> and Mg<sup>2+</sup>, GIBCO, Germany). After the aspiration of PBS, a proper amount of 0.25% trypsin/EDTA solution (Table 3-1) was added to the cells and incubated at 37°C, 5% CO<sub>2</sub> for about 5 minutes. The cell suspension was then transferred into a Falcon tube containing 10 ml ES cell medium. After centrifugation at 1200 rpm for 4 minutes at RT, the cell pellet was resuspended in ES medium and was ready for further expansion on plates or other purposes.

Types	Area (cm <sup>2</sup> )	Amount of medium (ml)	Amount of trypsin (ml)
15-cm dish	145	25	7.5
10-cm dish	56.7	10	4
6-cm dish	20.8	6	2
6-well plate	8.7	2.5	0.5
24-well plate	1.9	1	0.15
48-well plate	1	0.2	0.05

Table 3-1: Parameters of major cell culture plates or dishes

**3.2.4.3 Thawing and expanding of ES cells**

A vial of E14 ES cells (from 129 Ola strain) was quickly thawed in a 37°C water bath and then transferred to a falcon tube containing 10 ml ES cell medium. After centrifugation at 1200 rpm for 5 minutes at RT, the cell pellet was resuspended in 6 ml of ES cell medium, then plated onto a 6-cm feeder dish and incubated at 37°C, 5% CO<sub>2</sub> overnight. The next day,

the cells were re-fed with 6 ml of fresh ES cell medium and again incubated at 37°C, 5% CO<sub>2</sub> for another day. The cells were trypsinized, split onto 3 other feeder dishes and incubated at 37°C, 5% CO<sub>2</sub> for another 2 days. Thereafter, the cells were split again onto three 6-cm feeder dishes or gelatinized dishes (Gelatin pre-treatment of dishes was performed by incubation with 0.1% gelatin for about 30 minutes, afterward gelatin solution was aspirated and dishes were filled up with ES cell medium) for further expansion. After another 2 days, the ES cells were ready for electroporation.

#### **3.2.4.4 Freezing of ES cells**

Many people working with cultured cells take a general rule for granted: cells should be frozen slowly and thawed quickly (Matise, 2000; Robertson, 1986).

To freeze ES cells, they were mixed with freezing medium containing a cryoprotective (dimethyl sulphoxide, DMSO) at a final concentration of 10-20%. Again, the cells were trypsinized and a cell pellet was obtained by centrifugation. The cells were resuspended in pre-cooled freezing medium and transferred into freezing vials. The freezing tubes were quickly placed in a -20°C or a -70°C or -80°C freezer or the air phase compartment of a liquid nitrogen storage vessel. For longer storage, the cells should be stored under liquid nitrogen, where they survive almost indefinitely. The vials stored at -20°C should be transferred to lower temperatures after a couple of hours. Cells stored at -80°C are viable for some months (6 months) (Matise, 2000).

##### Freezing medium:

FCS + 15% DMSO (Dimethyl Sulfoxide, SIGMA, Cat.No. D-5879)

#### **3.2.4.5 Electroporation of ES cells, antibiotic selection, picking, expansion and freezing of resistant ES cell clones**

DNA can be introduced into the genome of ES cells by electroporation, an application of a high voltage electrical pulse to a suspension of cells and DNA (Potter *et al.*, 1984; Thomas and Capecchi, 1987). A high voltage discharge as it is used in this gene transfer technique induces cells to fuse via their plasma membranes by creating pores in the cell (Zimmermann and Vienken, 1982). Cells are then able to take up and express exogenous (Neumann *et al.*, 1982). The process of electroporation consists of the same major steps:

(a) Preparing ES cells:

ES cells are thawed and cultured on feeder cells and passaged for at least one time. ES cells on the 60 x 15 mm tissue culture dish 36 hrs before electroporation were trypsinized and transferred on a 100 x 20 mm dish containing feeder cells.

(b) Electroporation:

ES cells are trypsinized from plates with feeder cells and washed with PBS twice. The cells were centrifuged and resuspended in PBS. After counting the cells,  $7 \times 10^6$  cells in 0.8 ml of electroporation medium was prepared and mixed well with 20  $\mu$ g of DNA (the linearized targeting vector). The mix was transferred into electroporation cuvette. The electroporation was performed under the condition of 230 V, 500  $\mu$ F for about 6.0 milli-seconds with Bio Rad Gene Pulser. The cuvette was left at room temperature for 5 min and transferred to a 50 ml tube containing 17.5 ml ES medium. The whole content of ES medium and cells were distributed on 18 100 x 20 mm dishes with feeder cells containing ES cell medium.

(c) Selection:

The selection was started about 48 hrs after the electroporation with a regular change of the medium with ES cell medium following the day after the electroporation. For a positive-negative selection 450  $\mu$ g/ml of G418 and 2  $\mu$ M of ganciclovir were added to the medium; The time for selection differs from 6-10 days when individual drug-resistant colonies should have appeared, large enough to be picked. The selection time depends on the density of cells, the differentiation of the clones, and if one wishes to pick the clones with or without a microscope.

(d) Picking and further passaging of drug-resistant clones:

Each individual drug-resistant clone deriving from one transfected cell is isolated by picking it from the selection plates containing PBS, to a single 96- or 48-well with a drawn-out Pasteur pipette or a Gilson pipette (100  $\mu$ l). The single clones are then trypsinized in the individual wells and divided into two portions, one for the screening procedures and one as a frozen back-up. The clones can be trypsinized and splitted right after picking or one day later by picking them into wells containing a feeder layer. A part of the clones is splitted and transferred to either gelatinized 96-, 48-, or 24- well plates for the screening procedures

(“screening plates”) and the other part is transferred to either 48- or 24-well plates containing feeder cells as a back-up (“back-up plates”) for later procedures. Both plates containing the same clones are marked to identify both portions of one clone. The medium in both plates was changed until they reach about 80-90% confluence. The DNA from the cells on the “screening plates” was isolated and examined. The cells in the “back-up plates” were frozen by either replacing the medium with pre-cooled freezing medium or by mixing a cell suspension with pre-cooled freezing medium in each individual well. The plates were transferred to a  $-70^{\circ}\text{C}$  or a  $-80^{\circ}\text{C}$  freezer. When a specific clone turns out to be positive for homologous recombination in the screening procedures, the corresponding clone on the “back-up plate” can be thawed and cultured for further procedures.

Electroporation medium:

10 ml EMFI medium  
50  $\mu\text{l}$  5M NaCl

Phosphate-buffered saline (PBS),  $\text{Mg}^{2+}$  and  $\text{Ca}^{2+}$  free:

1 liter of PBS solution made in  $\text{H}_2\text{O}$  contains the following:  
10g NaCl  
0.25g KCl  
1.44g  $\text{Na}_2\text{HPO}_4$   
0.25g  $\text{KH}_2\text{PO}_4$   
Adjust pH 7.2

PBS is used routinely for washing embryonic fibroblast and ES cell layers prior to trypsinization.

Trypsin – EDTA:

0.1% trypsin in 0.04% EDTA  
GIBCO BRL, Cat. No. 35400-019

For routine passaging of EMFIS and ES cells, they were disaggregated by using 0.1% trypsin dissolved in Tris-saline/EDTA. After adding the trypsin, the cells were placed in the incubator for 5 minutes.

Geneticin:

G418-Sulphate: 35mg in 100mg ES cell medium  
GIBCO BRL, Cat. No. 066-1811



Gancyclovir:

Gancyclovir -Sodium, Cymeven®

Stock solution: 5.1µl Gancyclovir in 1 ml PBS, stored at –20°C

**3.2.4.6 Expansion of positive clones**

After the positive clones were examined by PCR and Southern-blot, the corresponding frozen clones in 48-well feeder plates were thawed quickly with warm medium, and expanded progressively onto feeder cells in the order of 48-well plates, 24-well plates, 3.5 cm dishes and 6 cm-dishes. The cells on 3.5 cm feeder dishes were trypsinized and resuspended in 1 ml E14 freezing medium, then transferred into one 1 ml freezing vial (Nunc). The vials were immediate transferred to –20°C or –80°C freezer, stored at –80°C for a few days and transferred into liquid nitrogen.

**3.3 Plasmid isolation from *E. coli*.****3.3.1 Mini-prep DNA isolation**

To check if the isolated single colonies contained the correct plasmid, a mini-prep DNA isolation was carried out. 2 ml of cells from mini culture was centrifuged (4500 rpm/10 min /RT, Heraeus) and the pellet was resuspended in 300 µl of P1 + RNase A buffer. 300 µl of P2 buffer was added into each tube. After the addition of 300 µl of P3 buffer into the tube, the cellular debris was centrifuged (14000 rpm/40min/RT, Heraeus) and the supernatant of each preparation was precipitated with 2.5 volumes of absolute ethanol and 0.1 volumes of 3 M sodium acetate. After washing the DNA pellet with 70% ethanol, the DNA pellet was air-dried and resuspended in 50 µl TE buffer (pH 8.0).

Buffer P1 (Resuspension buffer):

50 mM	Tris-Hcl, pH 8.0
10 mM	EDTA, pH 8.0

P1+ RNase A:

100 µg / ml	RNase A
-------------	---------

Buffer P2 (Lysis buffer):

200 mM	NaOH
1%	SDS

Buffer P3 (Neutralization buffer):

2.55 M KOAc, pH 4.8
---------------------

RNase A stock solution:

10 mg / ml	RNase A
10 mM	Tris-Hcl, pH7.5
15 mM	NaCl

The solution was boiled for 15 min, cooled slowly at RT and then aliquoted.

### 3.3.2 Maxi-prep DNA with Qiagen Plasmid Maxi Kits

A single colony was picked from a freshly streaked selective plate and inoculated in 500 ml LB medium containing the appropriate selective antibiotic. The culture was incubated at 37°C overnight with vigorous shaking (200 rpm). On the next day, the bacterial cells were harvested by centrifugation at 4500 rpm for 15 min at 4°C. The bacterial pellet was resuspended in 10 ml of buffer P1. 10 ml of buffer P2 were added and mixed well but thoroughly by inverting the tubes 4-6 times. 10 ml of chilled buffer P3 was given to the cells and mixed gently by inverting 4-6 times and incubated on ice for 20 min. The suspension was centrifuged twice at 4500 rpm for 40 min and the supernatant containing the plasmid DNA was removed promptly to a fresh tube.

The Qiagen-Tip 500 column was equilibrated by applying 10 ml buffer QBT and allowing the column to empty by gravity flow. The supernatant was applied on the column and allowed to enter the resin by gravity flow. The column was washed twice with 30 ml buffer QC and eluted with 15 ml buffer QF. The DNA was precipitated by adding 10.5 ml (0.7 volumes) room-temperature isopropanol to the eluted DNA. The solution was mixed well and centrifuged at 4500 rpm for 20 min at room temperature. The DNA pellet was washed once with 70% ethanol and centrifuged at 4500 rpm for 10 min. The DNA pellet was air-dried for 5 min and re-dissolved in a suitable volume of TE.

#### Buffer QBT (Equilibration buffer):

750 mM	NaCl
50 mM	MOPS, pH 7.0
15%	isopropanol
0.15%	Triton X-100

#### Buffer QC (Wash buffer):

1M	NaCl
50 mM	MOPS, pH 7.0
15%	isopropanol

#### Buffer QF (Elution buffer):

1.25 M	NaCl
50 mM	MOPS, pH 8.5
15%	isopropanol

## 3.4 Analysis and enzymatic digestion of DNA

### 3.4.1 DNA purification through phenol extraction and ethanol precipitation

The DNA to be purified was dissolved in TE, treated twice with an equal volume of phenol/chloroform/isoamylalcohol (25:24:1) and finally with 1 vol. chloroform/isoamyl alcohol (24:1) to remove any remaining phenol in the watery phase. The upper TE phase was precipitated with 2.5 volumes of absolute ethanol and 0.1 volumes of 3 M sodium acetate (pH 5.2) at -80°C for 30-60 min. The pellet obtained after centrifugation at 14000 rpm for 20 min was air-dried and resuspended in 50 µl TE.

### 3.4.2 Measurement of DNA concentration

The concentration of a DNA solution in TE can be calculated through measuring DNA at OD<sub>260</sub>. TE was used as the blank value. DNA concentration was calculated according to the following formula:

$$1 \text{ OD}_{260} = 50 \mu\text{g} / \text{ml DNA.}$$

Concentration of oligonucleotides was measured at OD<sub>260</sub> and calculated as follows:

$$\epsilon_{260} (\text{A}) = 15.0$$

$$\epsilon_{260} (\text{G}) = 1.8$$

$$\epsilon_{260} (\text{C}) = 8.8$$

$$\epsilon_{260} (\text{T}) = 7.4$$

$$\Sigma\epsilon_{260} (\text{oligonucleotide}) = 1 \mu\text{mol}/\mu\text{l}$$

### 3.4.3 Agarose gel electrophoresis of DNA

1% agarose gel in TBE buffer was used to separate DNA. Agarose was suspended in TBE buffer and boiled in a microwave stove until the agarose was totally dissolved in the buffer.

0.5  $\mu\text{g}/\text{ml}$  ethidiumbromid was added to the agarose solution at about 60°C. The gel solution was poured into a appropriate gel form and left to cool and solidify. 6 x loading buffer was given to DNA dissolved in H<sub>2</sub>O or TE and the DNA was loaded on the gel. The gel was run at 5-10 V/cm (length of the gel) in TBE buffer. The separated DNA bands were visible at a wavelength of 366 nm because of the inlay of ethidiumbromid into DNA.

#### TBE-buffer:

89 mM

89 mM

2 mM

Tris base

boric acid

EDTA

#### 6 x loading buffer:

10 mM

50 mM

10%

10%

0.01%

Tris-HCl, pH 8.0

EDTA, pH 8.0

ficoll

glycerol

bromophenol blue

### 3.4.4 Elution of DNA from agarose gel

#### 3.4.4.1 *Electro-elution of DNA*

Large amounts of DNA were purified from agarose gel by electro-elution. The apparatus used for electro-elution from Colora consists of 2 separate chambers connected with a special connector, which had two pieces of dialysis membranes on its both ends. The two chambers and the connector were filled with 1 x TBE buffer. An agarose gel slice was placed in the one end of the connector. Due to the electricity field between the two chambers the DNA ran to

another end of the connector, where DNA was collected and could be pipetted out. DNA was then precipitated and dissolved in suitable volume of TE.

#### **3.4.4.2 Elution of DNA with QIAquick Gel Extraction Kit**

The DNA fragment was excised from the agarose gel with a clean, sharp scalpel. The gel slice was weighed in a colorless tube and 3 volumes of buffer QG were added to 1 volume of gel (100 mg ~ 100 µl). The tube was incubated at 50°C for 10 min (or until the gel slice was completely dissolved). The gel was dissolved by vortexing the tube every 2 – 3 min during the incubation (After the gel slice has dissolved completely, the color of the mixture should be yellow). 1 volume of isopropanol was added and the tube was mixed well. A QIAquick spin column was placed in a provided 2-ml collection tube. The sample was applied to the column to let DNA bind to it and centrifuged for 1 min (3000 rpm). The flow-through was discarded and the column was placed on the same tube again. To wash the column, 0.75 ml of buffer PE was added and the column in tube was centrifuged for 1 min. The flow-through was discarded and the column was centrifuged for an additional 1 min. The column was then placed in a clean 1.5-ml tube. 50 µl of elution buffer EB (10 mM Tris-HCl, pH 8.5) or H<sub>2</sub>O was added to the center of column and the column was centrifuged for 1 min at maximum speed. Alternatively, for high DNA concentration, 30 µl of elution buffer was added to the center of the column and the column was centrifuged at maximum speed for 1 min.

#### **3.4.5 Sequencing double-stranded DNA**

Double-stranded DNA was sequenced by “thermo Sequenase Radiolabeled Terminator Cycle Sequencing Kit”(Usb), which is based on the principle that chain stops due to the addition of dideoxynucleotide during chain elongation from DNA-polymerase I.

a) Termination mixes: The termination mixes were prepared on ice. 2 µl of nucleotide master mix and 0.5 µl of [ $\alpha$ -<sup>33</sup>P] ddNTP (G, A, T, or C, one of each per sequence) were mixed to produce a termination mix for each ddNTP. Four tubes (G, A, T, and C) with 2.5 µl of each termination mix were labeled, filled and capped.

b) Reaction mixture: For multiple reactions with different primers and/or templates, a n+1 batch of reaction buffer, water and polymerase were prepared and aliquoted; Then the unique primer and the template in the appropriate concentration and volume were added to the aliquotes.

c) Cycling termination reactions

4.5 µl of reaction mixture was transferred to each termination tube (G, A, T, and C) from step (a) and mixed well. The mixture was overlaid with 10-20 µl of mineral oil (if need). The tube was placed in a thermal cycling instrument.

d) Cycling programm: The specific cycling parameters depend on the primer sequence and the amount and purity of the template DNA. Normally, 25-250 fmol of primer were used, and the reaction runs 36 cycles as follows:

95°C/30 s  
55°C/30 s  
72°C/60-120 s

x 36 cycles

e) Termination of the reactions: 4 µl of stop solution was added to each of the reactions and mixed well. The samples were kept on ice until they were loaded onto a gel.

f) Loading of the gel: Before loading, the samples have to be denatured at 70°C for 2-10 min. 3.0-5.0 µl of each sample was immediately loaded on the gel.

### **3.4.6 Polyacrylamid sequence gel electrophoresis**

#### **3.4.6.1 Gel preparation**

Glass plates must be clean and free of dried gel and soap residues. To remove residues, both plates were cleaned with ethanol. To ensure that the gel will not stick to the glass plates they were coated with Gel Slick or silicone. Glass plates were assembled with two 0.2 mm-spacers on the sequencing apparatus (Electrophoresis Sequencing System, Model S2). A 5% Long Ranger gel mixture was prepared:

##### 5% Long Ranger gel mixture:

10 ml	Long Ranger™ gel solution (FMC)
10 ml	10 x TBE
36 g	urea
52 ml	H <sub>2</sub> O

The solution was mixed well and then filtered through a 0.45 µm Membrane filter (Millipore™). 600 µl of APS and 60 µl of TEMED were added to the mixture and mixed well. The solution was poured between the plates of the gel apparatus and a comb was inserted between the plates. The gel was left to polymerize for 2 hrs. The comb was removed and the wells and top surface were rinsed with TBE buffer. The gel cassette was mounted onto the sequencing apparatus.

### 3.4.6.2 Electrophoresis

The anodal and cathodal chambers were filled with 1 x TBE buffer. The gel was pre-run at about 45 mA/80 Watt until it reached a temperature of 50°C. The comb was inserted between the plates and the samples were loaded onto the gel. The run time was monitored with the marker dyes bromophenol blue and xylene cyanol. After the run was finished, the sequencing apparatus was disconnected and the gel was transferred onto a Whatman 3 MM filter paper. The gel was dried and exposed to an X-ray film.

### 3.4.7 Restriction endonuclease digestion

Purified DNA was digested by restriction enzymes with their corresponding buffers. If necessary, BSA was added to the digestion. The digest was incubated at 37°C for 1-2 hrs and loaded onto an agarose gel after adding 6 x loading buffer.

### 3.4.8 Fill in of 5' overhanging ends with Klenow DNA-polymerase

5'-overhanging ends of DNA fragment can be filled in by Klenow fragment (big fragment of *E. coli* DNA polymerase) to generate blunt ends. After treatment, a 5'-overhanging DNA fragment can be cloned into a vector or labeled radioactively at the 5' end.

DNA was incubated with 20 – 40 µM desoxynucleotidtriphosphats (pH 7.0) with 1-5 units of Klenow fragment for 1 h at room temperature. The reaction was stopped by heating the mixture at 65°C for 15 min. Excessive dNTP should be given in the reaction to inhibit exonuclease activity of the Klenow DNA-polymerase.

### 3.4.9 Generation of blunt ends with T4 DNA-polymerase

5'- and 3'-overhanging ends of DNA can be treated with T4 polymerase to generate blunt ends due to its 5'-3' DNA-polymerase activity and 3'-5' exonuclease activity.

1 µg DNA was incubated with 1 U T4 DNA-polymerase, 1 x T4 DNA-polymerase buffer and 50 µM dNTPs in 20 µl for 1 hr at 37°C. The reaction was stopped by heating at 65°C for 15 min.

#### 5 x T4-buffer:

250 mM	Tris-Hcl, pH 8.8
75 mM	(NH <sub>4</sub> ) <sub>2</sub> SO <sub>4</sub>
35 mM	MgCl <sub>2</sub>
0.1 mM	EDTA
50 mM	β-mercaptoethanol

### 3.4.10 Dephosphorylation of DNA with alkaline phosphatase

The restriction-cloning vector was dephosphorylated (Maniatis, 1982) with calf intestinal alkaline phosphatase (CIP; Boehringer-Mannheim). 10 µg linearized plasmid DNA was dissolved in 90 µl 50 mM Tris-HCl (pH 8.0) and incubated with CIP (0.1 units/µg) for 1 hr at 37°C. Afterwards 1.0 µl of 0.5 M EDTA was added and the reaction was inactivated at 75°C for 10 min. The dephosphorylated DNA was then purified from agarose gel (3.4.4).

#### 10 x CIP buffer:

10 mM	ZnCl <sub>2</sub>
10 mM	MgCl <sub>2</sub>
100 mM	Tris-HCl, pH 8.0

## 3.5 Isolation of genomic DNA and enzymatic digestion

### 3.5.1 Preparation of genomic DNA from 48-well plates and enzymatic digestion

Genomic DNA from mice ES cells was isolated from 48-well plates directly (Ramirez-Solis *et al.*, 1992). The ES cells were allowed to grow on gelatin-coated plates until the medium turned yellow. When the cells were ready for DNA extraction procedure, the wells were rinsed with cold PBS and 100 µl lysis buffer were added to per well. The plate was incubated overnight at 50°C in a humid atmosphere. This was easily achieved by incubating the plate inside a closed Tupperware container with paper towels in a convenient 50°C oven. The next day, the plate was shortly centrifuged at 2500 rpm. For DNA precipitation, 200 µl of NaCl/ethanol mix (150 µl of 5M NaCl to 10 ml of cold absolute ethanol) was added to every well using a multichannel pipette. The 48-well plate was shook for 30 min at room temperature. During this time, the nucleic acids precipitated as a filamentous network. The plate was centrifuged again and carefully inverted to discard the solution while the nucleic acids remained attached to the plate. The plate was rinsed 3 times by rinsing each well with 300 µl of 70% ethanol using a multichannel pipette. The plate was shortly centrifuged and the ethanol was discarded by inversion. After the final wash, the plate was inverted and allowed to dry on the bench. 50 µl of TE were added to each well. The plate was incubated at 37°C overnight to let the genomic DNA dissolve well.

25 µl of genomic DNA was digested with a restriction enzyme the next day. A restriction digestion mix was prepared as follows: 1 x restriction buffer, 100 µg/ml RNase and 50 units of restriction enzyme. 25 µl of the mixture were added to 25 µl DNA and mixed well. The digestion reaction was incubated at 37°C overnight.

**Lysis-buffer:**

10 mM	Tris-HCl, pH 7.5
10 mM	EDTA, pH 8.0
10 mM	NaCl
0.5%	Sacrosyl
1 mg/ml	Proteinase K (add prior to use)

**3.5.2 Isolation of genomic DNA from a 10 cm-dish**

A big amount of genomic DNA from mammalian cells was isolated with Easy-DNA™ Kit (Invitrogen).

$10^3$  to  $10^7$  of cells were pelleted and resuspended in 200  $\mu$ l 1 x PBS. 350  $\mu$ l Solution A was added to the cell suspension, vortexed in second intervals until it evenly dispersed, and then incubated at 65°C for 10 min. 150  $\mu$ l Solution B were added and vortexed vigorously until the precipitate moved freely in the tube, and the sample was uniformly viscous (10 sec to 1 min).

500  $\mu$ l chloroform was added and vortexed until viscosity decreases and the mixture is homogeneous (10 sec to 1 min). The tube was centrifuged at maximum speed for 10-20 min at 4°C to separate phases and form the interface. The upper phase was transferred into a fresh microcentrifuge tube. 1 ml of 100% ethanol (-20°C) was added to the DNA solution and vortexed briefly. The tube was incubated on ice for 30 min and then centrifuged at maximum speed for 10-15 min. The ethanol was removed from the pellet with a drawn-out Pasteur pipette. The DNA pellet was washed with 80% ethanol and centrifuged once more at the maximum speed. The DNA pellet was air-dried and resuspended in 100  $\mu$ l TE. 2  $\mu$ l of RNase (2 mg/ml) was added and the DNA was incubated at 65°C for 30 min.

30  $\mu$ l of genomic DNA was digested with restriction enzyme overnight at 37°C as described in 3.4.7.

**3.5.3 Isolation of genomic DNA from mice tails**

Genomic DNA of mouse tails was isolated according to the protocol from Laird (Laird *et al.*, 1991).

500  $\mu$ l of lysis buffer was added into a tube containing a mouse tail, which was cut by a sterile scalpel to about 2 mm length. The tube was incubated with rocking at 55°C for at least 3 hrs or overnight. The tube was then centrifuged at maximum speed for 30 min. The supernatant was transferred carefully to a prelabeled tube containing 0.5 ml isopropanol and mixed well by inversion until DNA precipitation was completed. The sample was centrifuged at maximum speed for 15 min at room temperature and washed with 80% ethanol. The DNA pellet was dissolved in 60  $\mu$ l TE. Complete dissolution of DNA may require several hours of



agitation at 37°C or 55°C. It is important that the DNA is completely dissolved to ensure the reproducible removal of aliquots for analysis.

30 µl of genomic DNA were digested with restriction enzyme overnight at 37°C as described in 3.4.7.

Lysis buffer:

100 mM	Tris-Hcl, pH 8.5
5 mM	EDTA, pH 8.0
0.2%	SDS
200 mM	NaCl
100 µg/ml	Proteinase K (add right before use)

### **3.5.4 A quick method for the isolation of unpurified genomic DNA from ES cells for PCR**

Direct lysis of ES cells on from 48-well plates with Kawasaki buffer (Kawasaki, 1990) simplifies the genomic DNA purification process. Genomic DNA gained by this method can be directly used in PCR, but is not suitable for a Southern-blot.

ES cells on 48-well plate were rinsed twice with 1 x PBS. 80 µl of Kawasaki buffer and 10 µl of 1 mg/ml Proteinase K were added to per well. The plate was incubated at 60°C for 1 hr in a humid atmosphere and further incubated at 95°C for 20 min to inactive Proteinase K. The plate was centrifuged at 1200 rpm for 5 min to spin down the cell debris. The gomic DNA in the supernatant was used directly for PCR.

Kawasaki buffer:

20 mM	Tris-Hcl, pH 8.3
1.5 mM	MgCl <sub>2</sub>
25 mM	KCl
0.5%	Tween

## **3.6 Amplification of DNA-fragments by Polymerase chain reaction (PCR)**

### **3.6.1 Screening positive homologous recombined ES cell clones by PCR**

PCR with plasmid DNA, with purified genomic DNA from ES cells (3.5.1 and 3.5.2) or mice tails (3.5.3) and unpurified genomic DNA from ES cells (3.5.4) were performed with Biotag DNA polymerase (10 Units/µl) and corresponding buffer. Biotag DNA Polymerase is a 94 kDa heat-stable DNA Polymerase purified from *Thermus aquaticus* and is especially suitable for GC-rich PCR. For ES cells clone screening, primers P11M1 and Neo-primer (primer pair

1) were used. As a control PCR, P11M2 and Neo-primer (primer pair 2) were used to amplify a relative longer PCR product compared to the first primer pair.

20 ng of plasmid DNA, 100 ng purified genomic DNA (3.5.1, 3.5.2 and 3.5.3) or 2.0 µl of unpurified genomic DNA (3.5.4) were mixed with 4 pmol primers, 2.0 µl of 10 x reaction buffer, 0.05 mM dNTP, 2.5 mM MgCl<sub>2</sub>, ddH<sub>2</sub>O and 1 Unit of diluted Biotag DNA polymerase to an end volume of 20 µl. The PCR machine was prewarmed to 96°C and the PCR tubes were placed into the machine. The PCR was performed as followed:

96°C / 5min	1 cycle
96°C / 1min, 56°C / 1min, 72°C / 1 min 30 sec	36 cycles
72°C / 10min	1 cycle
4°C / ∞	

PCR products were analyzed by electrophoresis on a 1% agarose gel. If no specific bands could be seen, the gel was blotted and hybridized with a specific radioactively labeled probe.

Biotag-Dilution buffer:

20 mM	Tris-Hcl, pH 8.0
0.1 mM	EDTA, pH 8.0
100 mM	KCl
1 mM	DTT
0.5% (v/v)	Tween
0.5% (v/v)	NP40
50% (v/v)	glycerol

10 x reaction buffer:

677 mM	Tris-HCl, pH 8.8
166 mM	(NH <sub>4</sub> ) <sub>2</sub> SO <sub>4</sub>
0.1%	Tween 20

### 3.6.2 Amplification of Pura cDNA fragments of different length by PCR

Purα-cDNA fragments of different length were amplified by PCR. pcDNA3-Purα.ext plasmid containing full-length Purα cDNA was used as a template in PCR.

PCR reaction:

pcDNA3-Purα.ext plasmid	60 ng
10 µM Primer 1	2.0 µl
10 µM Primer 2	2.0 µl
4 mM dNTPs	2.5 µl
10 x Pwo-buffer (with Mg <sup>2+</sup> )	5.0 µl
25 Units Pwo	0.5 µl
Add H <sub>2</sub> O to 50 µl	

The PCR was performed as follows:

94°C / 5min	1 cycle
94°C / 1min, 50-54°C / 1min, 72°C / 1 min 40 sec	36 cycles
72°C / 10min	1 cycle
4°C / ∞	

Annealing temperature should be changed according to different primers.

### 3.6.3 Amplification of homologous arms for the target vector

Expand<sup>TM</sup> Long Template PCR System (Rosch) was used to amplify homologous arms of the targeting vector. Expand<sup>TM</sup> Long Template PCR System is composed of an unique enzyme mix containing thermostable Taq and Pwo DNA polymerases. This powerful polymerase mixture is designed to give a high yield of PCR products from episomal and genomic DNA. It amplifies fragments from human genomic DNA of up to 27 kb.

Genomic DNA of murine E14K ES cells was used as a template for this amplification.

#### PCR reaction:

E14K genomic DNA		100 ng
50 μM Primer 1	2.0 μl	
50 μM Primer 2	2.0 μl	
4 mM dNTPs		4.4 μl
10 X buffer (with 1.75 mM Mg <sup>2+</sup> )		5.0 μl
Enzymes mix		0.75 μl
Add H <sub>2</sub> O to 50 μl total volume		

The PCR was performed as follows: Annealing temperature should be changed according to different primers.

94°C / 2min	1 cycle
94°C / 15 sec, 47°C / 30 sec, 72°C / 1 min 30 sec	10 cycles
94°C / 15 sec, 47°C / 30 sec, 72°C / 1 min 30 sec (cycle elongation for more yield of 20 sec for each cycle)	20 cycles
72°C / 7min	1 cycle
4°C / ∞	

## 3.7 Radioactive labeling of DNA

### 3.7.1 5' end labeling with T4-polynucleotide kinase

T4 polynucleotide kinase catalyzed the transfer of terminal phosphate of ATP ( $\gamma$ ) to the 5'-hydroxyltermini of DNA and RNA. This reaction is very efficient; hence it is the general method for labeling 5' ends or phosphorylating oligonucleotides.

2-10 pmol of oligonucleotides was incubated with 10-50  $\mu\text{Ci}$  (3.3 to 16.5 pmol)  $[\gamma\text{-}^{32}\text{P}]\text{-ATP}$ , 1U T4 polynucleotidkinase and 10 x kinase-buffer for 1hr at 37°C. The labeled oligonucleotide was separated from unincorporated  $[\gamma\text{-}^{32}\text{P}]\text{-dATP}$  through a Sephadex G-50 column.

Kinase-buffer:

50 mM	Tris-HCl, pH 8.0
10 mM	DTT
20 mM	MgCl <sub>2</sub>
0.2 mM	spermidin
0.2 mM	EDTA

### 3.7.2 DNA labeling with Random prime kit

25 ng DNA was diluted with H<sub>2</sub>O to an end volume of 23  $\mu\text{l}$  and denatured by heating at 95°C for 5 min, then chilled rapidly in an ice bad. 15  $\mu\text{l}$  of random-primers-buffer was added into the tube and mixed well. Subsequently, 2  $\mu\text{l}$  dCTP, 2  $\mu\text{l}$  dGTP and 2  $\mu\text{l}$  dTTP were given to the mixture. At the end, 5  $\mu\text{l}$  (50  $\mu\text{Ci}$ )  $[\alpha\text{-}^{32}\text{P}]\text{-dATP}$  and 3 Units of Klenow-fragment were added. The mixture was incubated for 1 hr at 25°C and stopped by adding 5  $\mu\text{l}$  0.5 M EDTA. The labeled DNA was purified through a Sephadex G-50 column.

### 3.7.3 Removal of unincorporated dNTPs with a Sephadex G- 50 column

A small glass ball was placed on the bottom of a Pasteur pipette. The sephadex G-50 resin suspended in TE was filled onto this pipette and enough space of about 200  $\mu\text{l}$  was left for the the loading of the radioactively labeled DNA sample. The column was washed with 5 volumes of TE, loaded with the radioactive sample and eluted with TE. Unincorporated dNTPs bind to the column whereas labeled DNA can be found in the flow-through.

## 3.8 Southern-blot analysis

Southern-blotting is the transfer of DNA fragments from an electrophoresis gel to a membrane. The transfer results in immobilization of the DNA fragments, therefore the membrane carries a semi-permanent reproduction of the banding pattern of the gel. After immobilization, the DNA can be subjected to hybridization analysis, enabling the identification of bands with sequence similarity to a labeled probe.

### 3.8.1 Transfer of DNA on Nylon- or Nitrocellulose membrane

Hybond N<sup>+</sup>-membrane, a positively charged nylon membrane, is ideally used for hybridization.

The agarose gel was rinsed in distilled water and placed in a clean glass dish containing 10 gel volumes of 0.25 M HCl where it was shaken slowly for 6 min at room temperature. HCl was discarded and the gel was rinsed with distilled water. The gel was then shaken in 10 volumes of 0.4 M NaOH for 40 min to denature the DNA.

A sponge, with a size slightly larger than the gel, was placed in a plastic dish. The dish was filled with enough 0.4 M NaOH to leave the soaked sponge about half-submerged in buffer. Three pieces Whatman paper were cut and placed on the sponge. The gel was transferred onto the Whatman paper and air bubbles were squeezed out by rolling a glass pipet over the surface. A piece of Hybond N<sup>+</sup>-membrane was placed on the gel and 3 pieces of Whatman papers were put on the membrane. It was confirmed that there were no air bubbles between the membrane and the gel. Paper towels were piled up on Whatman papers and a glass plate on top of the pile. A weight was placed on the top to hold everything in place. It was left overnight, disassembled and the membrane was rinsed with 2 x SSC the next day.

### 3.8.2 Hybridization of oligonucleotides

The protocol from Woods *et al* (1982) was slightly changed as following:

The membrane was prehybridized overnight at 42°C with pre-hybridization-buffer containing 100 µg/ml yeast-tRNA to inhibit unspecific binding of the oligonucleotides onto the membrane. According to different container used for hybridization, variable amounts of pre-hybridization-buffer were used. After prehybridization, an appropriate quantity of hybridization solution with 100 µg/ml yeast-tRNA was added into the container. 2-10 µl radioactive labeled oligonucleotides were given into the hybridization tube and hybridization was performed overnight at 42°C.

The membrane was washed with 6 x SSC + 0.05% Na<sub>4</sub>P<sub>2</sub>O<sub>7</sub>, twice to three times at room temperature and then twice at 45°C. The wash process is variable according to different situations. The blot was covered with plastic wrap immediately.

The membrane was placed on a Phosphor Image Screen, which was scanned by Phosphor Image.

#### Pre-hybridization-buffer:

6 x	SSC
5 x	Denhardt-solution
0.05%	Na <sub>4</sub> P <sub>2</sub> O <sub>7</sub>
0.5%	SDS
100 µl /ml	yeast-tRNA (addition before use)

Hybridization-buffer:

6 x	SSC
5 x	Denhardt-solution
0.05%	Na <sub>4</sub> P <sub>2</sub> O <sub>7</sub>
100 µl /ml	yeast-tRNA (addition before us )

20 x SSC:

3 M	NaCl
0.3 M	Sodium citrate, pH 7.2

100 x Denhardt-solution:

10 g	Ficoll 400
10 g	Polyvinylpyrrolidon
10 g	BSA
add 50 ml H <sub>2</sub> O bidest.	

### 3.8.3 Hybridization with Church solution

According to Church and Gilbert 's protocol (1984), the membrane was hybridized with 10 ml hybridization buffer at 65°C for 1 h. An appropriate amount of the radioactive DNA-fragment was denatured by heating at 95°C for 5 min, chilled on ice, added to 10 ml of fresh hybridization buffer, and mixed well. The fresh hybridization buffer containing the DNA probe was given onto the membrane and hybridized at 65°C overnight.

The membrane was washed with low-stringency-buffer at 65°C for 5-10 min, then with high-stringency-buffer for several times at 65°C. The blot was covered with plastic wrap immediately.

The membrane was placed on a Phosphor Image Screen, which was scanned by Phosphor Image.

Hybridization-buffer:

1 mM	EDTA
0.5 mM	NaHPO <sub>4</sub> , pH 7.2
1%	BSA, crystal
7%	SDS

Low-stringency-buffer:

1 mM	EDTA
40 mM	NaHPO <sub>4</sub> , pH 7.2
0.5%	BSA, crystal
5%	SDS

High-stringency-buffer:

1 mM	EDTA
40 mM	NaHPO <sub>4</sub> , pH 7.2
1%	SDS

### 3.8.4 Hybridization with ExpressHyb™ Hybridization Solution

A specific single copy gene was detected in Southern-blot with ExpressHyb™ Hybridization Solution (Clontech) because of its high sensitivity and low background.

ExpressHyb™ Hybridization Solution was pre-warmed and stirred well at 60°C to be completely dissolved. A 10 x 10-cm membrane was prehybridized in a total volume of minimal 5 ml of ExpressHyb™ Hybridization Solution with continuous shaking at 60°C for 30 min. The radioactively labeled DNA probe was denatured at 95-100°C for 2-5 min and chilled on ice. The recommended radioactive labeled probe concentration is 2-10 ng/ml or 1-2 x 10<sup>6</sup> cpm/ml. The radioactively labeled probe was added to 5 ml ExpressHyb and mixed well. Replace the ExpressHyb Solution with the fresh solution containing the radiolabeled DNA probe. Be sure that all of the air bubbles were removed from the container and the ExpressHyb solution was evenly distributed over the entire blot. The hybridization was performed with shaking at 60°C for 1 hr.

The blot was rinsed several times in wash solution 1 at room temperature, while washing for 30-40 min with continuous agitation and replacing the wash solution several times. Thereafter, the blot was washed in wash solution 2 with continuous shaking at 50°C for 40 min with one change of fresh solution. The blot was covered with plastic wrap immediately.

The membrane was placed on a Phosphor Image Screen, which was scanned by Phosphor Image.

<u>Wash-solution 1:</u>		<u>Wash-solution 2:</u>	
2 x	SSC	0.1 x	SSC
0.05%	SDS	0.1%	SDS

### 3.8.5 Removing the radiolabeled DNA probe from the blot

To re-hybridize a blot with other DNA probes, the radiolabeled DNA on the blot can be removed from the blot as follows:

A hybridization tube was fully filled with 0.1 x SSC/0.1% SDS solution and heated to 90-100°C. The plastic wrap was removed from the blot and immediately placed in the heated solution without exposure to air. The solution containing the blot was shaken and incubated for 10 min at 95°C. The solution was discarded and the blot was slipped into a plastic bag and stored at -20°C until further use.

### 3.9 Screening recombinant DNA libraries

A 129/SvJ mouse genomic DNA bank in lambda phage was screened. The titer of this bank is about  $10^8$  pfu/ml. The bacteria strain for lambda phage is XLI Blue/MRA/P2.

#### 3.9.1 Preparation of phage competent bacteria

A single colony of bacteria was inoculated into 20 ml TYM, and the suspension was incubated at 37°C with moderate shaking (200 rpm). 5 ml of the culture was inoculated into 100 ml TYM and left to grow to an  $OD_{600} = 0.6$  to 0.8. The bacterial cells were centrifuged at 3500 rpm and the cell pellet was resuspended in sterile SM solution (to an end concentration of  $10^{10}$  bacteria/ml). 1 OD corresponded to  $8 \times 10^8$  bacteria/ml. After storage at 4°C for 2 hrs, the bacteria cells were ready to be infected with the phages. The further usage of these cells depends on the different strain of phage competent bacterial cells: XLI Blue should be used in the same day whereas K803 and LE392 could be stored at 4°C for up to 1 week.

#### NZCYM:

0.5%	NaCl
0.2%	MgSO <sub>4</sub>
0.5%	Yeast extract
1.0%	NZ Amin
0.1%	Casamino acid
adjust to pH 7.5	

#### λ-Dilution:

50 mM	Tris-Hcl, pH 7.5
100 mM	NaCl
10 mM	MgSO <sub>4</sub>

#### SM solution:

0.1%	Gelatine in λ- Dilution
------	-------------------------

#### 3.9.2 Titration of recombinant λ-phage

Phage stock solution or lysate were serially diluted ( $10^{-2}$ - $10^{-8}$ ) with λ-Dilution solution. 10 μl of the diluted phage were added to 100 μl of prepared bacteria cells ( $1 \times 10^{10}$  / ml). The phages were incubated with the bacteria at 37°C for 20 min. 8 ml of molten top agar were given to the suspension, mixed by inverting quickly and poured onto LB plates pre-warmed to 37°C. The top agar was allowed to harden and the plates were then incubated inverted at 37°C overnight.

The number of the plaques was counted on the next day and the titer of the phage was calculated.



Top agar:

0.5%	NaCl
0.2%	MgSO <sub>4</sub>
0.5%	Yeast extract
1.0%	NZ Amin
0.1%	Casamino acid
1.5%	Bacto-agar
adjust to pH 7.5	

### 3.9.3 Absorption of phages into host bacteria

Bacteriophages were plated onto agar plates at high density for the screening of 1 million different plaques. The bacteriophage plaques were then transferred to nitrocellulose- or Hybond-filters, denatured, and baked. The filters were then hybridized with a specific radiolabeled DNA probe.

$5 \times 10^4$  pfu were added to 100  $\mu$ l of prepared bacteria cells ( $1 \times 10^{10}$ /ml). The phages were incubated with bacteria at 37°C for 20 min. 8 ml of molten top agar were given, mixed by inverting quickly and poured onto LB plates pre-warmed to 37°C. 12 plates were generated. 8 ml of molten top agar was given to the suspension, mixed by inverting quickly and poured onto LB plates pre-warmed to 37°C. The top agar was allowed to harden and the plates were then incubated inverted at 37°C overnight.

### 3.9.4 Phage blotting and identification of positive phages

The 12 plates generated were incubated at 4°C for at least 2 hrs prior to the application of the filters. Two pieces of Hybond N<sup>+</sup> membranes (Amersham Pharmacia Biotech, UK) were prepared for each plate. The membranes were labeled with a ballpoint pen and applied face down (ink side up) on cold plates bearing bacteriophage plaques without air bubbles between the membrane and the plate. The membranes were left on the plates for 1 min to allow the transfer of phage particles onto the membranes. During the transfer period the orientation of the membrane to the plate was recorded by stabbing a needle through the filter into the agar at several asymmetric points around the edge of the plate. The second membrane was placed onto the plate for another blotting of 2 min. Remove the membrane slowly from the plates with blunt, flat forceps and transfer them into denature buffer. After 2 min, they were transferred into neutral buffer for 5 min. The membranes were shortly washed in 6 x SSC and then placed face up on Whatman paper to dry on air. Finally, the membranes were baked at 80°C for 4 hrs to fix the DNA.

The membranes were followed hybridized with a DNA probe with Church solution according to 3.8.3. A film was placed on every membrane and developed after storage at -80°C overnight.

### **3.9.5 Screening phage library for Pura genomic DNA**

Phage plates were correctly oriented to the autograph film to identify positive plaques. The plaques which showed positive signals on both membranes from the same plate were considered to be the plaques of interest. A plug of agarose (about 0.5 cm<sup>2</sup>) was picked from the primary plate, placed in Eppendorf tubes containing 300 µl of λ-Dilution. This solution was incubated for 3 hrs at room temperature with gentle shaking. A secondary phage library was plated with this solution. The plaques on the secondary plates were transferred onto nitrocellulose filters and hybridized with the same DNA probe. An isolated positive plaque was picked, placed in Eppendorf tubes containing 300 µl of λ-Dilution. With this solution a third phage library was generated. This process was repeated until the desired single plaque was purified.

The secondary and following screenings were carried out as the primary screening, with the difference that more diluted phages were plated out, and smaller surrounding areas of positive plaques were picked up from the original plates each time. Generally, 3-4 rounds of screening were required for the isolation of the identical phages.

### **3.9.6 Purification of λ-phage DNA**

#### ***3.9.6.1 Liquid lysate of λ-phage***

A single phage plaque was picked from an agar plate and transferred into a tube containing 500 µl of SM solution. The tube was placed at 4°C overnight. 100 µl of competent bacterial cells and 10-20 µl of phage plaque elute were inoculated in 50 ml NZCYM medium and incubated at 37°C for 8-10 hrs until the bacterial cells were totally lysed. 5 ml of chloroform was given to the culture. After centrifugation at 4500 rpm for 15 min, the supernatant including the phages was transferred into a new sterile tube. To this phage lysate, 30 µl of DNase (10 mg/ml) and 30 µl of RNase (10 mg/ml) were added and incubated at 37°C for at least 2 hrs or overnight. The phage lysate was centrifuged at 28000 rpm (SW 28 Rotor) at 4°C for at least 2 hrs. Phage DNA was isolated from the phage pellet.

#### ***3.9.6.2 Isolation of λ-phage DNA***

The bacteriophage pellet was resuspended in 700 µl of TE, 150 µl of 1 M NaCl, 100 µl of 10% SDS and 50 µl of Proteinase K (10mg/ml). The suspension was incubated at 55°C for at least 2 hrs or overnight.

1 ml of Phenol/TE was added, mixed and incubated at 55°C for 15 min with gentle shaking. The emulsion was transferred into a new tube and centrifuged at 1400 rpm for 5 min at room

temperature. The supernatant was treated with an equal volume of phenol/chloroform/isoamyl alcohol (25:24:1) twice and then with 1 volume of chloroform/isoamyl alcohol (24:1) to remove the remaining phenol in the watery phase. The upper phase was precipitated with 1 volume of isopropanol and 70  $\mu$ l of 3 M sodium acetate, pH 5.2 at  $-20^{\circ}\text{C}$  for 30 min. The pellet obtained after centrifugation at 14000 rpm for 20 min at room temperature, was washed, air-dried, and resuspended in 50-100  $\mu$ l TE.

### **3.10 Analysis of proteins**

#### **3.10.1 Preparation of cellular protein extracts from mammalian cells**

Cellular extracts from NIH3T3 and 293 cells were prepared. Approximately  $1 \times 10^6$  cells were resuspended in 500  $\mu$ l lysis buffer and lysed on ice for 30 min. The lysates were cleared by centrifugation. The protein concentration of the supernatant was determined using the Bio-Rad reagent.

##### Lysis buffer:

50 mM	Hepes, pH 7.9
1 mM	DTT
400 mM	NaCl
1 mM	EDTA
0.5%	NP40
10%	glycerol
1 mM	PMSF
1:1000	Aprotinin (10 $\mu\text{g}/\mu\text{l}$ )
1:500	Leupeptin

#### **3.10.2 Measurement of Protein concentration by Bradford assay**

Protein quantitation was performed by using the Bradford (Bradford, 1976) reagent supplied by Bio-rad. 1  $\mu$ l of protein sample was mixed with water and analyzed in a final volume of 800  $\mu$ l. 200  $\mu$ l of Bradford reagent was added and the solution was gently mixed and left at room temperature for 5 min to allow color development. The protein concentration in the samples was measured by spectrophotometry at  $A_{595}$ .  $\text{H}_2\text{O}$  was used as a standard and BSA was used for a calibrate-curve.

##### Bradford reagent:

0.01%	Coomasie Brilliant Blue G 250
8.5%	phosphoric acid
5%	methanol

### 3.10.3 Preparation of protein extracts from mice tissues and measurement of protein concentration

#### 1) Extraction of proteins from tissues

Tissue samples stored at - 80°C were weighed, placed in 5 ml plastic tubes and homogenized in protein extraction buffer with a tissue homogenizer for 1 min. 500 µl of extraction buffer was added to each 20 mg tissue. The homogenizer was washed with PBS after each sample.

#### Protein extraction buffer:

20 mM	Tris-HCl, pH 7.5
1%	Triton X-100
1 x	laemmli buffer

The samples were stored on ice, transferred to 1.5 ml centrifuge tubes and centrifuged at 12000 rpm at 4°C for 5 min. An aliquot was removed for the determination of protein concentration and samples were stored at - 20°C.

#### 2) Determination of protein concentration

The protein content in the samples was estimated by the bicinchoninic acid (BCA) protein assay. A set of protein standards of known concentrations was prepared by serially diluting a bovine serum albumin (BSA) stock solution (4 mg/ml) in PBS. 50 µl of the standards and of the samples of unknown concentration (diluted 1:10 in PBS) were pipetted into 96-well plates and 200 µl of a mixture of BCA and 4% CuSO<sub>4</sub> (50:1) were added to each well and mixed. The plate was incubated at 37°C for 30 min and the absorbance was measured at 562 nm. A standard curve was prepared by plotting the absorbance of the standards versus protein concentrations. The protein concentration of the samples was determined using the standard curve.

### 3.10.4 SDS-polyacrylamid gel eletrophoresis (SDS-Page)

This gel system uses the method described by Laemmli (1970). In this technique, the protein sample is denatured and coated with detergent by heating in the presence of SDS and a reducing agent. The SDS coating gives the protein a high net negative charge that is proportional to the length of the polypeptide chain. The sample is loaded on a polyacrylamid gel and high voltage is applied, causing the protein components to migrate toward the positive electrode (anode). Since all of the proteins have a net negative charge that is in proportion to

their size, the proteins are separated solely on the basis of their molecular mass, a result of sieving effect of the gel matrix. The molecular mass of the protein can be estimated by comparing the mobility of a band with protein standards. Shape banding of the protein components is achieved by using a discontinuous gel system, which is composed of stacking and separating gel layers that differ in either salt concentration or pH or both.

Resolving and stacking mini-gel solutions for the preparation of two 7 x 10 cm gels with a thickness of about 0.75-1.00 mm were prepared. 10% ammonium persulfate (APS) and TEMED were added just prior to pouring the gel. The resolving gel mix was poured into assembled gel plates, leaving sufficient space at the top for the stacking gel to be added later. The gel mix was gently overlaid with isopropanol and the gel was allowed to polymerize for at least 15-30 min. After polymerization, the isopropanol layer was removed and the surface of the resolving gel was rinsed with water. The remaining space was filled with the stacking gel solution and the comb was inserted immediately. After the stacking gel had polymerized, the comb was removed and the wells were rinsed with water to remove unpolymerized acrylamid. At least 1 cm of stacking gel should be present between the bottom of the loading wells and the resolving gel.

0.02 –25 µg of protein with 5 x loading buffer were heated at 95°C for 5 min and loaded onto the gel with a protein standard marker beside it. The gel was run in SDS gel running buffer at 200 V.

Acrylamid solution:

30%	Acryamid
0.8%	N,N'-Methylen-Bisacrylamid

Stacking gel solution:

1 ml	Acrylamid solution (30+0.8)
0.75 ml 1 M	Tris-Hcl, pH 6.8
65 µl	10% SDS
4.1 ml	H <sub>2</sub> O
100 µl	10% APS
7 µl	TEMED (N,N,N',N'-Tetramethylethylenamine)

Resolving Gel solution:

5 ml	Acrylamid solution (30+0.8)
4.75 ml	1 M Tris-Hcl, pH 8.8
125 µl	10% SDS
3.0 ml	H <sub>2</sub> O
150 µl	10% APS
15 µl	TEMED (N,N,N',N'-Tetramethylethylenamine)

SDS gel running buffer:

25 mM	Tris
192 mM	glycin
0.1%	SDS

5 x loading buffer:

10%	SDS
25%	$\beta$ -Mercaptoethanol
30%	glycerol
312.5 mM	Tris-Hcl, pH 6.8
0.01%	bromophenol blue
0.01%	xylyencyanol

### 3.10.5 In gel staining of proteins

#### 3.10.5.1 *Coomassie blue staining*

Detection of protein bands in a gel by Coomassie Blue staining can be achieved due to nonspecific binding of a dye, coomassie Brilliant Blue R, to the proteins. The detection limit is 20 ng to 1  $\mu$ g/protein band.

After the SDS gel was run, the gel was shaken in Coomassie Blue staining solution for 15 min to 16 hrs depending on the amount of protein. Coomassie Blue turned the entire gel blue and the gel should be destained by destaining solution. After destaining, the blue protein bands appeared against a clear background. The gel could be stored in acetic acid or water or was photographed or dried to maintain a permanent record.

Coomassie Blue staining solution:

50% (v/v)	methanol
0.05% (v/v)	Coomassie brilliant blue R-250
10%	acetic acid
40%	H <sub>2</sub> O

Destaining solution:

5%	methanol
7%	acetic acid
88%	H <sub>2</sub> O

#### 3.10.5.2 *Rapid Coomassie blue staining*

Roti-Blue (Roth) was used for rapid protein staining. Roti-Blue stains the protein bands after 30 min with very little background even after 15 hrs of staining, because the dye in Roti-Blue binds specifically to the protein but not to the gel matrix. The detection limit is almost the same as Silver staining (< 30 ng/protein). Gel was shook in Roti-Blue staining solution and then destained. The gel could be stored in acetic acid or water or was photographed or dried to maintain a permanent record.

Destaining solution:

25%	methanol
75%	H <sub>2</sub> O

### 3.10.6 Western-blot

The Western-blot Chemiluminescence Reagent Plus (NEN<sup>TM</sup> Life Science Products) was used, which is based on the enhanced version of a chemiluminescence reaction in which the enzyme horseradish peroxidase (HRP) catalyzes light emission from the oxidation of luminol.

Western-blotting can be used to separate 0.0005-25 µg of complex mixtures of proteins. A PVDF membrane was shaken shortly in absolute ethanol, washed in H<sub>2</sub>O and incubated in Western-blot buffer for 15 min with gentle continuous shaking. The gel was incubated in renature buffer for at least 30 min to renature the proteins. Then the gel was blotted onto a PVDF membrane using Miniprotean II (Biorad) at 60 V for 1 hr. The membrane was air-dried for at least 20 min and incubated in TBST buffer containing 5-10% FCS for 1 hr with gentle shaking to block unspecific bindings of antibody. Specific primary antibody was given to the blot and incubated for 1 hr with gentle shaking. Depending on the antibody's specificity and affinity, the antibody was diluted to 1:100 to 1:1000 in TBST containing 10% of FCS. After the membrane was washed for 3 times with TBST, the secondary antibody, peroxidase conjugated anti-IgG (mouse, rabbit, peroxidase-conjugated, Sigma) diluted to 1:5000-1:10000 in TBST containing 10% FCS was given and incubated for 1 hr with gentle shaking. The blot was washed with TBST for four times. The Western-blot Chemiluminescence Reagent was prepared by mixing 5 ml of the solutions from bottle 1 and bottle 2 and immediately given to membrane. The Chemiluminescence Reagent was incubated with the membrane for 1 min at room temperature. Use at least 0.125 ml per cm<sup>2</sup> membrane and incubate with shaking. The membrane was shortly drained between Whatman papers and placed between the covers of a polypropylene sheet. A film was laid on the membrane and exposed for 15 seconds and then developed. Repeat the film exposure, varying the time as needed for optimal detection.

#### Alkaline phosphatase buffer:

100 mM	Tris-HCl, pH 9.5
100 mM	NaCl
5 mM	MgCl <sub>2</sub>

#### TBST buffer:

10 mM	Tris-HCl, pH 8.0
150 mM	NaCl
0.05%	Tween

#### Renature buffer:

50 mM	Tris-HCl, pH 7.5
20%	glycerol

### 3.10.7 Eletro mobility shift assay – EMSA

The mobility shift assay was developed by Schneider et al (1994) on the basis of the observation from Fried and Crother (1981). In native polyacrylamid gel, the protein-DNA-

complex keeps stable and runs differently from free protein or free DNA. Protein-DNA-complex runs slowly than protein alone but faster than the free DNA.

The washed glass plates and 1.5 mm spacers were assembled for casting the gel, which was 16cm x 16cm x 1.5mm big. The 8% polyacrylamid gel solution was poured between the plates. Let the gel polymerize for at least 1 hr. The gel was prerun at 90V for 1hr.

10-50 fmol  $^{32}\text{P}$ -labeled oligonucleotide was incubated shortly on ice with the protein in binding buffer in the presence of 1-2  $\mu\text{g}$  poly-[d(I-C)] and 10-20  $\mu\text{g}$  of BSA. 10 x loading buffer was given before loading.

The electrophoresis was conducted in TBE buffer at 150 V for 4 hrs before the bromphenol blue approached the bottom of the gel. A phosphor Image was laid on the gel and followed scanned by Phosphor Image.

Binding buffer:

50 mM	Hepes, pH 7.9
10 mM	$\text{MgCl}_2$
150 mM	$\text{NaCl}$
1 mM	DTT
1 mM	EDTA
10%	glycerol

10 x loading buffer:

625 mM	Hepes, pH 7.9
100 mM	DTT
25%	glycerol
0.05%	bromphenol blue
0.05%	xylencyanol

8% gel solution:

13.3 ml	30% Acryamid, 0.8% N,N'-Methylen-Bisacrylamid
5 ml	10 x TBE
$\text{H}_2\text{O}$ add to 50 ml	
Polymerization through addition of 120 $\mu\text{l}$ of 10% APS and 100 $\mu\text{l}$ of TEMED	

### 3.10.8 Antibody supershift assay

Supershift assay is a useful variation of the mobility shift assay using antibodies to identify proteins present in the protein-DNA complex (Kristie and Roizman, 1986a; Kristie and Roizman, 1986b). Addition of a specific antibody to a binding reaction can have one of several effects. If the protein recognized by the antibody is not involved in complex formation, addition of the antibody should have no effect. If the protein that forms the complex is recognized by the antibody, the antibody can either block complex formation, or it can form an antibody-protein-DNA ternary complex and thereby specifically result in a further reduction in the mobility of the protein-DNA complex (supershift).

10  $\mu\text{l}$  of anti-Pur $\alpha$  antibodies was added to the binding reaction (described in 3.10.7). The mixture was incubated shortly on ice. A nonspecific antibody was needed as a negative



control. Thereafter, the reaction was stopped by adding 10 x loading buffer and loaded on a 8% polyacrylamid gel as described in 3.10.7.

### 3.10.9 Immunprecipitation

Protein G-sepharose was used for immunprecipitation. All of the anti-Pur $\alpha$  antibodies used were monoclonal and from rat. Protein G-sepharose beads were equilibrated with 1 ml of PBS, mixed and centrifuged (1000rpm/1min). This process was repeated five times and the beads were resuspended in 1 ml 1 x PBS.

Most of the anti-Pur $\alpha$  antibodies are not IgG, which can directly bind to protein G-sepharose. Therefore, 2  $\mu$ g of “Goat anti Rat unconjugated (IgG + IgM)” was coupled at first with 30  $\mu$ l of equilibrated protein G-sepharose on the Vibrax (1000rpm) for about 1 hr at room temperature. Thereafter, 1 ml of anti-Pur $\alpha$  antibody was given and incubated on vibrax (1000 rpm) for an additional 1 hr. The beads were washed twice with 5 ml of PBS containing 5mg/ml BSA. After each wash, the mixture was centrifuged at 1000 rpm for 1min. The supernatant was carefully aspirated with a fine-tipped Pasteur pipet and 100  $\mu$ l of fluid above the pellet was left. The tube was placed on ice for 5 min and all of the processes followed were performed at 4°C or in cold room. Protein crude extract (500-1000  $\mu$ g) was given and incubated on Vibrax (1000 rpm) for 1 hr. The beads was followed washed four times with 5 ml of ice cold PBS and centrifuged. After each wash, the mixture was centrifuged at 1000 rpm for 1min. The supernatant was carefully aspirated with a fine-tipped Pasteur pipet and 100  $\mu$ l of fluid above the pellet was left. The pellet was resuspended in 20  $\mu$ l of 1 x SDS loading buffer. The supernatant was loaded on 12% SDS gel after heating at 95°C for 5 min. After the gel was run, the gel was blotted onto a PVDF membrane and detected with Western-blot analysis.

### 3.10.10 In vitro transcription and translation

The TNT<sup>®</sup> Quick Coupled Transcription/Translation System (Promega) was used to synthesize [<sup>35</sup>S]-labeled Pur $\alpha$  protein in *vitro*. The TNT<sup>®</sup> Quick Coupled Transcription/Translation System (minus Methionine) is convenient single-tube, coupled transcription/translation reactions for eukaryotic *in vitro* translation. It is available for transcription and translation of genes cloned downstream from the T7 or SP6 RNA polymearse promoters. To use this system, 0.2 – 2.0  $\mu$ g of either circular or linear DNA and 4.0  $\mu$ l of Redivue<sup>™</sup>L-[<sup>35</sup>S] methionine (10 mCi /ml) is added to an aliquot of TNT<sup>®</sup> Quick Master mix, which was removed from the freezer and allowed to thaw on ice before using. TNT<sup>®</sup> Quick Master mix contains TNT<sup>®</sup> rabbit reticulocyte lysate, TNT<sup>®</sup> reaction buffer, TNT<sup>®</sup> RNA polymearse, amino acid mixture minus methionine, and RNasin ribonuclease

inhibitor. The reaction was then incubated in a 50  $\mu$ l volume for 60-90 minutes at 30°C. The synthesized protein was analyzed by SDS-polyacrylamide gel electrophoresis (SDS-PAGE) and autoradiography.

### 3.10.11 Pull-down assay

30  $\mu$ l of glutathione-sepharose beads were washed with 1.0 ml of binding buffer twice for every reaction. 10  $\mu$ l of *in vitro* translated [<sup>35</sup>S]-labeled Pur $\alpha$  protein was added to 5  $\mu$ g of GST-Pur $\alpha$  in binding buffer to an end volume of 200  $\mu$ l and incubated on ice for 30 min. The mixture was transferred into the tube containing the washed glutathione-sepharose beads. The tube was shaken at 4°C for 1 hr. After centrifugation at 1000 rpm for 1 min, the glutathione-sepharose beads were washed with 1 ml of binding buffer five times. After the last wash, 15  $\mu$ l of 2 x SDS loading buffer was added to every tube to elute the proteins immobilized on glutathione-sepharose beads. The proteins were then analyzed by SDS-polyacrylamide gel electrophoresis (SDS-PAGE) and autoradiography.

#### Binding buffer:

50 mM	Hepes, pH 7.9
10 mM	MgCl <sub>2</sub>
150-300 mM	NaCl
1 mM	DTT
1 mM	EDTA
10%	glycerol
0.1%	NP40

### 3.10.12 Expression and purification of GST- fusion proteins

PGEX vectors can be used in bacterial systems to express foreign polypeptides as fusions with glutathione-S-transferase (GST). In general, such fusion proteins are soluble and are easily purified from lysed cells under nondenaturing conditions by absorption with glutathione-sepharose beads, followed by elution in the presence of free glutathione.

#### 3.10.12.1 Induction of expression of GST-fusion proteins

A colony of the pGEX transformant was inoculated into 100 ml LB/ampicillin medium and incubated at 37°C overnight with shaking (200 rpm). The culture was diluted 1:10 into 1 liter of fresh LB / ampicillin medium, incubated at 37°C with shaking for about 1 hr until its OD<sub>600</sub> = 0.5. IPTG (100  $\mu$ M) was given and the culture was incubated at 37°C for an additional 3 hrs. The culture was centrifuged (4500 rpm/10 min, room temperature). The bacterial pellet was washed three times with 50 mM Tris-HCl, pH8.0 / 100 mM NaCl, resuspended in 10 ml lysis buffer on ice and lysed using a sonicator (15 impulses, 30% output and repeat for 3

times, Branson Sonifier 250). After sonication, the suspension was centrifuged (20000 rpm/30 min/ 4°C, Heraeus HFA 22.50). The GST-fusion protein was purified from supernatant by incubating with glutathione-sepharose beads.

Lysis buffer:

50 mM	Hepes, pH 7.9
500 mM	NaCl
1 mM	EDTA
5 mM	DTT
0.5%	Nonidet
0.1%	Triton X-100

### **3.10.12.2 Purification of GST-fusion proteins**

Glutathione-sepharose beads (Pharmacia) were washed and equilibrated twice with wash buffer. The supernatant from above was incubated with 300-400 µl of equilibrated glutathione-sepharose beads at 4°C for at least 1 hr with gentle shaking. The mixture was centrifuged (2000 rpm/2min/4°C, Heraeus, RS5315). The sepharose pellet was washed with wash buffer for 5 times, it is necessary to incubated the beads with wash buffer for 5 min on ice to destroy the unspecific interactions with the beads. GST-fusion protein was eluted three times by adding the same volume of the elution buffer, mixing well at 4°C for 5 min and centrifuging (2000 rpm/2min/4°C, Heraeus, RS5315). Each Fraction was analyzed by SDS-PAGE. Stored the eluted protein in aliquots containing 10% glycerol at -70°C.

Wash buffer:

50 mM	Hepes, pH 7.9
1000 mM	NaCl
1 mM	EDTA
5 mM	DTT
1%	Triton X-100

Elution buffer:

150 mM	Hepes, pH 7.9
500 mM	NaCl
1 mM	EDTA
5 mM	DTT
1%	Nonidet
1%	Triton X-100
100 mM	glutathione

### **3.10.12.3 Regeneration of glutathione-sepharose beads**

To regenerate glutathione-sepharose beads, the beads were washed with 5 volumes of regeneration buffer and equilibrated with wash buffer.

Regeneration buffer:

50 mM	Hepes, pH 7.9
3000 mM	NaCl
1 mM	EDTA
5 mM	DTT
1%	Triton X-100

**3.10.12.4 Dialysis of GST-fusion protein**

Slider-A-Lyzer Dialysis Cassette was used to dialyze GST-fusion protein. Low molecular weight contaminant removal, buffer exchange, desalting and concentration can be accomplished with this device. Dialysis was performed in dialysis buffer at 4°C overnight.

Dialysis buffer:

25 mM	Mes, pH 6.5
0.1 mM	EDTA
50 mM	NaCl
20%	glycerol
5 mM	MgCl <sub>2</sub>
1 mM	DTT

**3.10.13 Unwinding assay****3.10.13.1 Generation of different substrates**

## 3.10.13.1.1 Preparation of 5'-labeled unwinding substrate

The DNA substrate used in unwinding assays consists of <sup>32</sup>P labeled complementary oligodeoxynucleotide annealed to single-stranded M13mp19 phage DNA to create a partial duplex. The oligodeoxynucleotide (17-mer) was mainly used except as otherwise stated (Tuteja *et al.*, 1994; Tuteja *et al.*, 1990). A total of 10 pmol of oligonucleotide was labeled at the 5'-end with T4 polynucleotide kinase and [ $\gamma$ <sup>32</sup>P]-ATP. After 1 hr of incubation at 37°C, the reaction was stopped by heating at 95°C for 20 min. 7.5  $\mu$ l of M13mp19 DNA and 3.0  $\mu$ l of annealing buffer were given to the reaction. The mixture was heated at 95°C for 5 min to denature the oligonucleotide and M13mp19. After short centrifugation, it was transferred to a 60°C water bath, slowly cooled and hybridized overnight. Non-hybridized oligonucleotide was removed by gel filtration through a sepharose 4B (Pharmacia) column with elution buffer.

<u>Annealing buffer:</u>		<u>Elution buffer:</u>	
400 mM	Tris, pH 7.5	10 mM	Hepes, pH7.4
100 mM	MgCl <sub>2</sub>	100 mM	NaCl
1000 mM	NaCl	1 mM	EDTA
10 mM	DTT		

### 3.10.13.1.2 Preparation of blunt ended duplex and small linear DNA unwinding substrate

For the preparation of blunt ended duplex DNA substrate, 10 pmol of 17-mer was radioactively labeled and annealed to 40 pmol of complementary 17-mer. Small linear substrates were prepared by labeling 10 pmol of 17-mer and annealing it with 20 pmol of 101-mer.

A total of 10 pmol oligonucleotide (17-mer) was labeled at the 5'-end with T4 polynucleotide kinase and [ $\gamma^{32}\text{P}$ ]-ATP. After 1 hr of incubation at 37°C, the reaction was stopped by heating at 95°C for 20 min. 20 pmol of oligonucleotide (101-mer) or 40 pmol of oligonucleotide (complementary 17-mer) and 3.0  $\mu\text{l}$  of annealing buffer were given to the reaction. The mixture was heated at 95°C for 5 min to denature the oligonucleotide and M13mp19. After short centrifugation, it was transferred to a 60°C water bath, which was then turned off. The hybridization was performed overnight.

Non-hybridized oligonucleotide was removed by gel filtration through a sepharose 4B (Pharmacia) column with elution buffer.

### **3.10.13.2 DNA Unwinding assay**

The unwinding assay measures the unwinding of a  $\gamma^{32}\text{P}$  labeled DNA fragment from a partial duplex DNA molecule. The assays were performed in a final volume of 20  $\mu\text{l}$  containing 200 mM Mes (pH 6.5), 10 mM MgCl<sub>2</sub>, 10 mM DTT, about 200 ng of GST-Pur $\alpha$  or truncated GST-Pur $\alpha$  and  $^{32}\text{P}$ -labeled unwinding substrate. The reaction was incubated at 37°C for 30 min and terminated by adding 4.0  $\mu\text{l}$  of 5 x loading buffer. The product was separated by electrophoresis on a 12% nondenaturing polyacrylamid gel. A phosphor Image Screen was laid on the gel and followed scanned by Phosphor Image.

<u>5 x loading buffer:</u>	
75 mM	EDTA
2.25%	SDS
37.5%	glycerol
0.3%	bromophenol blue

### **3.10.13.3 Generation of point-mutations in a *Pura* deletion mutant**

Point mutation of Pur $\alpha$  cDNA was made using QuickChange<sup>TM</sup> Site-Directed Mutagenesis Kit (Stratagene). QuickChange<sup>TM</sup> Site-Directed Mutagenesis Kit allows site-specific mutation in virtually any double-stranded plasmid and requires no specialized vectors, unique restriction sites, or multiple transformations.

#### 1) Setting up the PCR reaction:

Two complementary oligonucleotides containing the desired mutation, flanked by unmodified nucleotide sequence were designed. The reaction was prepared as below:

5  $\mu$ l of 10 x reaction buffer  
50 ng of pGPur $\alpha$   
12.5 pmol oligonucleotide primer 1  
12.5 pmol oligonucleotide primer 2  
0.5 mM dNTP mix  
ddH<sub>2</sub>O to a final volume of 50  $\mu$ l  
1  $\mu$ l of Turbo Pfu DNA polymerase (2.5 U /  $\mu$ l)

Each reaction was overlaid with 30  $\mu$ l of mineral oil.

#### 2) Running PCR:

95°C / 1min	1 cycle
95°C / 1min, 65°C / 1min, 68°C / 8 min	16 cycles
68°C / 10min	1 cycle
4°C / $\infty$	

#### 3) Digestion of the products:

1.0  $\mu$ l of Dpn I restriction enzyme (10 U/ $\mu$ l) was directly added to each amplification reaction below the mineral oil overlay using a small, pointed pipette tip. The mixtures were incubated at 37°C for 1 hr to digest the parental supercoiled dsDNA.

4) After PCR products were transformed into XLI Blue Competent Cells, plasmid DNA was isolated from the cells and sequenced to check the point mutation.

## 4 Results

SPSF I and II were purified from calf thymus by Dr. Marion Jurk during her Ph.D work in our laboratory. Both proteins bind specifically to ssDNA. Peptide sequences derived from purified SPSF I and II revealed the identity of SPSF I protein with the so-called Hela Pur $\alpha$  factor. The DNA binding properties of the Pur protein to single-stranded oligonucleotides of different lengths and sequences were quantified by determination of DNA-binding constants. Hela Pur $\alpha$  cDNA was isolated from a Hela cDNA library and cloned successfully in our laboratory (Jurk *et al.*, 1996).

This dissertation is divided into two parts concentrating on the analysis of Pur $\alpha$ 's function. Since Pur $\alpha$  has been implicated in diverse cellular functions, including transcriptional activation and repression, translation and cell growth, we decided to generate Pur $\alpha$  knock-out (KO) mice to analyze its function *in vivo*. Thus, the first part of this dissertation reports the generation and characterization of Pur $\alpha$  KO mice. While analyzing Pur $\alpha$  enzymatic activities, we found accidentally that Pur $\alpha$  displayed helicase activity *in vitro*. Therefore, the second part of this work reports this new property of Pur $\alpha$  and the characterization of its function as a DNA unwinding enzyme.

### 4.1 The generation of Pura knock-out mice

For the generation of knock-out mice, two essential prerequisites must be fulfilled: (i) The gene to be deleted should be a single copy gene; (ii) the corresponding genomic sequence of this gene locus have to be known. Recent work has shown that mouse Pur $\alpha$  is a single copy gene, however, the genomic DNA sequence of Pur $\alpha$  is unknown. Thus, this work was started by an analysis of the structure of Pur $\alpha$  genomic DNA.

#### 4.1.1 Structure of Pura genomic DNA

For the generation of a Pur $\alpha$  targeting vector for homologous recombination in ES cells, two homologous regions are needed. A Hela Pur $\alpha$  cDNA fragment was used to screen a mouse genomic DNA library, since the Pur $\alpha$  protein is highly conserved among eucaryotic organisms.

##### 4.1.1.1 Isolation of Pura genomic DNA

To isolate the mouse Pur $\alpha$  genomic DNA, a 129/SvJ Mouse Genomic Library in Lambda FIX II vector (Stratagene) was used for screening.

The phages were propagated in phage competent bacteria prepared as described in 3.9.1.1-3. Lambda phages on plates were blotted onto membranes and hybridized (3.8.3) with a 777 bp human Pur $\alpha$  cDNA fragment, which was radioactively labeled as described in 3.7.2. The positive plaques were isolated and used for the second screening (3.9.5). Three cycles of screening were performed. Thereafter a few single plaques were isolated from phage plates. Large scale lambda DNA of positive phage was prepared as described in 3.9.6.

DNA of the isolated plaques was digested with different restriction enzymes. To ensure the complete digestion of phage DNA, the reactions were carried out at 37°C overnight. Different restriction enzymes digested lambda DNA in different patterns. For analysis of the digestions, the reactions were loaded on a 1% agarose gel. According to the digestion patterns, two different independent phages were isolated containing mouse Pur $\alpha$  genomic DNA. They were designated p5/1 and p14/2.

Both phages were used to analyze the genomic structure of the Pur $\alpha$  gene by restriction mapping and partial sequencing.

#### **4.1.1.2 Analysis of phage p5/1**

In 129/SvJ Mouse Genomic Library, inserts of genomic DNA were cloned into a *XhoI* site, however, this site is not able to be recreated. Insert of genomic DNA can be excised by *NotI*. Therefore, the whole insert of genomic DNA can be isolated by *NotI* digestion of the phage clone, provided that the genomic DNA does not contain *NotI* restriction sites. Mouse Pur $\alpha$  cDNA contains two *NotI* restriction sites at position 135 and 1007. It is not clear, if Pur $\alpha$  genomic DNA has further *NotI* restriction sites. *PstI* cleaves mouse Pur $\alpha$  cDNA twice, too. Therefore, the mapping was started with *NotI* and *PstI* digestion.

DNA of p5/1 was digested by *NotI* or *PstI* separately. From *NotI* digestion a 2.1 kb fragment was seen instead of the expected 832 bp fragment of Pur $\alpha$  cDNA, suggesting the presence of an intron between the two *NotI* restriction sites. The 2.1 kb *NotI* fragment was subcloned into the *EagI* site of the pGMUT vector. A 4.5 kb fragment of the *PstI* digestion was subcloned into pGEM4Z vector linearized by *PstI*. Plasmids pG26 and pG3 were identified as correct plasmids according to the digestion patterns. DNA of both plasmids were isolated and sequenced from both sites. PG26 contained a part of Pur $\alpha$  cDNA to position 1007 (*NotI*) while pG3 contained Pur $\alpha$  cDNA downstream of the *PstI* restriction site (1456). Both DNA was digested with different enzymes and 6 fragments were subcloned into pGEM4Z. The sequencing analysis showed that subclone pZ14-9 with a 1.5 kb *XhoI/NruI* fragment contained a part of the Pur $\alpha$  cDNA sequence from position 389 to 394. The sequence of the Pur $\alpha$  cDNA before position 388 was not found on this subclone, suggesting that mouse Pur $\alpha$  genomic DNA might be composed of at least two exons. From the restriction map of murine



Pur $\alpha$  cDNA, subclones of pG26, pG3 and some other subclones, a partial restriction site map of phage p5/1 was derived (Figure 4-1).

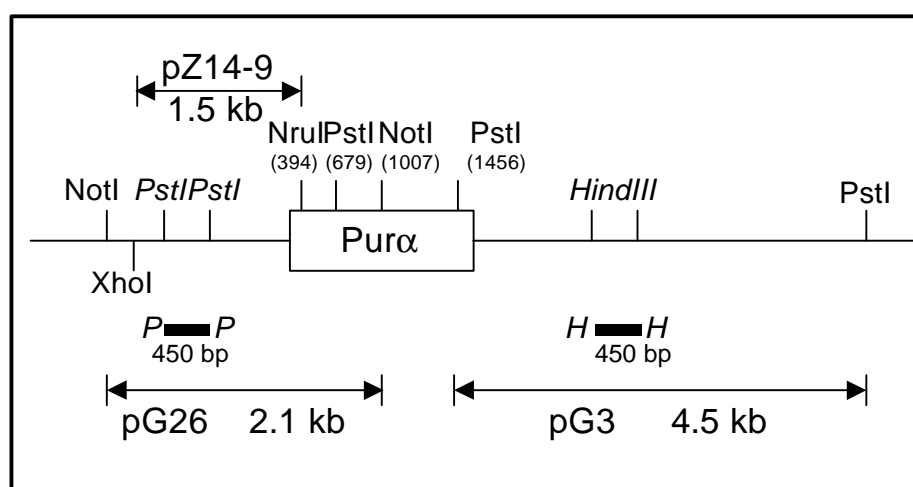


Figure 4-1: Partial of restriction map of p5/1. Pur $\alpha$  cDNA already mapped is illustrated by a box. The numbers in parentheses shows the nucleotide position of the restriction site of the respective enzymes in Pur $\alpha$  cDNA.

*PstI* 450 bp and *HindIII* 450 bp fragments were used as probes for further mapping of Pur $\alpha$  genomic DNA. Therefore, both fragments were subcloned into pGEM4Z. *PstI* and *HindIII* fragments were excised from the plasmids, purified from agarose gel with QIAquick Gel Extraction Kit (3.4.4.2) and labeled radioactively (3.7.2).

For the further analysis of Pur $\alpha$  genomic sequence, DNA of phage p5/1 and p14/2 was digested with the following combinations of enzymes: *NotI/HindIII*, *NotI/PstI*, *NotI/EcoRI*, *NotI/XbaI*, *NotI/SmaI*, *NotI/BamHI*, *NotI/EcoRV*, *NotI/BglIII*, *NotI/SalI* and *NotI*. The restriction reactions were loaded onto a 1% agarose gel and blotted onto a Hybond N<sup>+</sup>-membrane. The membrane was then hybridized with the 450 bp *HindIII* fragment isolated and labeled as described above. The blot was stripped (3.8.5) and then hybridized with the 450 bp *PstI* fragment.

Figure 4-2 shows the blot of p5/1 hybridized with 450 bp *PstI* or *HindIII* fragments. The sizes of the DNA fragments obtained in the Southern-blot are listed in the appendix (Table 8-1). From these two Southern-blot, a more detailed restriction map for p5/1 was derived as shown in Figure 4-3.

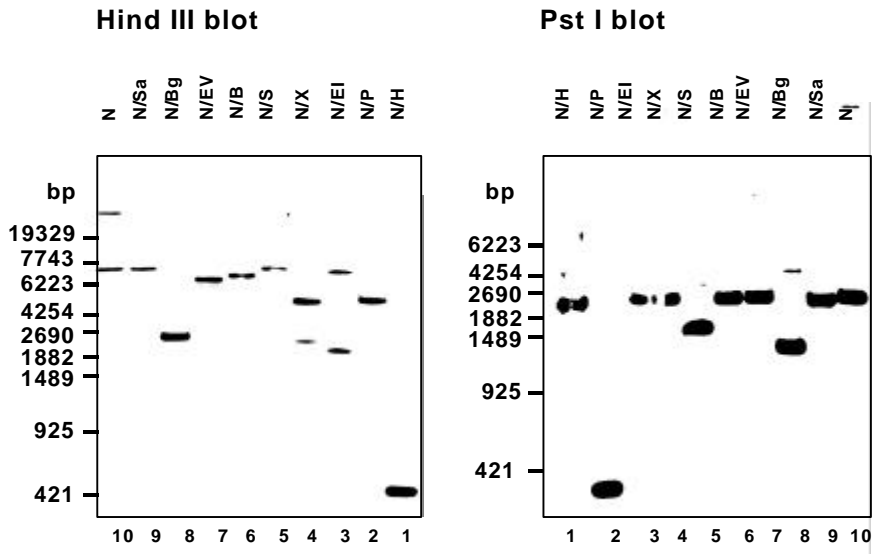


Figure 4-2: p5/1 DNA was digested with different enzyme combinations: N (*NotI*), H (*HindIII*), P (*PstI*), E (*EcoRI*), X (*XbaI*), S (*SmaI*), B (*BamHI*), Ev (*EcoRV*), Bg (*BglII*), Sa (*SalI*). The blot was hybridized with 450 bp *PstI* or *HindIII* fragments.

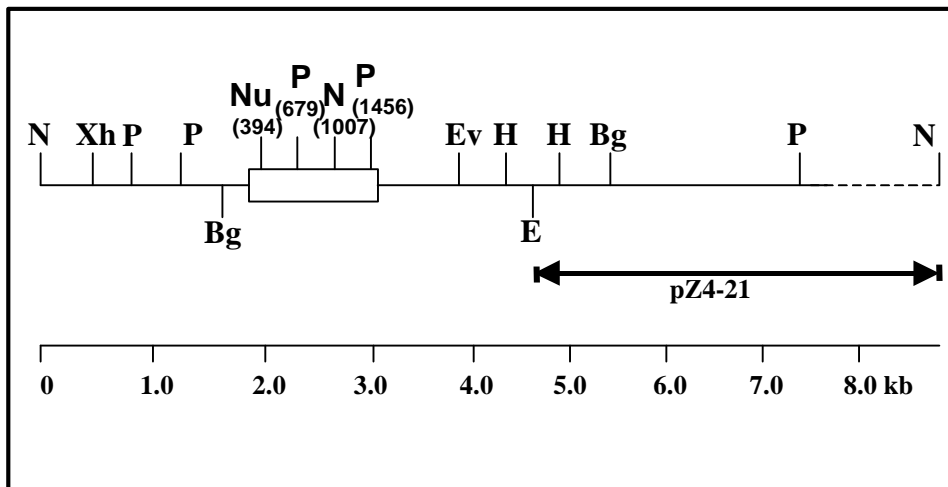


Figure 4-3: Partial restriction map of p5/1: N (*NotI*), H (*HindIII*), P (*PstI*), E (*EcoRI*), Xh (*XhoI*), Ev (*EcoRV*), Bg (*BglII*), Nu (*NruI*). The approximate size of the Pur locus is represented by the scale shown beneath the diagram.

The large fragment (>>7.0 kb) from the *NotI/EcoRI* digestion of p5/1 DNA was subcloned into a pZERO vector linearized with *NotI/EcoRI*. The resulting plasmid was pZ4-21, which was digested with *HindIII* and some other enzymes to get more information about restriction sites. From subclone pZ4-21 and the partial restriction map of p5/1, a more refined restriction map of p5/1 was obtained as shown in Figure 4-4.

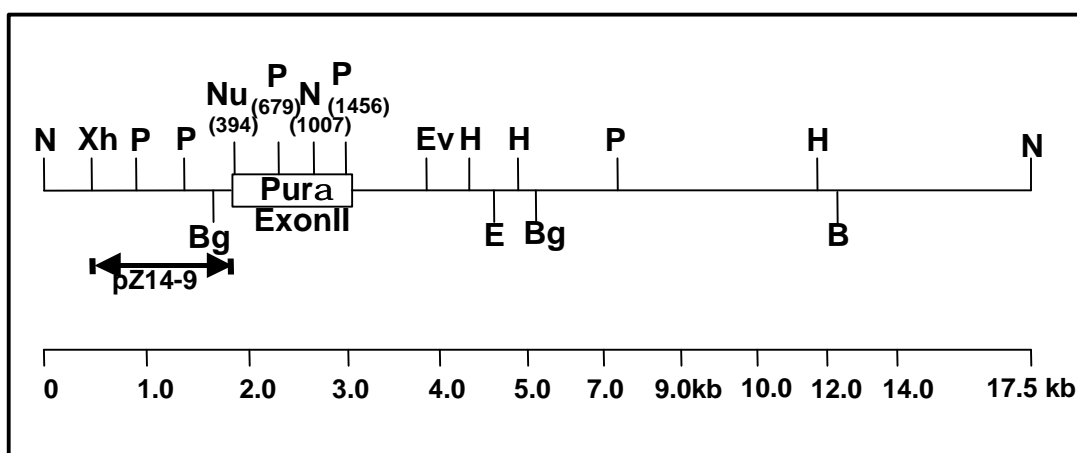


Figure 4-4: The complete restriction map of p5/1: N (*NotI*), H (*HindIII*), P (*PstI*), E (*EcoRI*), Xh (*XhoI*), Ev (*EcoRV*), Bg (*BglII*), Nu (*NruI*), B (*BamHI*). The approximate size of the Pur $\alpha$  locus is represented by the scale shown beneath the diagram.

From the whole restriction mapping and sequencing analysis of p5/1, the following can be concluded: A) p5/1 contains about 17.5 kb genomic DNA of the Pur $\alpha$  locus. B) The murine Pur $\alpha$  gene consists of at least 2 exons, the second one contains the whole open reading frame of Pur $\alpha$ . C) Sequencing analysis of the subclone pZ14-9 confirmed that the second exon begins at 389 bp of Pur $\alpha$  cDNA.

#### 4.1.1.3 Analysis of phage p14/2

Blot p14/2 was hybridized with the 450 bp *PstI* or *HindIII* fragments as described for blot p5/1. The sizes of the DNA bands obtained are presented in the appendix (Table 8-2). From these Southern-Blots and the murine Pur $\alpha$  cDNA sequence, a partial restriction map of p14/2 was derived as shown in Figure 4-5.

The 7.0 kb *NotI* fragment was subcloned into pZERO linearized with *NotI*, yielding plasmid pZ2-12. Sequencing analysis showed that pZ2-12 starts at nucleotide 135 and ends at nucleotide 1007 of Pur $\alpha$  cDNA and includes the 6.0 kb intron between nucleotides 388 and 389. Taken together, these data revealed the genomic structure of the Pur $\alpha$  as shown in Figure 4-6.

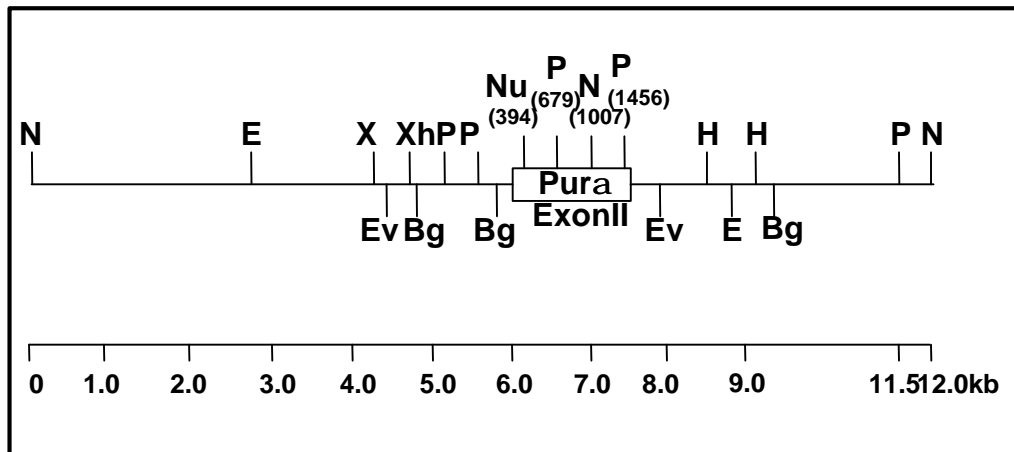


Figure 4-5: The partial restriction map of p14/2: N (*NotI*), H (*HindIII*), P (*PstI*), E (*EcoRI*), Xh (*XhoI*), Ev (*EcoRV*), Bg (*BglII*), Nu (*NruI*), B (*BamHI*), X (*XbaI*). The approximate size of the Purα locus is represented by the scale shown beneath the diagram.

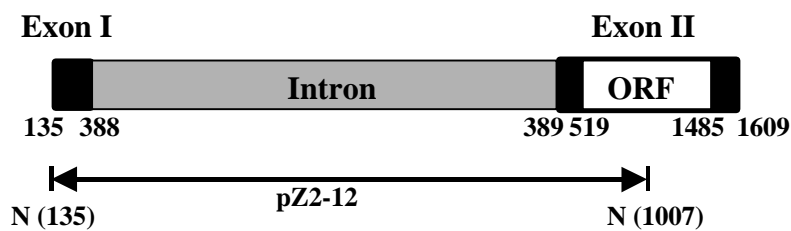


Figure 4-6: The Purα gene contains at least two exons, which are represented by black boxes. The complete open reading frame (519-1485) is located in the second exon. The two exons are separated by an intron of about 6.0 kb. The numbers under the box indicate nucleotide positions in Purα cDNA.

As already mentioned the Purα cDNA has two *NotI* restriction sites located at positions 135 and 1007. As described above, the digestion of Purα genomic DNA with *NotI* did not show a band of 872 bp, indicating the existence of at least one intron between nucleotide position 135 and 1007. Restriction analysis and sequencing confirmed the presence of a 6.0 kb intron between the two exons. The first exon contains nucleotides 135 to 388 as confirmed by sequencing. However, it remains unclear whether further intron(s) is present between position 1 and 135 of the first exon.

To answer this question, two oligonucleotides were designed for further mapping of intron-exon junction. P2M1 represents nucleotides 94-119 of mouse Purα cDNA and P2M2 is homologous to 346-369. The p14/2 blot was stripped and hybridized with P2M2. The blot was stripped again and then hybridized with P2M1. The lengths of DNA bands obtained from the Southern-blot are listed in the appendix (Table 8-2). From these two blots, a complete restriction map for p14/2 was derived as followed in Figure 4-7.

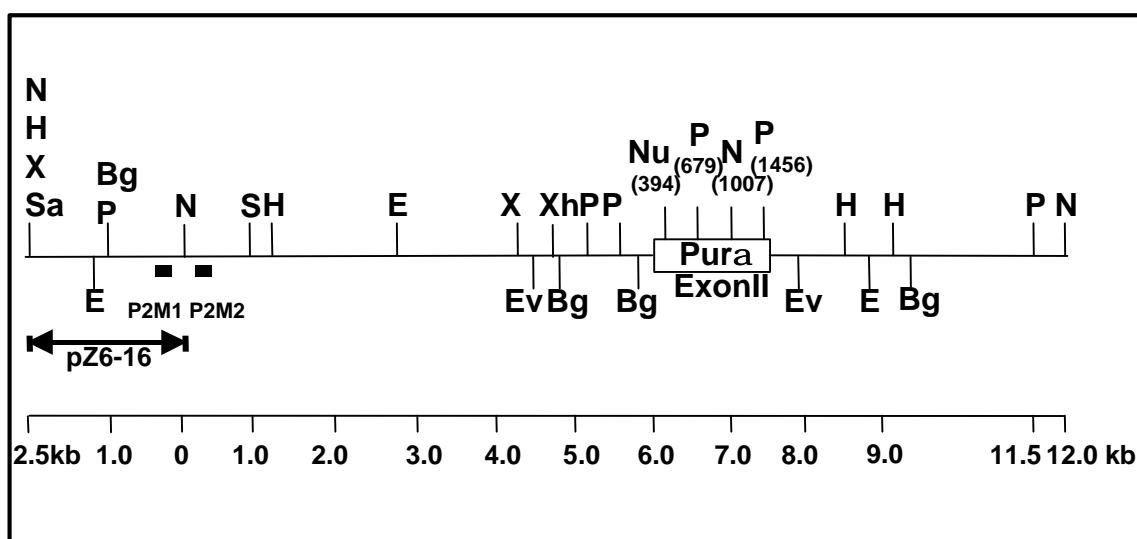


Figure 4-7: The complete restriction map of p14/2: N (*NotI*), H (*HindIII*), P (*PstI*), E (*EcoRI*), Xh (*XhoI*), Ev (*EcoRV*), Bg (*BglII*), Nu (*NruI*), X (*XbaI*) B (*BamHI*), Sa (*SalI*), S (*SmaI*). The approximate size of the Pur locus is represented by the scale shown beneath the diagram.

A 2.5 kb *NotI/XbaI* fragment was subcloned into pZERO linearized with *NotI* and *HindIII*. Sequence analysis of the resulting subclone pZ6-16 identified the first 135 bp of Pur $\alpha$  cDNA ending at the *NotI* restriction site. There were no additional intron in these 135 bp. Therefore, we conclude that the Pur $\alpha$  gene contains two exons, the first spanning 388 bp of the 5' UTR while the second exon comprising the remaining part of the 5' UTR, the translational start site, and the complete open reading frame followed by 113 bp of the 3' UTR, as found in the mouse cDNA. The intron present in the mouse Pur $\alpha$  gene is approximately 6.0 kb long. The complete Pur $\alpha$  genomic structure is shown in Figure 4-8.

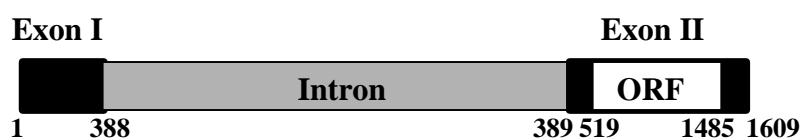


Figure 4-8: Schematic genomic structure of the Pur $\alpha$  gene. The Pur $\alpha$  gene contains two exons, which are represented as black boxes. The whole open reading frame (519-1485) is located in the second exon. Between the two exons is an intron of about 6.0 kb, which is represented as gray box. The numbers indicate the positions in Pur $\alpha$  cDNA.

#### 4.1.1.4 Genomic structure of the *Pura* locus

About 25 kb of genomic Pur $\alpha$  sequence were analyzed with different restriction enzymes and partially sequenced. There is about 6.0 kb overlapping sequence between these two phage fragments. The overlapping region is from *XhoI* restriction site to *PstI* restriction site. P5/1

contains the 5'-UTR with a 6.0 kb intron while the p14/2 contains the 3'-UTR. Figure 4-9 shows the structure of the inserts of phage p5/1 and p14/2.

For the complete restriction mapping, a few fragments were excised from phage DNA and subcloned into plasmids. These cloned fragments and the corresponding subclones are shown in Figure 4-11, which represents the Pur locus schematically with detailed restriction sites. In addition, the DNA probes used for phage screening are also indicated in this figure.

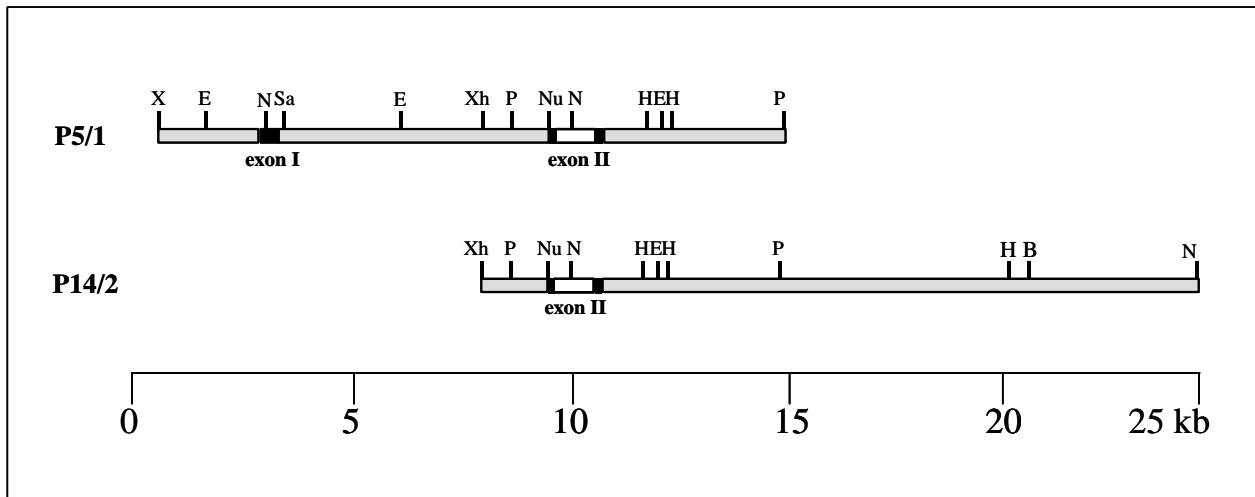


Figure 4-9: Schematic representation of the genomic inserts of phage p5/1 and p14/2. The two phage clones contain about 25 kb genomic Pur $\alpha$  and overlaps for about 6.0 kb. Exons are illustrated by black boxes. The open area within the boxes is the open reading frame (ORF) of Pur $\alpha$ . The restriction maps show the position of the restriction enzymes sites. X (*Xba*I), E (*Eco*RI), N (*Not*I), Sa (*Sal*I), Xh (*Xho*I), P (*Pst*I), Nu (*Nru*I), H (*Hind*III), B (*Bam*HI), Ev (*Eco*RV). The approximate size of Pur locus is indicated by the scale shown beneath the diagram.

#### 4.1.1.5 The exon/intron junction of the Pura gene

Finally, the exon/intron junctions of the Pur $\alpha$  gene were determined. There are two exons and one intron. The intron is located within the 5'-UTR after 388 bp of the cDNA. Exon II contains the remaining part of the 5'-UTR, the translational start site, the ORF and the 3'-UTR. Figure 4-10 shows the nucleotide composition at the junctions of exon I and exon II.

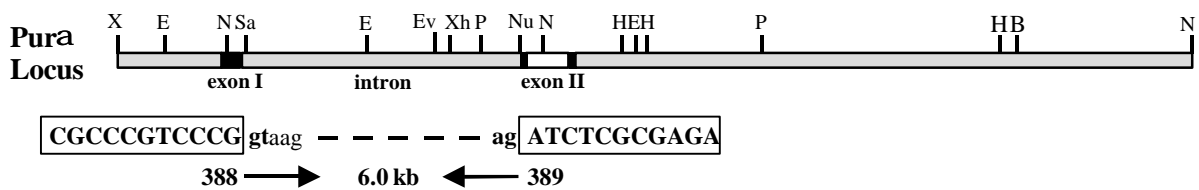


Figure 4-10: Nucleotide composition of the Pur $\alpha$  gene at the junctions of exon I and II. The gt, ag splice sites of the donor and acceptor sequences of the intron are shown in bold. Boxed sequences represent the end of the first exon and the beginning of the second exon.

# Puro $\alpha$ genomic structure

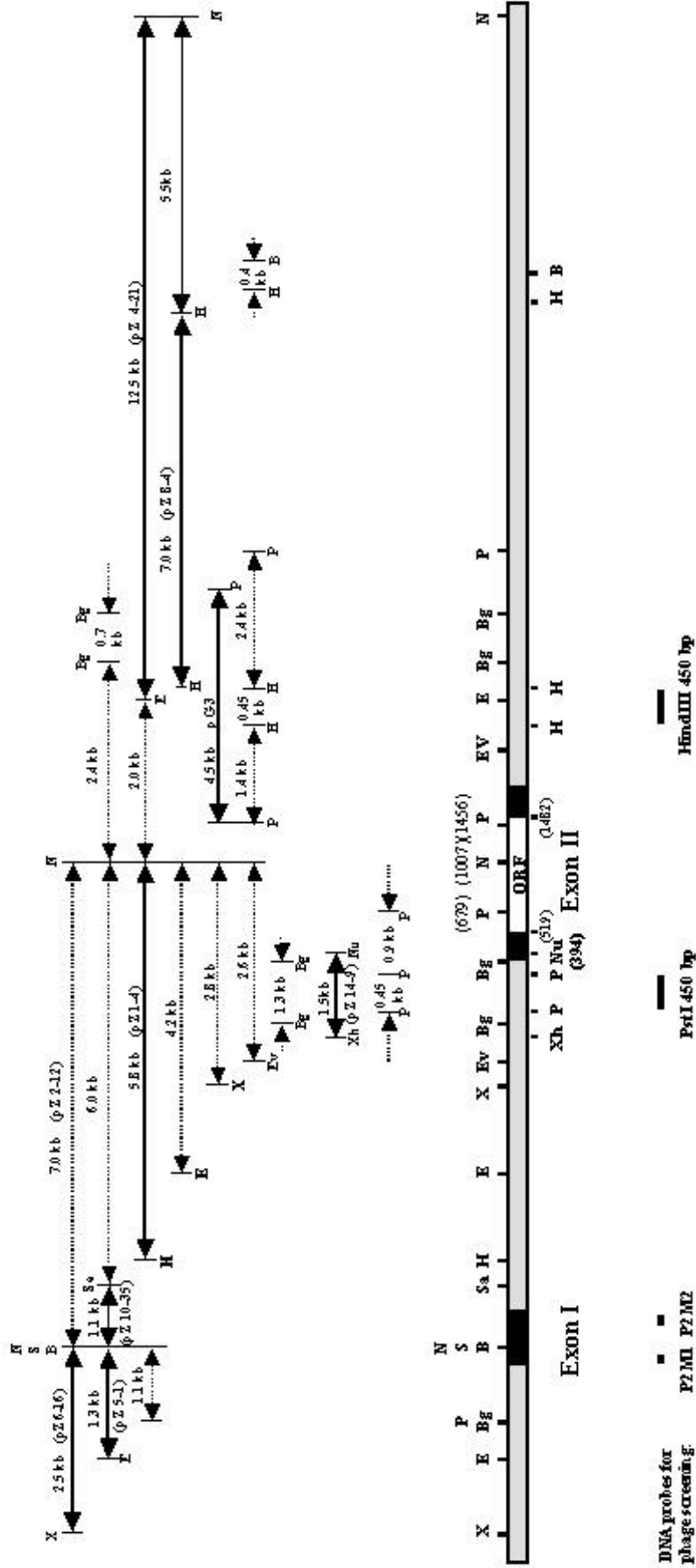


Figure 4-11: Genomic DNA structure of Puro $\alpha$ .

#### 4.1.2 The targeting constructs for the generation of Pura knock-out mice

A targeting vector is designed to recombine with and thereby mutate a chromosomal locus. The minimal components of such a vector are sequences which are homologous with the desired chromosomal integration site, a positive selection marker and a plasmid backbone. Since both the transfection efficiency and targeting frequency of such a vector usually are low, it is desirable to include other components in the vector such as additional positive and negative selection markers which provide strong selection for the targeted recombination product. The positive marker in a targeting vector may serve two functions. Firstly, it provides a selection marker to isolate rare transfected cells that have stably integrated DNA (which occurs at a frequency of about one in every  $10^4$  treated cells); Secondly, it replaces essential sequences of the target gene which leads to its inactivation upon homologous recombination. Two distinct vector designs can be used for targeting in mammalian cells, replacement and insertion vectors. Replacement vectors (Figure 4-12) are the most widely used vector type, whose fundamental elements are homology to the target locus, a positive selection marker, bacterial plasmid sequences, and a linearization site outside of the homologous sequences of the vector. In some cases a additional negative selectable marker may be used to enrich the transfected cells against random integration events (A.L.Joyner, 1999).

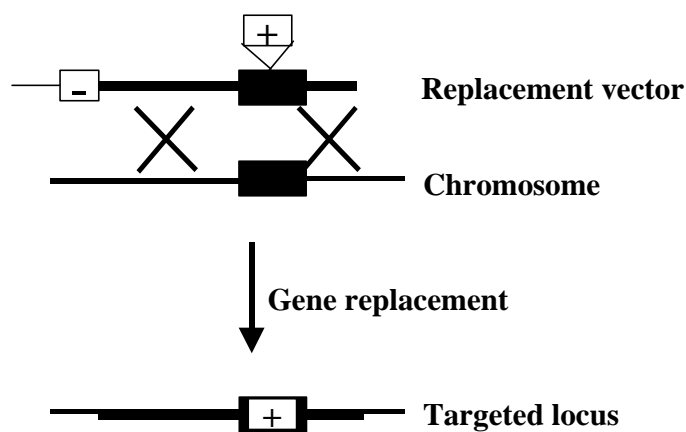


Figure 4-12: Replacement vector. Thick lines represent sequences homologous to the target locus, thin lines represent bacterial plasmid, line of intermediate thickness represents the target locus in the chromosome. Black rectangle represents an exon. Positive selection marker, a box that contains a '+', negative marker, a box containing a '-'. The positive selection marker deletes and replaces a part of the coding region of the target gene. The replacement vector is linearized outside the target homology prior to electroporation. Gene targeting results in a simple gene replacement product.



#### 4.1.2.1 Design of the targeting vector for deleting *Pura* locus

The genomic structure of the murine *Pur $\alpha$*  gene described in 4.1.1 was used to design the *Pur $\alpha$* -KO targeting vector.

To obtain a targeted disruption of *Pur $\alpha$*  gene, we decided to use the positive-negative selection strategy (Mansour *et al.*, 1988). This strategy enriches for homologous recombination events by simultaneously selection for Neo-resistance and against a herpes simplex virus thymidine kinase (HSV-TK) gene placed at the 3' end of the targeting sequence. The *Pur $\alpha$*  targeting vector was constructed by insertion of a PGK-Neo cassette into exon II thereby replacing the whole ORF. "Neo" encodes neomycin phosphotransferase whose expression is driven by the human PGK (phosphoglycerate kinase) promoter. ES cells with this antibiotic resistance gene have the ability to survive in the presence of the neomycin derivative geneticin (G418). The HSV-TK gene was placed at the 3' end of the targeting sequence. In ES cells, in which the targeting construct is inserted at the correct locus, the TK gene is deleted during homologous recombination. Therefore, these cells can survive in the presence of gancyclovir (GANC), while the ES cells, where the construct was inserted randomly still contain the TK gene and cannot survive in the presence of GANC (Thomas and Capecchi, 1987).

The homologous sequences in the vector should be derived from genomic libraries isogenic with the specific murine ES cells used in the targeting experiment. The number and extent of polymorphic variation between two mouse strains in any given locus is usually unknown and may vary from gene to gene (A.L.Joyner, 1999). For the restriction map of the *Pur $\alpha$*  gene a 129/SvJ Mouse Genomic Library was used. The ES cells used for electroporation in our laboratory are derived from mouse strain 129/Ola. Further complications arose from the recent finding that 129/SvJ, which is the source of several commonly used genomic libraries, is a genetically contaminated substrain containing genomic regions of non-129 origin (Threadgill *et al.*, 1997). Therefore, to ensure the highest possible homologous recombination frequency, the two homologous arms for the targeting vector were amplified by PCR from genomic DNA of E14 ES cells.

**Amplification of the left homologous arm (1.2 kb PCR fragment: F40):** A 1.2 kb fragment was amplified by PCR using a sense primer P11M2 and an antisense primer P7M1E as shown in Figure 4-13. Both primers contain linker sequences to introduce *Sma*I recognition sites into the amplified fragment. PCR was carried out as described in 3.6.1. The DNA fragment was excised from agarose gel and purified with QIAquick Gel Extraction Kit (see 3.4.4.2). The fragment F40 was achieved after digestion with *Sma*I and subcloned into the pKO vector.

**Amplification of the right homologous arm (7.0 kb PCR fragment: F39):** A 7.0 kb fragment was amplified by PCR using a sense primer P10M1A and antisense primer P10M2 as shown in Figure 4-13. Both of the primers contain linker sequences to introduce *Xho*I recognition sites into the amplified fragment. PCR was performed as described in 3.6.3. The DNA fragment was isolated from agarose gel and purified with QIAquick Gel Extraction Kit (see 3.4.4.2). The fragment F39 was achieved after digestion with *Xho*I was then subcloned into pKO vector.

The two homologous arms synthesized by PCR for targeting vector and the corresponding PCR primers are shown in Figure 4-13.

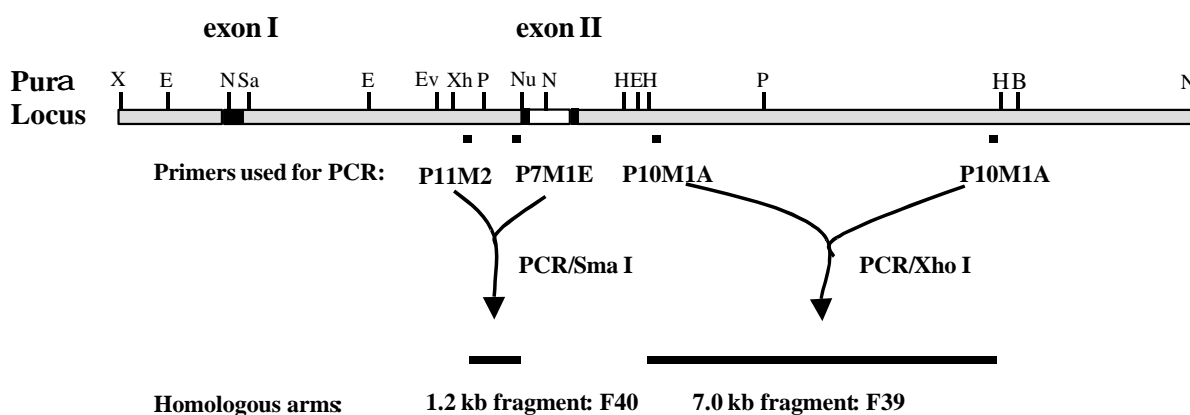


Figure 4-13: Location of the homologous arms for the targeting vector. Locations of the primers are indicated by bold black lines. After PCR amplification and enzyme digestion, the left homologous arm F40 and the right homologous arm F39 were achieved.

#### 4.1.2.2 Generation of the targeting vector for deletion of the *Pura* locus

To generate the  $\text{Pur}\alpha$  targeting vector, the plasmid pKO Scrambler V920 (Lexicon Genetics Incorporated) was used. The PGK-Neo cassette was released from pKO SelectNeo (Lexicon Genetics Incorporated) with *Asc*I. The pMC1-TK cassette was excised from plasmid pKO SelectTK (Lexicon Genetics Incorporated) with *Rsr*II.

**Subcloning of the PGK-Neo, pMC1-TK and two homologous arms into pKO vector:** The PGK-Neo-cassette was first subcloned into the *Asc*I restriction site of pKO in antisense direction. Then the pMC1-TK cassette was subcloned into pKO at the *Rsr*II site. Finally, the two homologous arms were ligated into *Sma*I and *Xho*I sites. The process to generate the  $\text{Pur}\alpha$  targeting vector is shown in Figure 4-14. The correct orientation of the fragments was verified by restriction analysis and sequencing.

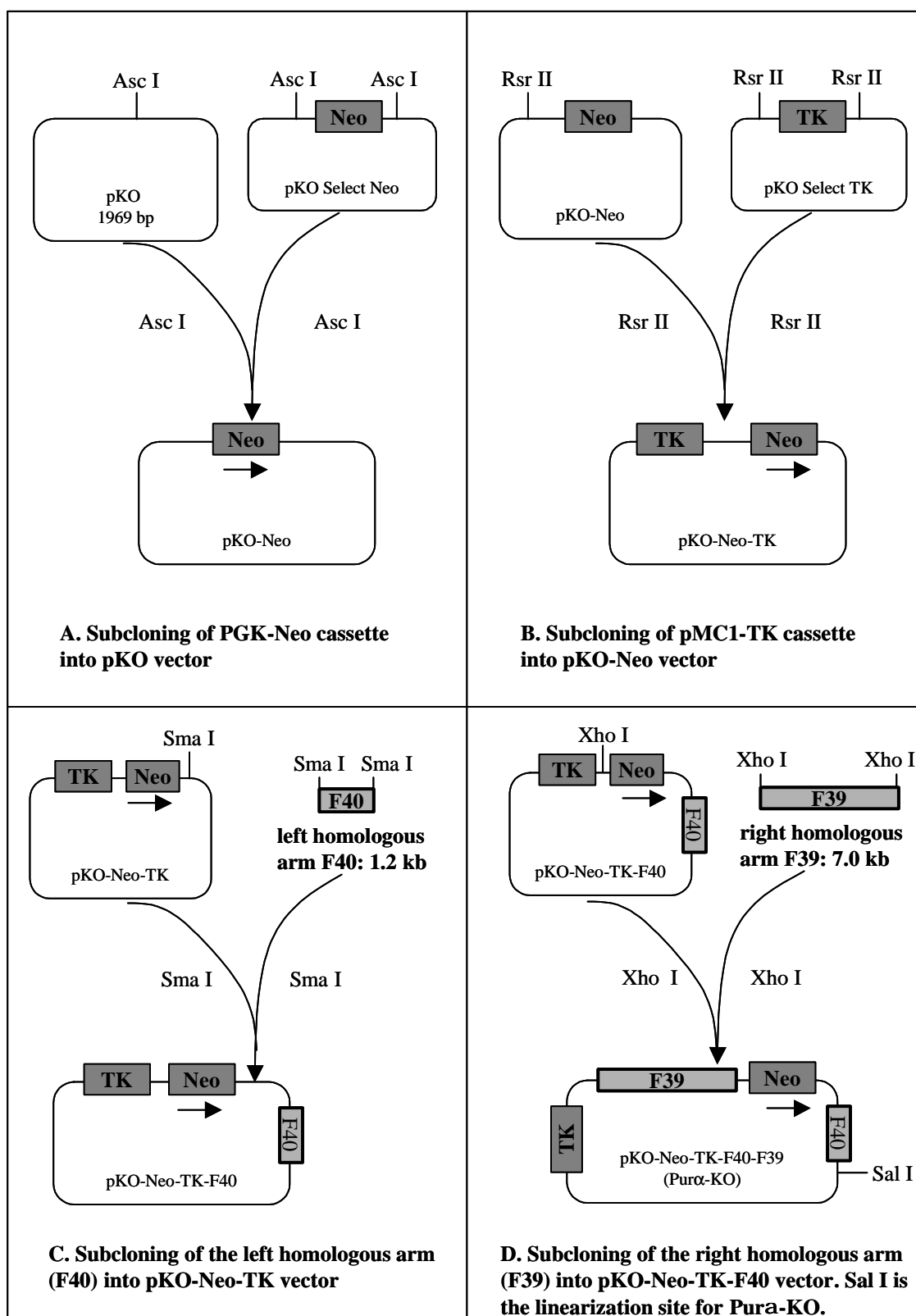


Figure 4-14: Cloning steps to generate Pur $\alpha$  targeting vector. The targeting vector Pur $\alpha$ -KO contains PGK-Neo cassette, pMC1-TK cassette and two homologous arms. Pur $\alpha$ -KO could be linearized by *Sal*I.

### 4.1.3 Generation of Pura knock-out mice

100  $\mu$ g of the Pur $\alpha$ -KO targeting vector (Figure 4-14) were completely linearized by *SalI* digestion. 20  $\mu$ g of the linear DNA were electroporated into E14 mouse embryonic stem (ES) cells. After geneticin G418 and gancyclovir selection, resistant colonies were visible and 480 single colonies were picked into 48 well feeder plates and expanded on 48 well feeder plates for freezing. Replicate gelatinized plates were produced for late screening analysis.

To confirm that the ES cell clones surviving selection with G418 and gancyclovir are the results of homologous targeting events and not from random insertion, it is necessary to further characterize these cell lines by either polymerase chain reaction (PCR) or Southern-blot analysis.

#### 4.1.3.1 Screening of positive ES clones by PCR

ES cells on 48-well plates were directly lysed with Kawasaki buffer (Kawasaki, 1990) (3.5.4). Using this method, the isolated genomic DNA can be directly used in PCR, but is not suitable for a Southern-blot. For the screening PCR one primer anneals to the novel sequences, e.g. the positive selection marker which replaces the targeted gene. The second primer lies just upstream of the homologous sequences of the shorter arm used for the vector. In this way, a correctly sized PCR product is only generated when the knock-out construct has been integrated by homologous recombination at the correct locus in the genome. PCR reaction was carried out as described in 3.6.1. The PCR screening strategy of ES cell clones targeted at the Pur $\alpha$  gene locus is shown in Figure 4-15.

The screening PCR with primer P11M1 and Neo-primer yields a 1.2 kb DNA fragment in ES cell clones mutated by homologous recombination. This 1.2 kb PCR fragment was only seen in correctly targeted clones (KO) but not in wild type cells (Figure 4-15, lane 1 and 2). The control PCR with primers P11M1 and P7M1E yields a slightly shorter product in all clones confirming integrity of DNA (Figure 4-15, lane 3). It is necessary to blot the PCR gel on membrane, if the PCR quality is not good enough. The blot could be hybridized with the 450 bp *PstI* fragment (Figure 4-1).

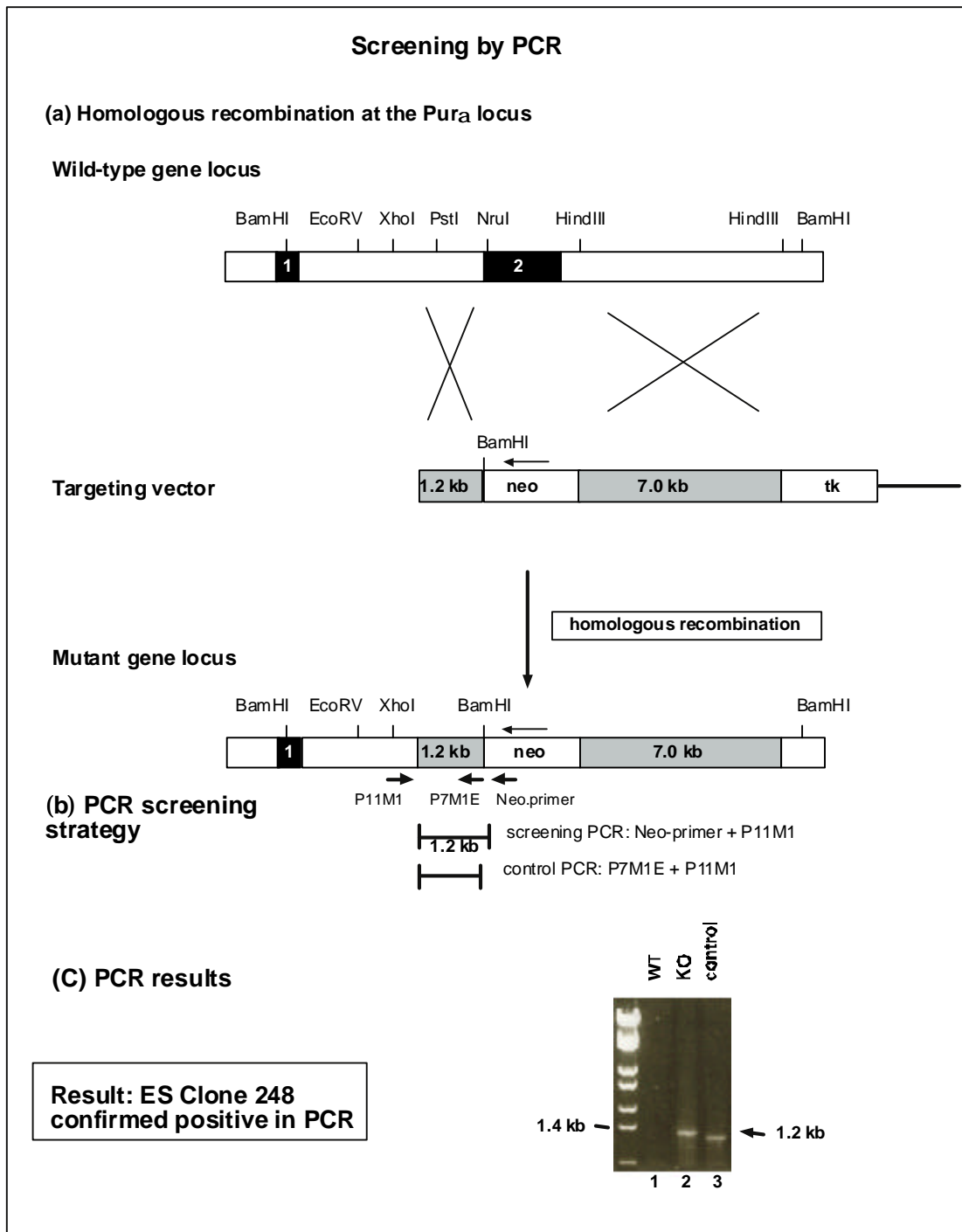


Figure 4-15: PCR screening strategy of ES cell clones targeted at the *Pur $\alpha$*  gene locus. (a) Targeting vector and homologous recombination at the *Pur $\alpha$*  locus. The targeting vector contains a neomycin cassette replacing exon II. The mutant gene locus shows the predicted map of the mutated *Pur $\alpha$*  allele following homologous recombination with the targeting vector. (b) PCR screening strategy. The screening PCR with primer P11M1 (within the region of homology) and Neo-primer yields a 1.2 kb DNA fragment in ES cell clones mutated by homologous recombination. The control PCR with

primers P11M1 and P7M1E yields a slightly shorter fragment in all ES cells. (c) PCR results. With screening primers P11M1 and Neo-Primer, a 1.2 kb PCR fragment in targeted clones (KO) was seen but not in wild type cells (lane 1 and 2). The control PCR with primers P11M1 and P7M1E yields a slightly shorter product in all clones (lane 3).

#### **4.1.3.2 Screening of positive ES clones by Southern-blot**

The PCR screening of positive ES clones is simple and the process to carry out PCRs is quick. But this method is not reliable because PCR quality is unstable and should always be blotted onto a membrane and hybridized with a DNA probe. In contrast, the screening of positive clone by Southern-blot is much more trustworthy although the process is relatively complicated.

To perform a Southern-blot analysis, it is necessary to design the vector in a way that the digestion with appropriate restriction enzymes allows unambiguous identification of targeted clones. The wild-type and the targeted alleles must therefore be readily distinguishable. In case of a replacement vector, Southern-blot analysis is performed with a probe that is not present in the target vector (external probe) and a restriction enzyme is used, with which correctly targeted ES clones can be distinguished from the wild type or random integration clones (Thomas and Capecchi, 1987). As shown in Figure 4-16, at the *Pur $\alpha$*  gene locus, one *Bam*HI restriction site is located in exon I and another one lies downstream of exon II, both sites are not present in the targeting vector. However, there is an additional *Bam*HI site in the targeting vector between the first exon and the Neo cassette. Therefore, wild type and targeted ES clones show different *Bam*HI digestion patterns. To avoid false negative results, Southern-blot analysis should be performed with several restriction enzymes and different probes. It is also important to analyze both the 5' and 3' ends of the targeted locus by using external probes from flanking sequences. Moreover, an internal probe which hybridizes to the selectable marker can be used to distinguish between a unique gene replacement and random integration events.

After the positive ES clone was confirmed by PCR, the corresponding frozen clone in 48 well plates was thawed quickly at 37°C in a water bath, and expanded progressively on feeder cells. The cells on 10 cm feeder dishes were used for preparation of genomic DNA as described in 3.5.2. 10-15  $\mu$ g of genomic DNA was digested with *Bam*HI and used for Southern-blot.

A part of the ES cell clones on 48 well plates were directly screened by Southern-blot because of its inherent reliability. Genomic DNA from ES cells was isolated as described in 3.5.1. 10-15  $\mu$ g of genomic DNA was digested with *Bam*HI overnight at 37°C, separated on a 0.8% agarose gel, and blotted as described in 3.8.1. The blot was hybridized with a 5' or 3' probe located outside the targeting vector as described in 3.8.4.

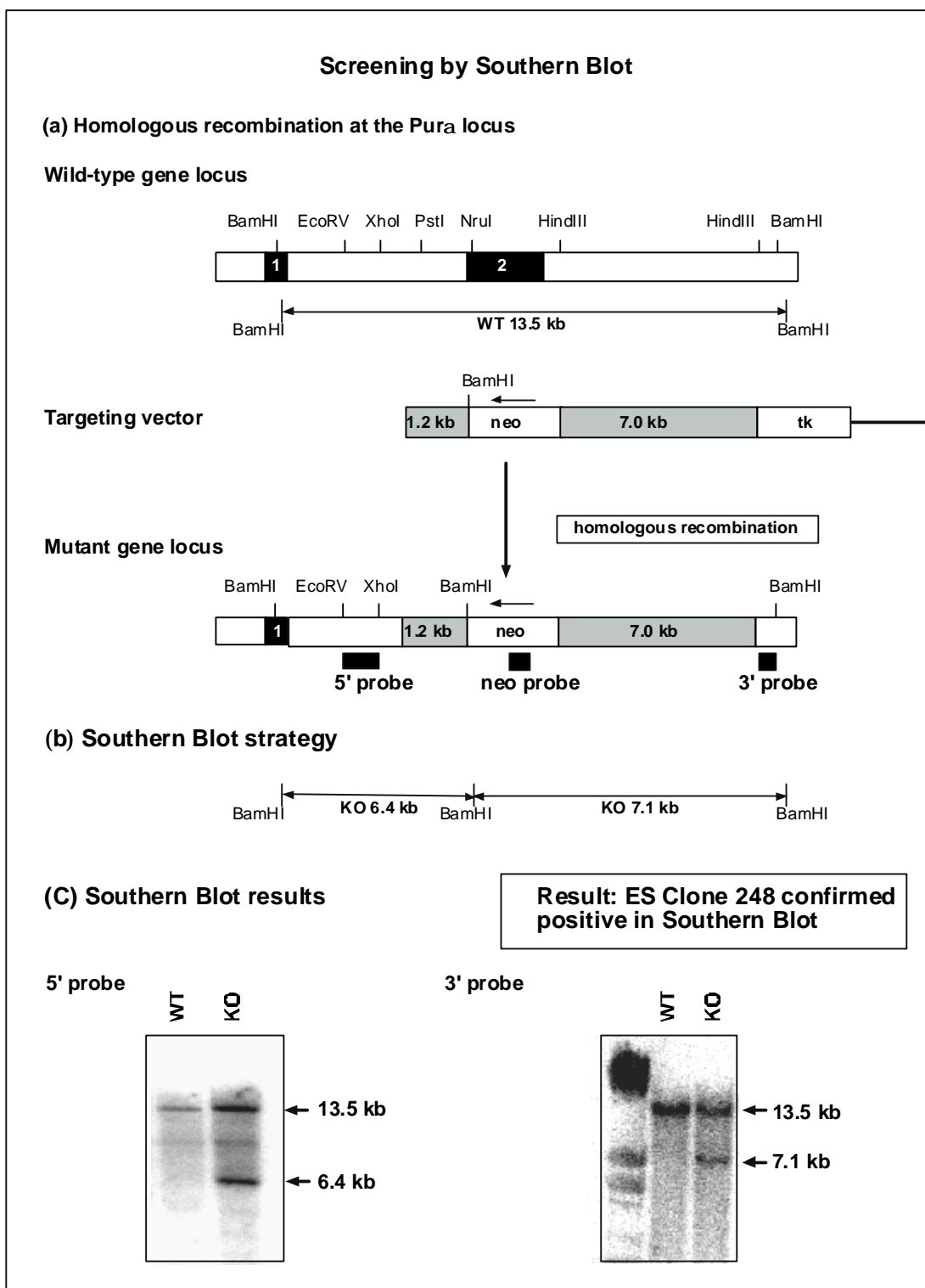


Figure 4-16: Southern-blot analysis screening strategy of ES cell clones targeted at the *Purα* gene locus. (a) The mutant *Purα* gene locus shows the predicted map of the mutated *Purα* allele after homologous recombination with the targeting vector. Restriction sites are indicated by vertical lines

and enzyme designation above the vector. Black boxes show the probes used for Southern-blot. 5'-probe was used for screening for correct recombination of the left arm, 3'-probe was used for correct recombination of the right arm, and neo-probe for confirmation of possible simple integration. (b) Southern-blot strategy. (c) Southern-blot results. With the 5'-probe, restriction digest with *Bam*HI resulted in a 13.5 kb fragment from the wild type gene locus and an additional 6.4 kb fragment from the mutant gene locus. With the 3'-probe, restriction digest with *Bam*HI resulted in a 13.5 kb fragment from the wild type gene locus and an additional 7.1 kb fragment from the mutant gene locus. Figure 4-16 shows the localization of the probes for Southern-blot. The 5' external probe to screen the mutant ES clone is a 500 bp *Xho*I/*Eco*RV fragment excised from pZ1-4 (Figure 4-11). The 3' external probe to screen the mutant ES clone is a 400 bp *Hind*III/*Bam*HI fragment excised from pZ4-21 plasmid (Figure 4-11). The Neo-probe is a 400 bp *Sph*I fragment excised from pKO-Select-Neo.

The Southern-blot screening strategy of ES cell clones targeted at the *Pur* $\alpha$  gene locus is shown in Figure 4-16. According to PCR and Southern-blot analysis ES clone 248 was confirmed to be the sole positive clone out of 2400 ES clones tested. The 5' external probe (a 500 bp *Xho*I/*Eco*RV fragment) resulted in a 13.5 kb fragment in wild-type clones and a 6.4 kb fragment in KO clone. The 3' external (a 400 bp *Hind*III/*Bam*HI fragment) resulted in a 13.5 kb fragment in wild-type clones and a 7.1 kb fragment in KO clones. It was essential to hybridize the blot with a Neo-probe to check for possible multiple integrations into the genome to avoid unknown disruption of the other genes. With the Neo-probe only a 7.1 kb band was detected as expected (data not shown). Therefore, ES KO248 was confirmed to be the sole clone out of 2400 ES clones tested that contains the mutated *Pur* $\alpha$  locus.

#### **4.1.3.3 Generation of chimeras and germ line transmission**

After screening for correct homologous recombinants, KO248 was thawed and injected into BALB/c mouse derived blastocysts. The E14 ES cell is originally derived from mouse strain 129/Ola with agouti color of fur, while BALB/c is albino. Therefore, the chimeric mice produced from these combinations will be a color mix of agouti/white and the percentage of chimerism was evaluated on the basis of the coat color of the chimeras. Eight chimeras with 30-95% chimerism were born, one chimera was found dead after birth. One male chimera and one female with 30-70% chimerism gave agouti color of pups.

#### **4.1.3.4 Generation and detection of *Pura* heterozygous knock-out mice**

F1 generation was got by breeding the male and female chimeras or breeding the chimeras with BALB/c mice. Altogether there were 23 F1 mice born. Southern-blot was carried out to detect if some of them are *Pur* $\alpha$  heterozygous KO mice. The genomic DNA was prepared from mice tails (3.5.3). 10-15  $\mu$ g of genomic DNA was digested with *Bam*HI overnight at



37°C and loaded onto a 0.8% agarose gel. The gel was blotted as described in 3.8.1. The blot was hybridized with the 5' probe (3.8.4), which is located outside the targeting vector. 12 of 22 F1 offspring carried the heterozygous  $Pur\alpha$  KO locus, 2 of which were female and 10 were male. Figure 4-17 shows one of the Southern-blots.

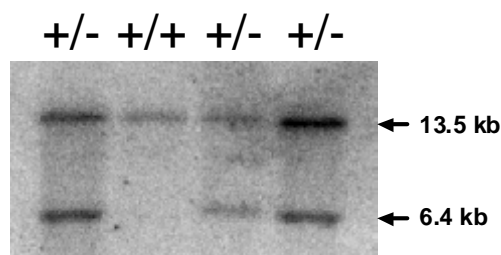


Figure 4-17: Southern-blot analysis of F1 mice.

#### 4.1.3.5 Generation and detection of *Pura* homozygous knock-out mice

By mating male and female heterozygous  $Pur\alpha$  KO mice, 168 F2 animals were born. Southern-blots were carried out (as described in 4.1.3.4) to detect if some of them are homozygous for the  $Pur\alpha$  KO locus. 2 mm tail clips was used for preparation of genomic DNA (3.5.3). 45 of 168 F2 offspring were confirmed as homozygous  $Pur\alpha$  KO mice and 81 F2 offspring were confirmed as  $Pur\alpha$  heterozygous KO mice while 42 F2 offspring were wild type mice. Figure 4-18 shows one of the Southern-blots.

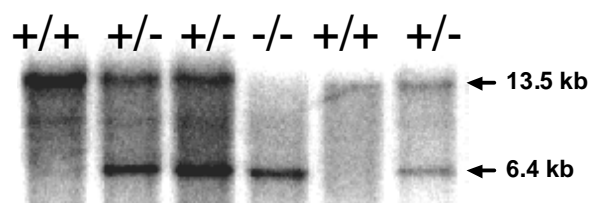


Figure 4-18: Southern-blot analysis of F2 mice.

To simplify the detection of heterozygous and homozygous  $Pur\alpha$  KO animals, a PCR method was established. In  $Pur\alpha$  homozygous mice the Neo-cassette replaces exon II of  $Pur\alpha$  while  $Pur\alpha$  heterozygous mice contain the Neo-cassette on one allele and the normal exon II of  $Pur\alpha$  on the other allele. Wild type mice do not have a Neo-cassette. A pair of neo-primers (neo2a and neo2b) and a pair of  $Pur\alpha$ -primers (HeM4 and HeM5, see Figure 4-38) from exon II were designed to amplify a 349 bp  $Pur\alpha$  fragment and a 450 bp neo Fragment. Neo-primers will amplify genomic DNA from  $Pur\alpha$  homozygous mice while  $Pur\alpha$  primers should not yield a fragment. DNA from heterozygous animals should produce products with both sets of primers while in wild type mice only the  $Pur\alpha$  primers give an amplification product.

Two PCRs were carried out separately using Neo primers or Pur $\alpha$  primers (3.6.1). PCR products were analyzed on an agarose gel as shown in Figure 4-19.

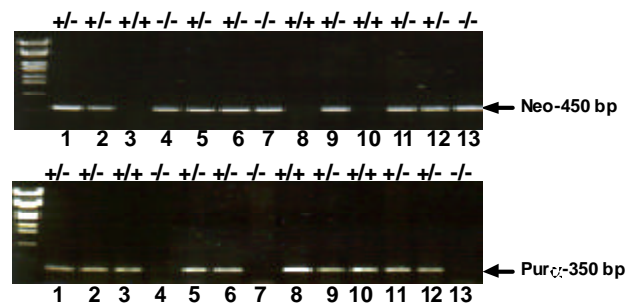


Figure 4-19: PCR analysis of F2 mice.

#### 4.1.3.6 Pura Western-blot

Pur $\alpha$  was found to be widely expressed in the mouse brain, especially abundant in the cerebral cortex and cerebellum (Osugi *et al.*, 1996). To analyze Pur $\alpha$  expression in both heterozygous and homozygous Pur $\alpha$  KO mice, protein extracts were prepared from the brain stems. The brain stems were homogenized in lysis puffer and protein concentrations were measured (3.10.3). 30  $\mu$ g of protein were electrophoresed through a pre-poured 12.5% SDS gel and electroblotted onto a PVDF membrane. Western-blot detection was carried out as described in 3.10.6. The blot was immunoprobed with a primary monoclonal antibody 3C12 against Pur $\alpha$  followed by goat anti-rat peroxidase conjugated anti-IgG+IgM (Sigma) and enhanced Chemiluminescence detection.

As shown in Figure 4-20, wild type mice (lane 5 and 6) show a Pur $\alpha$  protein band, which was not present in Pur $\alpha$  deficient mouse (lane 1 and 2). Heterozygous Pur $\alpha$  KO mice express about half the amount of Pur $\alpha$  (lane 3 and 4) as wild type mice.

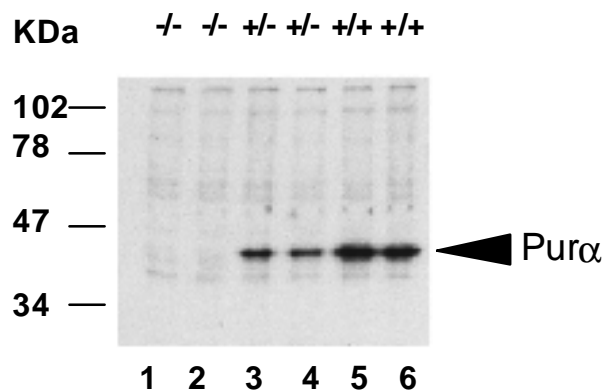


Figure 4-20: Detection of Pur $\alpha$  by Western-blot. 30  $\mu$ g of protein prepared from the mice brain stems were loaded on a 12.5% SDS gel. Lane 1 and 2: homozygous Pur $\alpha$  KO mice; Lane 3 and 4: heterozygous Pur $\alpha$  KO mice; Lane 5 and 6: Wild type mice.

#### 4.1.4 Primary phenotypic analysis of Pura knock-out mice

Pur $\alpha$  KO mice were live born with normal size and weight. At birth and for the following 10-12 days no phenotype other than wild type was apparent with either heterozygous or homozygous Pur $\alpha$  null mutants. From postnatal day 11-14 (p11-14) an increasingly severe and continuous tremor phenotype commenced in the homozygous Pur $\alpha$  KO mice, continuing unabated until the animals were sacrificed or natural death occurred. Pur $\alpha$  KO mice could not walk normally as their hind limbs apparently are too weak. These KO animals also showed a hyperexcitability on noise and tactile stimulus (contact with humans) resulting in uncontrollable movements of the KO mice. To confirm the genotype of the mice, Southern-blot analysis was performed. All mice showing the tremor phenotype were homozygous for the Pur $\alpha$  knock-out. Mice identified to be heterozygous for the Pur $\alpha$  knock-out displayed no obvious phenotype.

An additionally visible characteristic of the most homozygous KO mice is the crossing incisors beginning from different postnatal day. Normally, the mice incisors are maintained at a suitable length since they are ground by eating. Thus, the crossing of the incisors resulted not only in their continuous growth but also the reduced food intake. The incisors had to be cut if needed depending on their length. Additionally, to confirm proper food uptake, special soft cakes were fed to the KO animals.

With the onset of the tremor phenotype of Pur $\alpha$  KO mice, whether due to severe shaking, mis-positioned teeth, some other unknown factor, or a combination of these, the mice showed a reduced food intake and they started to lose weight from this time (Figure 4-22 A and B). In order to keep the KO animals alive some of them were injected with glucose once or more. While wild type and heterozygous mice showed continuous weight increase, KO mice showed significant slower weight increase until day 20-25 postnatally (p20-25). From p25 on KO mice recovered from weight loss resulting in the same weight as wild type at about p50 (female) or p70 (male) (Figure 4-21). Strikingly, the female KO mice displayed a more significant increase of weight than the males. KO females were always heavier than KO males whereas the male wild type mice were heavier than females (Figure 4-22 A and B). While wild type mice stabilize weight at the age of 2-3 months, body weight of KO mice increased continuously, becoming progressively more obese (Figure 4-21).

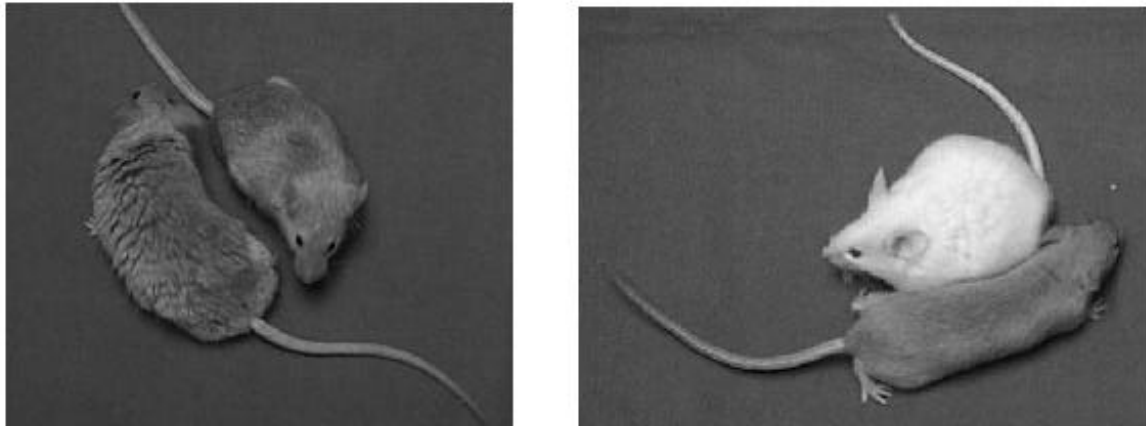


Figure 4-21: Pur $\alpha$  KO mice are bigger than their wild type littermates from postnatal day 70 because of obesity. (See color picture in page 136)

The weight loss of the male KO mice just after the onset of tremor at p11-15 was more severe than females and their weight recovery lasted longer than females until they reached the same weight as the wild type (Figure 4-22 A and B). Unlike heterozygous and wild type mice, whose weight reached a steady status after an increase phase, the weight of KO mice increased continuously until about day 120 postnatally and decreased shortly before they died (Figure 4-22 A, B, D and F).

Compared to the Pur $\alpha$  KO mice, the heterozygous KO mice did not display any visible phenotypes, such as tremor or the crossing incisors. The weight of the young heterozygotes did not decrease between postnatal days 12-14 as KO mice but increased continuously and evidently exceeded that of the wild type mice from day 30-40 postnatally (Figure 4-22 A and B).

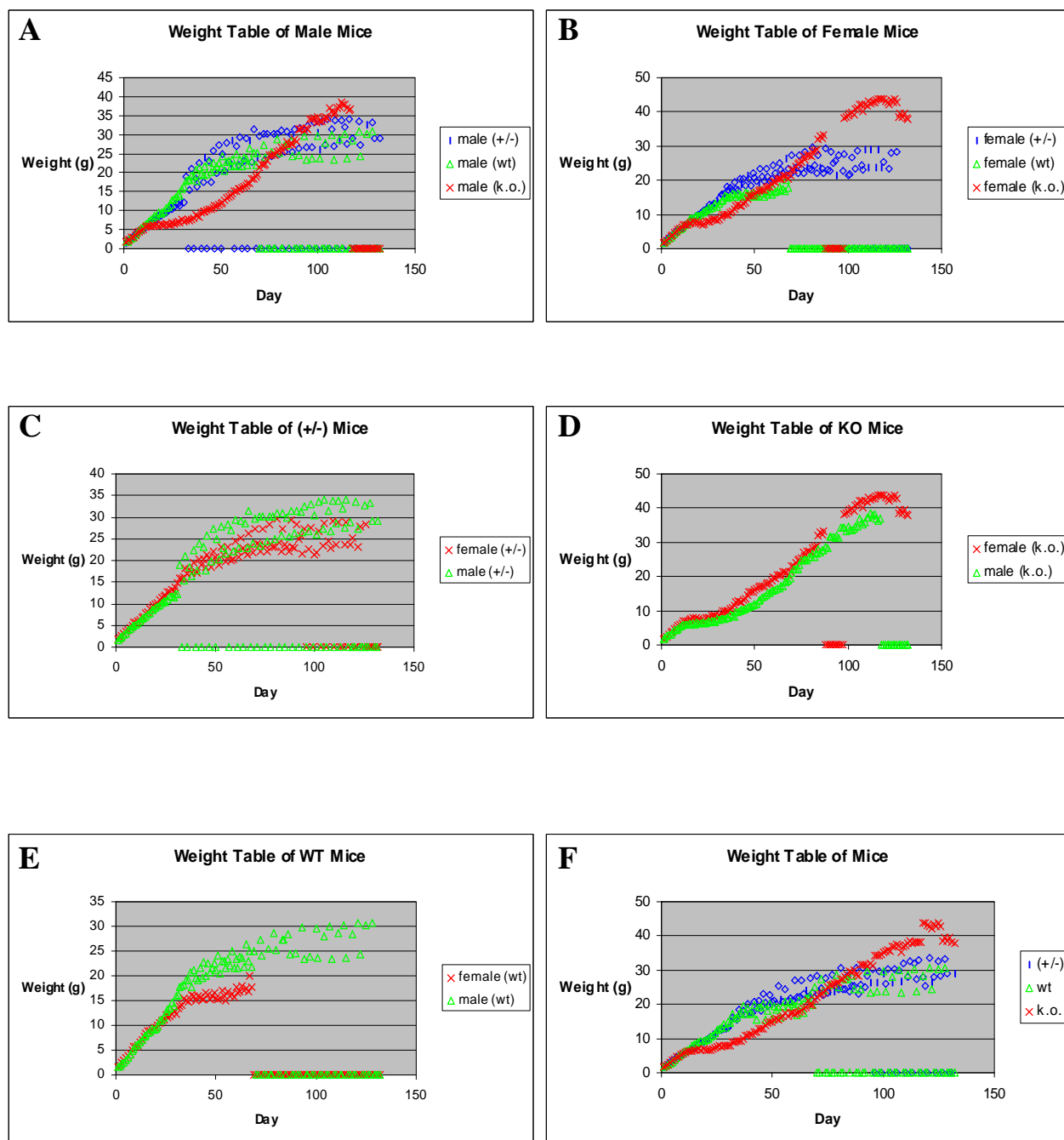


Figure 4-22: Weight tables of the  $Pur\alpha$  KO, heterozygous and wild type mice. (See color diagrams in page 137)

#### 4.1.5 Dissection of Pura knock-out mice

In 16-day-old mice, optical and weight analyses of the organs revealed no obvious differences in lungs, heart, liver etc, however significant differences were observed in 60-66 days old mice.

Firstly, the organ to body weight ratio of the brain was significantly higher in KO mice than that in wild type (see Table 4-1). The brain was visibly enlarged and the weight was increased by 30% compared to wild type (Figure 4-23 A). According to the enlarged and heavier brains of  $Pur\alpha$  KO mice, the brains from KO and wild type mice of 48 days postnatally (p48) were prepared and cerebrum, cerebellum, brain stem, hippocampus, and sensoric cortex were weighed separately. Detailed brain analysis showed brain stem enlarged and significantly heavier (about 3 times as heavy as those of the normal mice) (Figure 4-23 B), while the hippocampus and sensoric cortex were enlarged but lighter in KO mice. The enlargement of the cerebral cortex is accompanied by an increased surface, which can be seen in Figure 4-23 C.

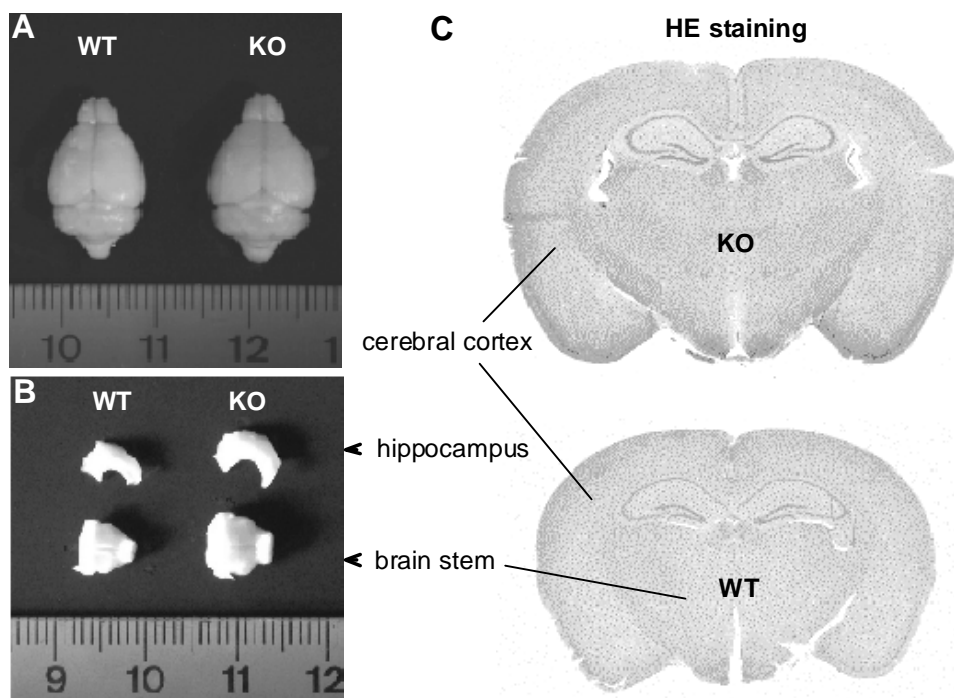


Figure 4-23: (A) The whole brain of  $Pur\alpha$  KO and wild type mice (p48). (B) The brain stem and hippocampus prepared from the brains of the KO and wild type mice. (C) HE staining of the brains of the KO and wild type mice. (see the color picture in page 136)

Secondly, as shown in Table 4-1, both male and females had increased abdominal and subcutaneous fat layers but interestingly, female mice have much more fat than male mice. Heterozygotes, although showing no phenotypic changes, had brain weights and amounts of

subcutaneous fat that lay exactly between homozygous KO and wild type levels (Table 4-1). Bones and muscle mass of homozygous KO mice were clearly lighter. Thus, overall increased animal weight was apparently due to fat deposits, while they seemed to have weaker musculature (see carcasse to body weight ratio in Table 4-1). The bones of the homozygous KO mice were also more fragile, and less elastic, for example the skull not only appeared thinner but also splintered easily upon dissection.

Investigations of mice at postnatal day 16 (p16) did not reveal any detectable changes in the brain at this stage, when the tremor phenotype was already manifest. Enlargement of the brain appears to be a developmental problem, possible a trial compensate for some other yet unknown defects.

Dissections of heterozygous and homozygous Pur $\alpha$  KO mice of all other organs did not display any abnormality.

Mouse Nr.	Geno-type	Sex	Age (days)	Total weight (g)	Length (nose-tail end) (cm)	Brain (g)	Abdominal fat (g)	Subcutaneous fat (g) (%)	Carcasse (g) (%)
1	WT	m	63	18,7	8,1	0,5532	0,2714	0,0581 (0.3%)	8,3085 (44%)
2	WT	m	59	22,9	8,7	0,4395	0,8966	0,3348 (1.4%)	9,2336 (40%)
3	WT	f	66	16,5	7,8	0,4552	0,9419	/	7,8828 (47%)
4	WT	f	66	18,0	8,1	0,4779	1,0435	/	8,6373 (48%)
5	+/-	m	63	24,8	9,2	0,649	0,4574	0,3805 (1.5%)	10,489 (42%)
6	+/-	f	59	23,6	8,9	0,5395	1,0949	1,1625 (4.9%)	9,0301 (38%)
7	+/-	f	59	19,5	8,9	0,54	0,7005	0,8073 (4.1%)	7,8392 (40%)
8	K.O.	f	66	29,5	9,2	0,6905	3,0804	3,505 (11.8%)	10,7601(36%)
9	K.O.	f	66	23,0	8,7	0,6636	2,4072	1,7595 (7.6%)	9,2584 (40%)
10	K.O.	f	59	19,0	8,3	0,7536	1,0112	1,1018 (5.8%)	6,5386 (34%)
11	K.O.	f	59	15,9	7,9	0,6971	0,623	0,6856 (4.3%)	5,6863 (35%)
12	K.O.	m	57	14,8	8,2	0,6916	0,2971	0,4906 (3.3%)	5,6377 (38%)
13	K.O.	m	63	14,8	7,2	0,7208	0,4888	0,7702 (5.2%)	5,1619 (34%)

Table 4-1: Weight of mice organs. (% means the organ to body weight ratio.)

#### 4.1.6 Clinical investigations

Clinical chemistry with the blood serum was performed with 60-66 day old wild type, heterozygous and homozygous KO mice. While most parameters were unchanged, triglycerides levels and glucose levels were strongly reduced but alkaline phosphatase levels were elevated. Surprisingly, although obesity was observed, there was no increase in cholesterol level while triglycerides level was decreased (Table 4-2).

The blood of 60-day-old wild type (1 female and 2 males), heterozygous (2 females and 2 males) and homozygous KO (2 females and 1 male) mice were analysed by blood smears. These blood smears showed an increased amount of lipid droplets in heterozygotes and homozygotes; however, this phenotype was more severe in homozygotes. Moreover, the degree of lipid droplets in female KO mice is more severe than male KO mice.

Parameter	Unit	WT		+/-		K.O.	
		X	s	X	s	X	s
NA	mmol / l	137,33	1,15	137,00	1,41	136,40	3,29
K	mmol / l	5,00	0,50	4,80	0,00	4,94	0,51
Ca	mmol / l	2,20	0,10	2,40	0,00	2,42	0,15
CL	mmol / l	89,33	1,15	90,00	0,00	85,60	3,29
PHOS	mmol / l	2,63	0,12	2,65	0,35	2,72	0,31
TP	g / dl	5,07	0,23	5,00	0,28	4,96	0,43
CREA	mg / dl	0,27	0,06	0,25	0,07	0,24	0,05
HST	mg / dl	44,67	6,43	29,00	7,07	23,20	4,87
HSR	mg / dl	1,53	0,81	0,90	0,14	0,92	0,41
CHOL	mg / dl	157,33	17,24	121,00	7,07	158,00	38,94
TG	mg / dl	130,67	74,57	168,00	2,83	87,60	35,76
CK	U / l	620,00	675,43	127,00	1,41	403,20	570,53
GPT	U / l	10,67	1,15	8,00	2,83	12,80	3,03
GOT	U / l	45,33	20,13	25,00	4,24	52,80	20,96
AP	U / l	247,33	33,84	360,00	53,74	489,00	139,62
AMY	U / l	3371,33	354,21	3101,00	151,32	3321,60	406,95
GLUC/S	mg / dl	172,00	19,08	176,00	2,83	117,20	23,05

Table 4-2: Parameters measured using the blood serum. NA: sodium; K: potassium; Ca: calcium; CL: chloride; PHOS: anorganic phosphate; TP: total protein; CREA: creatinine; HST: urea; HSR: uric acid; CHOL: cholesterol; TG: triglycerides; CK: creatinine kinase; GPT: glutamic-pyruvic transaminase; GOP: glutamic-oxaloacetic transaminase; AP: alkaline phosphatase; AMY:  $\alpha$ -amylase; GLUC: glucose.

#### 4.1.7 Shorter life span of Pura knock-out mice

Normally, a mouse can live up to 1-2 years. In our study it has been shown that the homozygous  $Pur\alpha$  KO mice have shorter life span than the heterozygous and wild type mice. It was observed that 10 out of 45  $Pur\alpha$  KO mice went to natural death at different postnatal day while the heterozygotes and wild type animals lived normally. 6 KO mice died between postnatal days 20-25, which suggests this period just after the onset of tremor phenotype is a critical phase for the survive of KO mice. Many of KO mice in this phase had to be injected



with glucose once or more to help them survive. After this period, 3 other KO mice died between postnatal days 40-65. The two oldest female KO mice died between 5-6 months, still persistently shaking. However, no wild type and heterozygous mice have died. Up to now, the reason for the shorter life span is not yet clear.

#### 4.1.8 Histological staining

Cryostat sections of paraformaldehyde perfused brains from a Pur $\alpha$  KO and a wild type mouse were analyzed using three different histological stainings: HE staining (labels nuclei and plasma), Sudan black (lipid staining), and myelin sheaths staining. Micrographes were taken from three areas: anterior commissure, facial nerve, and pyramidal tract.

As shown in Figure 4-24 (see color pictures in page 138 - 140), HE staining did not show any difference between KO and wild type mice. Interestingly, Sudan black staining displayed stronger labeling of brain tissue of KO mice, especially the myelin. In addition, labeling of myelin sheaths resulted in a slightly reduced staining of myelin in KO brain tissue. The increased Sudan black staining in combination with the slightly reduced labeling of the myelin sheaths suggests the presence of more lipids in the brains of KO animals.

#### 4.1.9 Detection of MBP levels in Pura knock-out mice

Mice mutated for the myelin basic protein (MBP) displayed a severe tremor phenotype beginning at day 11-15 postnatally, which is comparable to that of Pur $\alpha$  knock-out mice. In addition, Pur $\alpha$  has been shown to be able to increase transcription of the MBP promoter both *in vitro* and *in vivo* (Haas *et al.*, 1995). Therefore, the level of MBP was detected by Western-blot analysis using mice of 16 days postnatally. The mice were divided into male and female groups. For every group, brain stems from wild type, heterozygous, and homozygous Pur $\alpha$  KO mice were prepared for protein extractions (3.10.3).

0.05  $\mu$ g of whole protein extract were loaded on a 15% SDS gel, which was blotted on a PVDF membrane with blot buffer at 30 V for 12 hrs. The blot was immunoprobed with a primary monoclonal anti-MBP antibody followed by goat anti-rat peroxidase conjugated anti-IgG+IgM (Sigma) and enhanced Chemiluminescence detection. In the meantime, a 12% SDS gel was loaded with 30  $\mu$ g of whole protein extract for a Pur $\alpha$  Western-blot. As shown in Figure 4-25, the MBP level in KO mice is about half of that in heterozygous and wild type mice, independently of the sex. The corresponding Pur $\alpha$  Western-blot shows the genotypes of the mice.

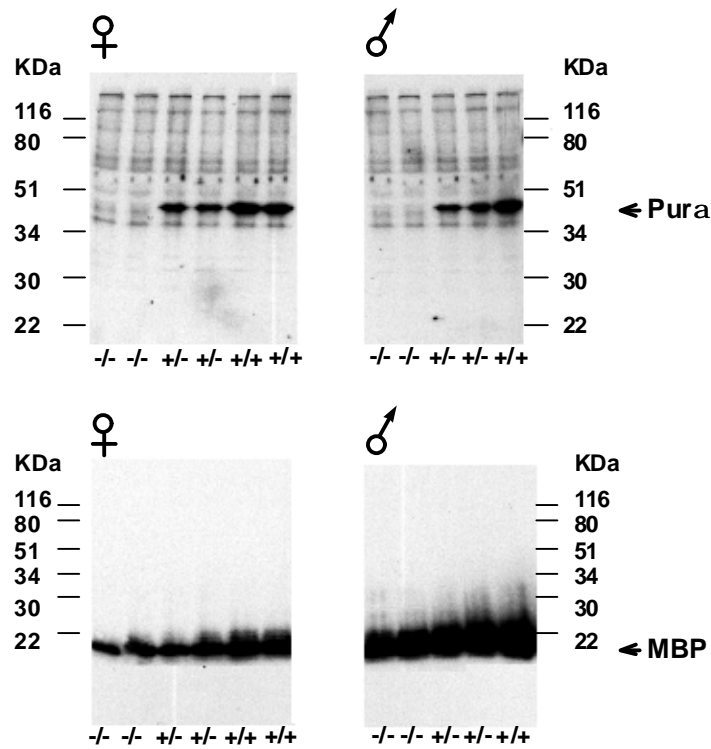


Figure 4-25: Detection of MBP level of 16-day-old mice by Western-blot. Lane 1 and 2: KO mice, lane 3 and 4: heterozygous mice, lane 5 and 6: wild type mice. The upper panel shows MBP Western-blot and the bottom panel shows Pur $\alpha$  Western-blot. Left Western-blot of the female mice group are shown and right of the male mice group.

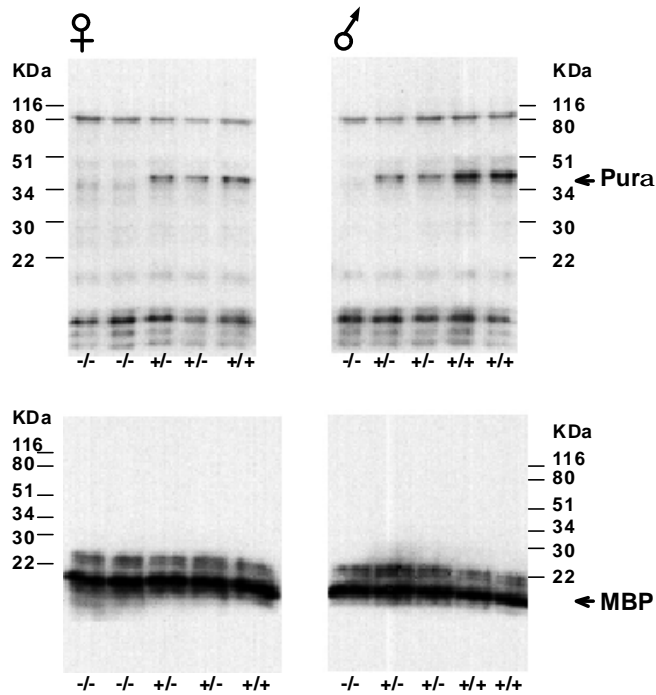


Figure 4-26: Detection of MBP level of 60-day-old mice by Western-blot. Lane 1 and 2: KO mice, lane 3 and 4: heterozygous mice, lane 5 and 6: wild type mice. The upper panel shows MBP Western-blot and the bottom panel shows Pur $\alpha$  Western-blot. Left Western-blot of the female mice group are shown and right of the male mice group.

Thereafter, the MBP level in 60-day-old mice was detected as above, to see if the adult mice have also a decreased MBP level. As shown in Figure 4-26, the MBP level of KO, heterozygous and wild type mice are indistinguishable, which suggests the restoration of MBP levels between postnatal days 16-60.

## 4.2 Biochemical characterization of Pura

Accidentally, Pur $\alpha$  was identified as a DNA helicase in our laboratory. Therefore, the detailed analysis to characterize its helicase activity was carried out.

### 4.2.1 DNA unwinding activity of Pura purified from calf thymus

Pur $\alpha$  protein was purified from calf thymus in our lab as described by Jurk et al (1996). After elution from the fourth column (DNA affinity chromatography) the Pur $\alpha$  fraction was nearly homogen. The protein was dialyzed (3.10.11.4) and tested in unwinding assay.

For the unwinding assay substrate Hel1/M13 was generated as described in 3.10.12.1.1. Hel1 is a 17-mer oligonucleotide, which was radioactively labeled and annealed to single-stranded M13mp19 phage DNA to create a partial duplex. A total of 10 pmol of oligonucleotide was labeled at the 5'-end with T4 polynucleotide kinase. 1.875  $\mu$ g of M13mp19 ssDNA was annealed to the labeled 17-mer overnight. Non-hybridized oligonucleotide was removed by gel filtration through a Sepharose 4B column.

For the unwinding reaction about 40 ng of purified Pur $\alpha$  protein was incubated with the substrate in a reaction mix containing ATP and Mg<sup>2+</sup> ions. As controls, substrate was incubated without protein (no unwinding, Figure 4-27 lane 1) and loaded directly on the gel or heated 5 min at 98°C prior to loading (complete unwinding, lane 3). The unwinding reactions were subjected to a 12% native PAA gel to separate the free, unwound 17-mer oligonucleotide from the annealed partial duplex. Signals were detected using a Phosphor Image.

As shown in Figure 4-27, native Pur $\alpha$  purified from calf thymus is capable to unwind at least a 17 bp duplex DNA. For further analysis of Pur $\alpha$  DNA unwinding assay we decided to use in *E. coli* expressed GST-Pur $\alpha$  fusion protein, particularly because GST protein can be expressed in high amounts and purified easily.

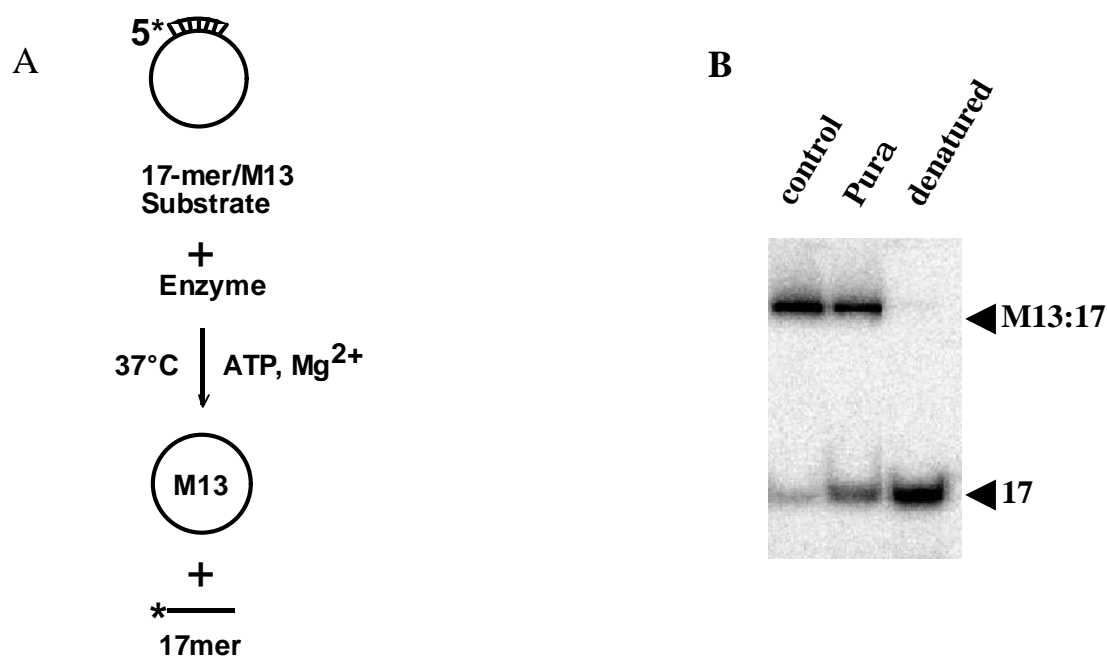


Figure 4-27: (A) Scheme of a DNA unwinding assay. (B) Helicase assay with purified Pura from calf thymus. dsDNA unwinding reaction was carried out for 30 min at 37 °C with 40 ng of purified Pura and <sup>32</sup>P labeled 17-mer/M13 DNA substrate. Reaction mix contains 2.5 mM ATP, 1.0 mM MgCl<sub>2</sub>, 1.0 mM DTT. Reaction was terminated by adding 4 µl of 5 x buffer (see 3.10.13.2). The products were separated on a 12% native polyacrylamid gel. The 'control' lane corresponds to a reaction without enzyme and the 'denatured' lane to heat denatured substrate.

#### 4.2.2 Cloning Pura cDNA in the expression vector pGEX4T1

A very simple and fast method to get high amount of a protein is to express it as fusion protein with *Schistosoma japonicum* Glutathion-S-Transferase (Smith *et al.*, 1986). For the expression of a GST-fusion protein, different pGEX-vectors were developed by Smith and Johnson (1988), each of them contains an open reading frame encoding GST, followed by unique restriction endonulease sites for *EcoRI*, *BamHI* and so on for in frame cloning, followed by termination codons in all three frames.

To clone human Pura cDNA into pGEX4T1, a PCR was carried out using primers HelM2-A and HelM1-C1 to amplify Pura cDNA from 1-322 aa. To simplify the cloning process, both of the primers were designed containing a link sequence to introduce a restriction site into the amplified PCR fragment. HelM2-A contains an *EcoRI* recognition site and HelM1-C1 a *SalI* recognition site. After PCR (3.6.2), PCR fragments were digested directly with these two enzymes and cloned into pGEX4T1, without changing the open reading frame. The plasmid was proved by sequencing analysis and was ready for expression and purification of GST-Pura fusion protein.

### 4.2.3 Expression of GST-Pur $\alpha$ fusion protein in *E. coli* and its purification

The purification of Pur $\alpha$  from calf thymus is a complicated and time-consuming process. To get a big amount of Pur $\alpha$  protein, GST-Pur $\alpha$  was expressed and purified from *E. coli*.

For the expression of GST-Pur $\alpha$  fusion protein, the *E. coli* culture in logarithm growth was induced with 100  $\mu$ M IPTG for 3 hrs (see 3.10.11.1). The bacterial pellet was washed, resuspended in 10 ml lysis buffer on ice and lysed using a sonicator. After centrifuging, the GST-fusion protein was purified from supernatant through incubated with pre-equilibrated glutathione-sepharose beads.

Binding of glutathione-S-transferase to glutathione-sepharose is very strong and firm; therefore the glutathione-sepharose could be washed with high volumes of wash buffer containing 1 M NaCl to wash away any unspecific bound proteins. (3.10.12.2). The GST-Pur $\alpha$  was eluted 3 times with 100 mM glutathione, which competes for the binding of the fusion protein to glutathione-sepharose. Figure 4-28 shows the purified fusion protein and GST as a control. GST has a molecular weight of 27.5 kDa, and Pur $\alpha$  of 42 kDa. The fusion protein was dialyzed with Mes 6.5 dialyze-buffer overnight at 4°C (3.10.12.4). It was important to aliquot the protein in small volume and stored at -80°C. The protein should not be thawed more than 3 times.

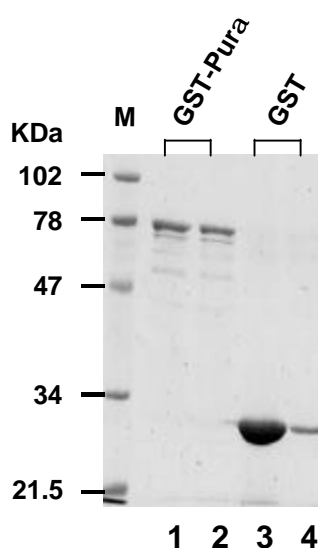


Figure 4-28: SDS polyacrylamid gel electrophoresis of purified GST fusion protein. M is protein standard (Biorad). The first two lanes show 200 ng of purified GST-Pur $\alpha$ . As a control, purified GST protein was loaded in the Lane 3, and 1:10 diluted GST was loaded in lane 4, which shows the same amount as the purified GST-Pur $\alpha$ .

The molecular mass of GST-Pur $\alpha$  fusion protein is 69.5 kDa. In fact, the main band of GST-Pur $\alpha$  on a SDS gel ran at about 70 kDa (lane 1 and 2). Co-purification of small amounts of

partially degraded GST-Pur $\alpha$  could not be avoided and a few degradation bands could always be seen on the SDS gel. Since GST alone was expressed much more efficient than GST-Pur $\alpha$ . Before using it as a control in DNA unwinding assays, the GST protein was diluted 1:10 (Figure 4-28).

#### 4.2.4 DNA-binding activity of GST-Pura

To test whether the GST-Pur $\alpha$  protein can be purified in an active form, we tested its DNA binding activity. Therefore, EMSAs were performed to test if GST-Pur $\alpha$  is capable of binding to single-stranded oligonucleotide Ori-1 coding for the lower strand of the origin of replication of the Bovine Papilloma Virus. Oligo nucleotide Ori-1 was end labeled (see 3.7.1). 25 fmol of purified Ori-1 was incubated with 200 ng of GST-Pur $\alpha$  protein (see 3.10.7). All binding assays were performed with a vast excess of unlabeled poly(dI-dC) to eliminate nonspecific DNA binding. Identical amount of purified GST was used as a negative control. Figure 4-29 shows the protein/DNA-complex formed exclusively by GST-Pur $\alpha$ , whereas GST alone displayed no DNA binding activity at all.

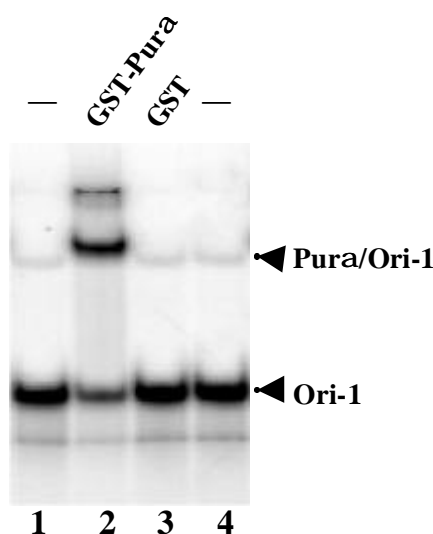


Figure 4-29: DNA-binding activity of GST-Pur $\alpha$ . The GST-Pur $\alpha$  protein was incubated with 25 fmol 5'-end-labeled oligonucleotide Ori-1 in binding buffer (3.10.7). Lane 1 and 4: no protein added; Lane 2: GST-Pur $\alpha$ ; Lane 3: GST as a negative control.

#### 4.2.5 dsDNA unwinding activity of GST-Pura

To analyze DNA unwinding activity of GST-Pur $\alpha$  protein, 17-mer/M13 was generated and used as substrate (3.10.13.1). Unwinding reaction was carried out as described in 3.10.13.2. As shown in Figure 4-30, purified GST-Pur $\alpha$  was capable of unwinding the 17-mer/M13 complex. Only incubation with the recombinant GST-Pur $\alpha$  protein resulted in the appearance

of free oligonucleotide whereas incubation of the substrate with comparable amounts of GST alone did not result in any DNA unwinding.

Therefore we concluded, that the GST-Pur $\alpha$  protein expressed in *E. coli* displayed identical DNA binding and unwinding activity compared to native Pur $\alpha$  and can be used for further analysis of Pur $\alpha$  enzymatic activity.

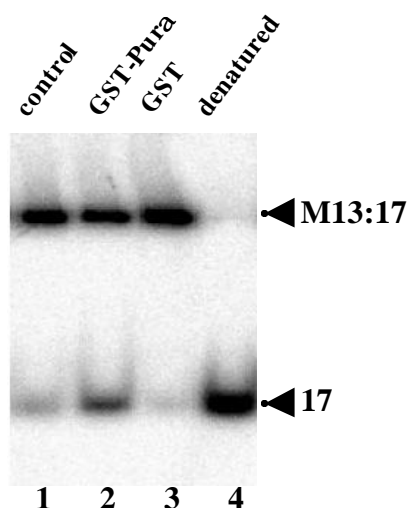


Figure 4-30: Unwinding reaction was carried out for 30 min at 37°C with 200 ng of purified GST-Pur $\alpha$  and  $^{32}\text{P}$  labeled 17-mer/M13. Lane 2 is GST-Pur $\alpha$ , and lane 3 is GST as negative control. The 'control' lane corresponds to a reaction without enzyme and the 'denatured' lane to that with a substrate heated at 95°C for 5min.

#### 4.2.6 Titration of amount of GST-Pura for maximal unwinding activity

The amount of GST-Pur $\alpha$  was increased in the unwinding reaction to identify the optimal amount of fusion protein in the unwinding assay. 50 ng to 1500 ng GST-Pur $\alpha$  were used. Figure 4-31 shows that at least 150 ng of GST-Pur $\alpha$  is necessary to detect its unwinding activity.

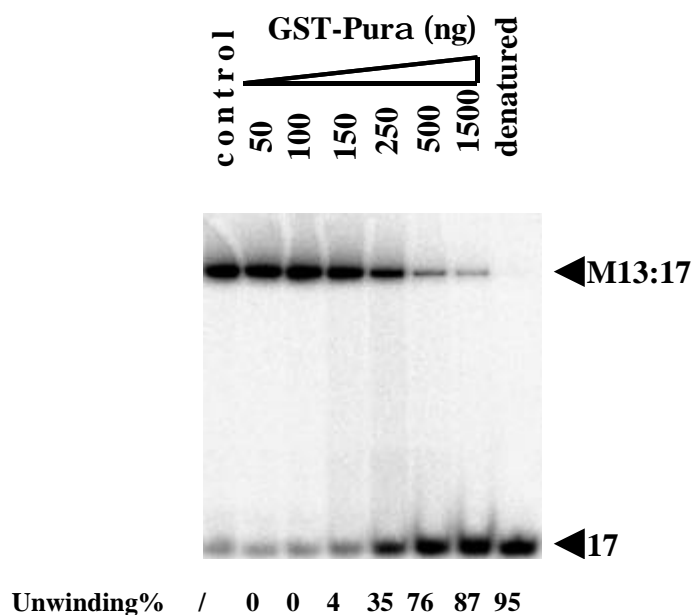


Figure 4-31: Titration of the amount of GST-Pur $\alpha$  required for maximal unwinding activity. The panel shows the autoradiographical evaluation of the experiment. The amount of GST-Pur $\alpha$  is indicated at the top of each lane. Percentage of unwinding for every lane is indicated at the bottom.

#### 4.2.7 dsDNA unwinding activity with various substrates

To further characterize Pur $\alpha$  DNA unwinding activity we generated different DNA substrates (3.10.13.1). As shown in Figure 4-32, Pur $\alpha$  was tested with different substrates in unwinding assay. We constructed substrates containing a poly(dT)<sub>15</sub> overhang at the 3' or 5'-end of the 17-mer respectively, thereby forming a fork-like structure. GST-Pur $\alpha$  was capable of unwinding both types of substrates with no significant higher efficiency compared to the tail-less 17-mer (Figure 4-32 D and E). However, unwinding capacity of Pur $\alpha$  decreased dramatically if the hybrid region of tail-less substrate was increased to 25 bp (Figure 4-32 B). While 90% of the 17-mer substrate was unwound, the same amount of protein could only unwind 7% of a substrate containing a 25-mer. If the duplex was increased to 32 bp, no unwinding was detected.

In addition, we used a linear substrate to test the unwinding capacity of Pur $\alpha$ . A 17-mer was annealed to the 5' or 3' end of a 101 bp single-stranded oligonucleotide to generate a duplex region with a blunt end and a 5' or 3' overhanging end respectively. A third 17-mer was annealed to the middle of the 101 bp oligonucleotide resulting a duplex with 5' and 3' overhanging ends. Pur $\alpha$  was capable of unwinding all three different substrates with no obvious differences (Figure 4-32 F-H). However, a duplex 17-mer with both sides blunt ended was not unwound by Pur $\alpha$  (Figure 4-32 I). Assuming that Pur $\alpha$  is not capable of



unwinding duplexes starting from a blunt end, the unwinding experiments using substrates of Figure 4-32 F and H indicates that Puro $\alpha$  has no directionality for strand displacement.

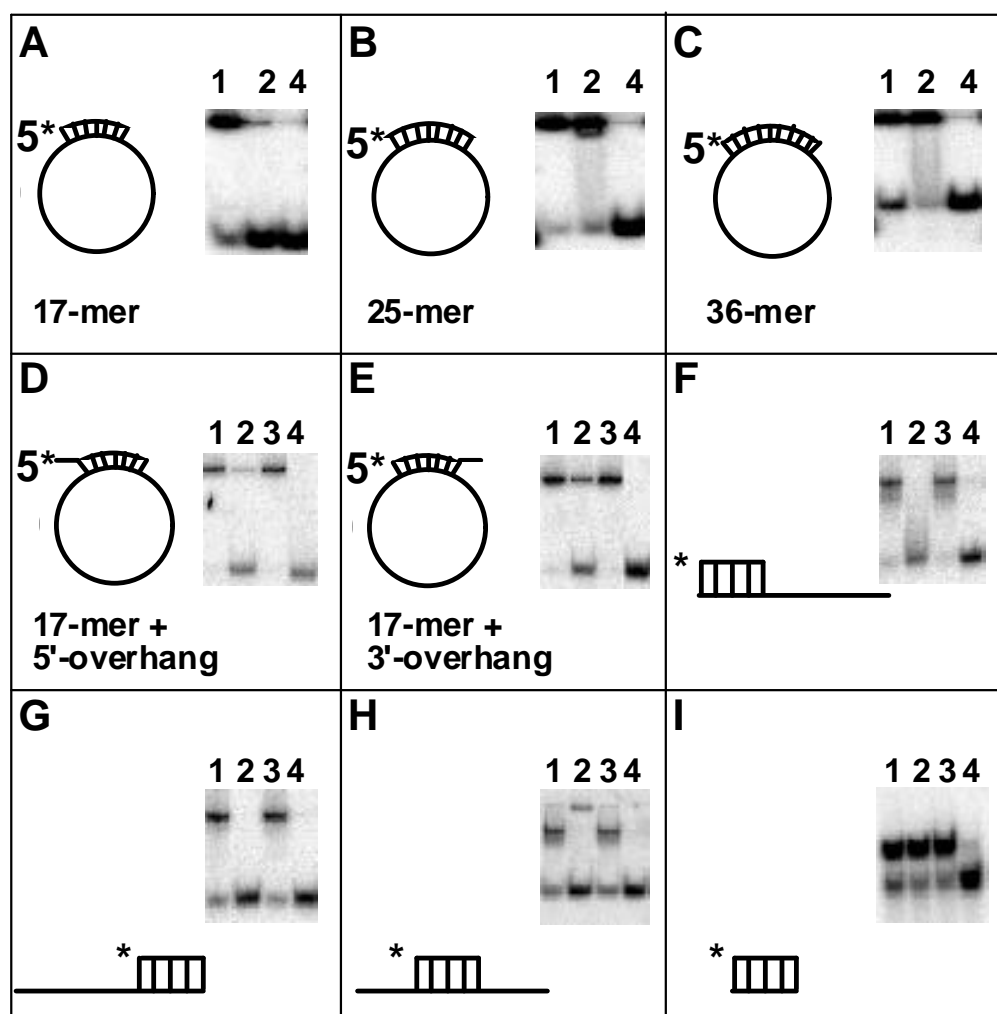


Figure 4-32: DNA unwinding assay with various substrates. The star indicates the labeled end. In all experiments, 200 ng of GST-Puro $\alpha$  was used. Lane 1 and 4: no protein added; Lane 2: GST-Puro $\alpha$ ; Lane 3: GST as a negative control.

#### 4.2.8 Pura DNA Unwinding activity is not influenced by ATP or Mg<sup>2+</sup> concentration

The results obtained in the unwinding assay described above raised evidence that Puro $\alpha$  might display a DNA helicase activity. All helicases known are dependent on DNA binding and hydrolysis of a nucleoside 5'-triphosphates (NTP or dNTP). Therefore, ATP, CTP, GTP, TTP, dATP, dCTP and dUTP were tested in unwinding assay. Strikingly, GST-Puro $\alpha$  could unwind the double-stranded DNA without hydrolyzing NTPs or dNTPs (Figure 4-33).

To verify this result that Pur $\alpha$  DNA unwinding activity is independent on NTPs or dNTPs, the experiment was repeated twice and always led to the same result.

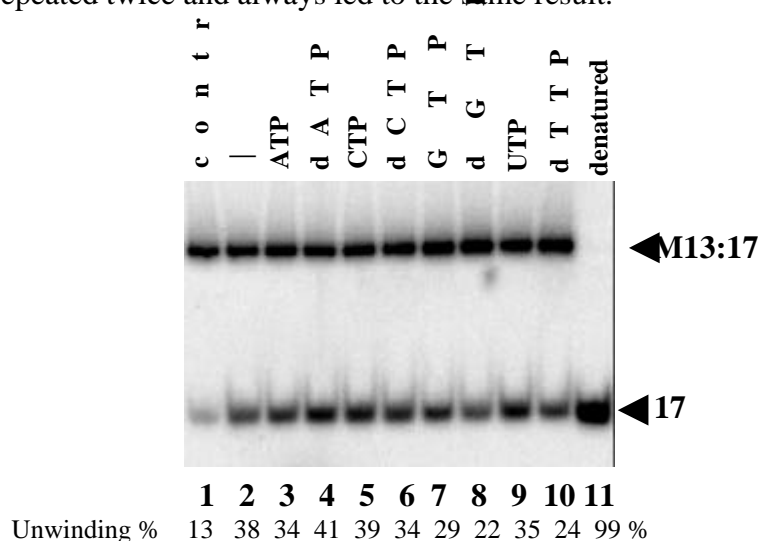


Figure 4-33: Effect of NTP and dNTP on DNA unwinding activity. GST-Pur $\alpha$  was dialyzed to 25 mM MES (pH 6.5), 0.1 mM EDTA, 50 mM NaCl, 1.0 mM DTT, 5 mM MgCl<sub>2</sub> prior to use. NTPs and dNTPs were added to 5 mM. Percentage of unwinding is shown in the bottom.

To avoid experimental artifacts GST-Pur was dialyzed against a buffer containing no Mg<sup>2+</sup> ions and ATP. The dialyzed fraction was used in DNA binding and DNA unwinding assays, supplemented with Mg<sup>2+</sup> and/or ATP or lacking Mg<sup>2+</sup> and ATP. Strikingly, adding Mg<sup>2+</sup> ions to 5 mM to the DNA binding reaction resulted in a slight decrease in DNA binding activity (Figure 4-34 A, lane 1 and 2), while addition of ATP to 5 mM significantly increased DNA binding activity of the Pur $\alpha$  protein (Figure 4-34 A, lane 3). If ATP and Mg<sup>2+</sup> were added together, only a slight effect on DNA binding was observed (Figure 4-34 A, lane 4). In contrast, addition of Mg<sup>2+</sup> ions, ATP, or Mg<sup>2+</sup> and ATP only poorly influenced DNA unwinding activity of Pur $\alpha$  (Figure 4-34 B, lane 1-4).

These results indicate a mechanism that Pur $\alpha$  DNA unwinding activity is independent of any dNTP and NTP hydrolysis.

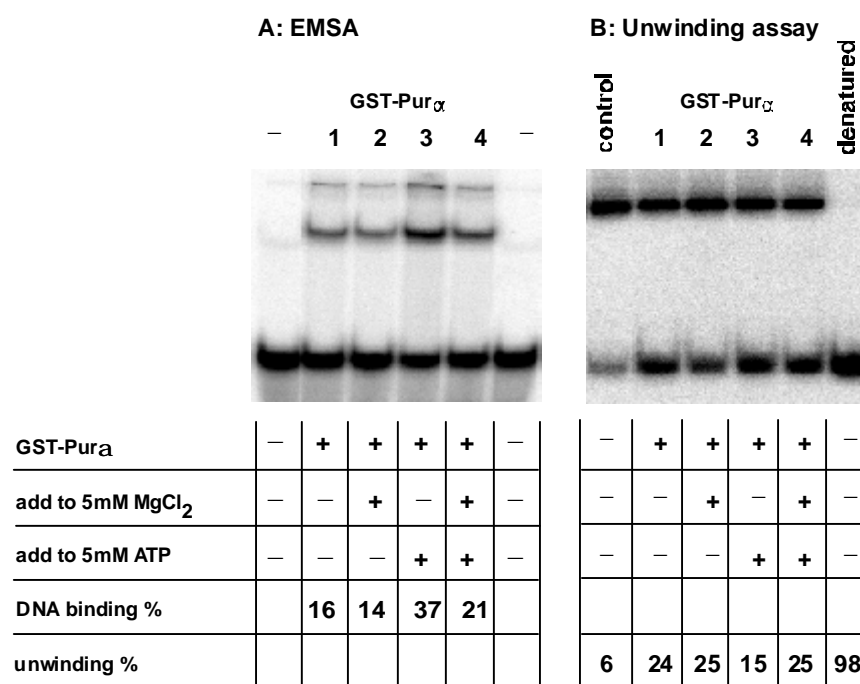


Figure 4-34: Influence of Mg<sup>2+</sup> and ATP on GST-Pur $\alpha$  DNA binding and unwinding activity. (A) Influence of Mg<sup>2+</sup> and ATP on GST-Pur $\alpha$  DNA binding activity. GST-Pur $\alpha$  was dialyzed to 25 mM MES (pH 6.5), 0.1 mM EDTA, 50 mM NaCl, 1.0 mM DTT prior to use. Dialysis buffer did not contain Mg<sup>2+</sup> and ATP. Binding reaction was adjusted to 150 mM NaCl. MgCl<sub>2</sub> and ATP were added as indicated. (B) Influence of Mg<sup>2+</sup> and ATP on GST-Pur $\alpha$  DNA unwinding activity. GST-Pur $\alpha$  was dialyzed as described in (A). DNA unwinding reactions were performed in a buffer containing 20 mM MES (pH 6.5), 1.0 mM DTT. MgCl<sub>2</sub> and ATP were added to the reaction as indicated.

#### 4.2.9 Pura unwinding activity can be inhibited by specific oligonucleotides

Pur $\alpha$  binds single-stranded DNA in a sequence-specific manner. One of the bound oligonucleotide is PUR1, which contains a purine rich motif originally identified by Bergemann and Johnson (1992). Pur $\alpha$  does not bind the unrelated oligonucleotide Mage11-2. To test whether Pur $\alpha$  strand displacement activity can be inhibited by its binding to specific oligonucleotides, we performed unwinding assays in the presence of specific or unspecific oligonucleotides. Addition of 2 pmol PUR1 oligonucleotide completely abolished DNA unwinding activity whereas addition of an identical amount of unspecific Mage11-2 oligonucleotide did not influence unwinding activity (Figure 4-35). These results indicated that the unwinding activity of Pur $\alpha$  is coupled with the DNA binding activity and could be abolished by an excess of oligonucleotides containing sequences specifically bound by Pur $\alpha$ .

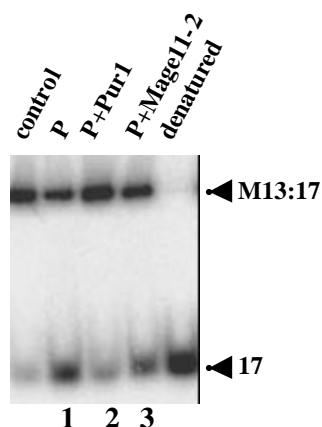


Figure 4-35: Specific oligonucleotides inhibit Pur $\alpha$  unwinding activity. Unwinding reaction was performed as described in Figure 4-27. 2 pmol competitor oligonucleotides were added to the reaction mix prior to addition of the protein. Lane 1: 200 ng of GST-Pur $\alpha$ , no competitor added; Lane 2: 200 ng of GST-Pur $\alpha$ , 2 pmol PUR1 added; Lane 3: 200 ng of GST-Pur $\alpha$ , 2 pmol Mage11-2 added.

#### 4.2.10 Generation of different GST-Pur $\alpha$ deletion mutants

As shown in Figure 4-36, Pur $\alpha$  is composed of several modular domains (Bergemann *et al.*, 1992; Bergemann, 1992). The central region contains three aromatic and basic repeats (class I) interspersed with two acidic leucine-rich repeats (class II). In addition to this central repeat region, Pur $\alpha$  possess an amino terminal glycine-rich region, an amphipathic  $\alpha$ -helix, and a glutamate-glutamine rich region near the carboxy terminus. To identify the regions responsible for DNA binding and dsDNA unwinding activity, a series of N- and C-terminal deletion mutants fused to GST were generated and tested in DNA binding and dsDNA unwinding assays.

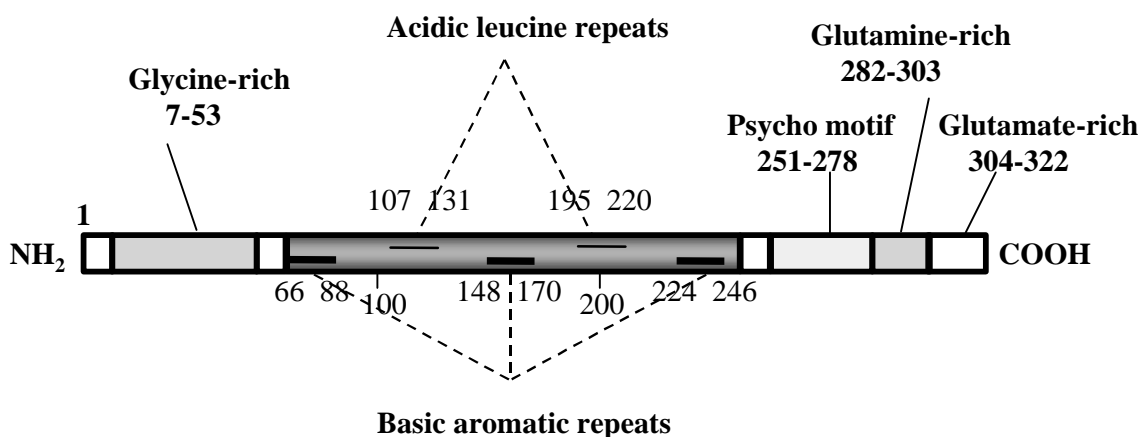


Figure 4-36: Schematic structure of Pur $\alpha$ .

Firstly, according to the Pur $\alpha$  cDNA sequence, different pairs of primers were designed, with which different long Pur $\alpha$  cDNA fragments were amplified. Most of the primers have an annealing temperature of 54°C, therefore different primer combinations could be used to amplify different Pur $\alpha$  cDNA fragments. Sense primers contain an additional *EcoRI* recognition site, and antisense primers an additional *SalI* recognition site. Addition of these two restriction sites ensured the correct orientation of the PCR-fragments cloned into the pGEX4T1 vector without changing the Pur $\alpha$  reading frame. Pur $\alpha$  cDNA is 1049 bp long and consists of 322 amino acids. pCDNA3-Pur $\alpha$ .ext plasmid containing full length of Pur $\alpha$  cDNA was used as a template to amplify truncated Pur $\alpha$  cDNA fragments. PCR was performed as in 3.6.2. Altogether 16 truncated human Pur $\alpha$  cDNA variants were amplified using 16 pairs of primers (see Table 8-4 in appendix). The schematic representation of the truncated Pur $\alpha$  cDNA fragments is shown in Figure 4-38.

The different Pur $\alpha$  fragments were cloned into the *EcoRI* and *SalI* restriction sites of the vector pGEX4T1 resulting in in-frame fusion of the truncated Pur $\alpha$  cDNAs to GST sequence. Correct cloning of the fragments was verified by sequencing.

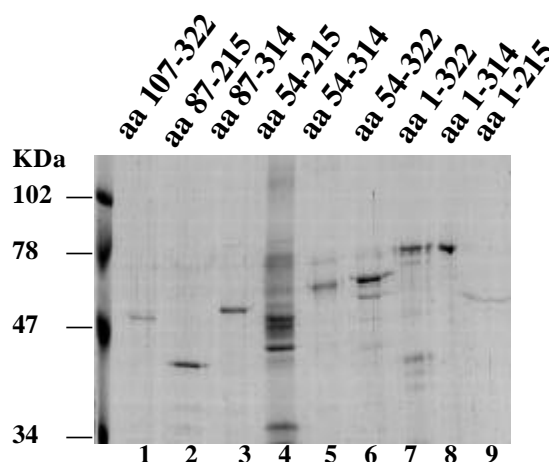


Figure 4-37: Various GST-Pur $\alpha$  deletion mutants were purified from bacteria *E. coli* TOP10F' and analyzed on SDS-PAGE. Pur $\alpha$  amino acids fused to GST are indicated at the top of the lanes.

Various truncated GST-Pur $\alpha$  proteins were expressed in *E. coli* TOP10F' and purified as described in 3.10.12. The purified proteins were dialyzed with Mes (pH 6.5) buffer overnight at 4°C (3.10.12.4) and the correct size of the fusion proteins was confirmed by SDS-page. Figure 4-37 shows nine truncated GST-Pur $\alpha$  variants after purification from *E. coli*. It was necessary to aliquot the proteins in small volumes and store at -80°C. The proteins should not be thawed more than 3 times; otherwise, they lost their unwinding activity. N-terminal truncated GST-Pur $\alpha$ , for example, GST-Pur $\alpha$  54-322, and 74-322 are not stable at 4°C and

began to degrade 4 days after dialyze. After one week at 4°C, the proteins could not be detected on a SDS gel any more.

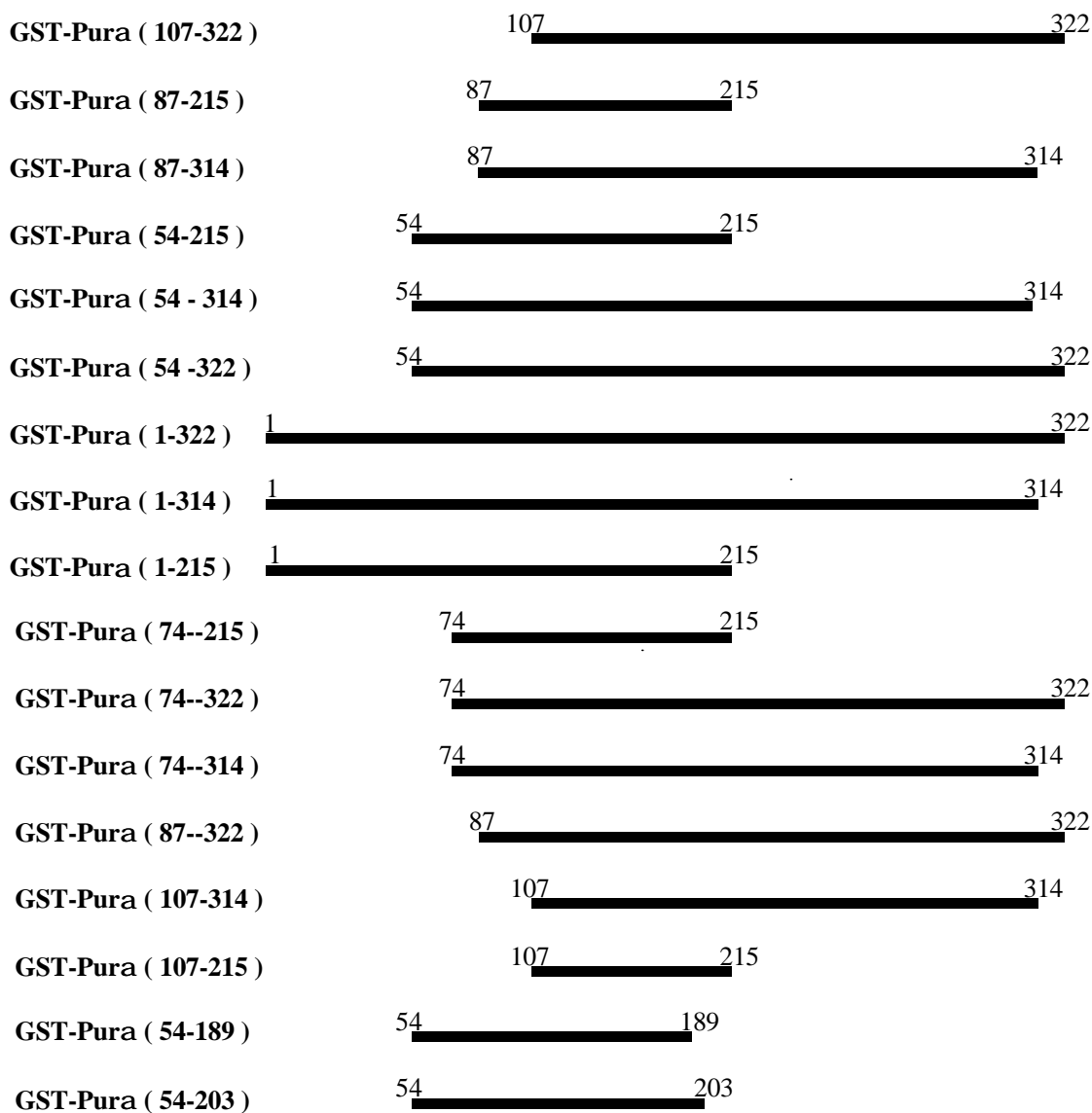
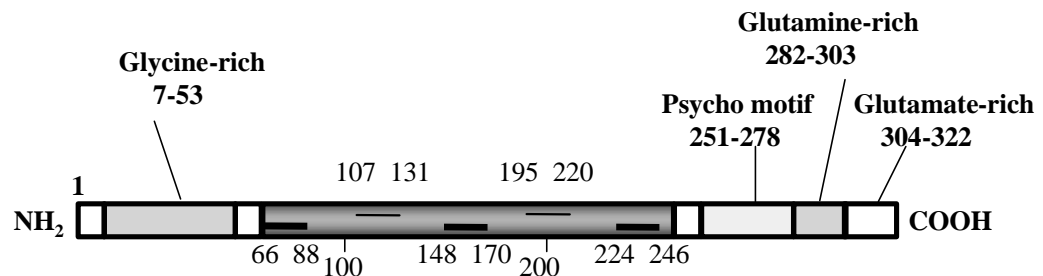


Figure 4-38: Schematic representation of the various human Purα cDNA fragments.

#### 4.2.11 DNA binding activity with different deletion mutants

The series of deletion mutants described above was utilized to determine protein domains involved in binding to the Pur $\alpha$  recognition element. The same amount of proteins was used in the assays to compare their activities.

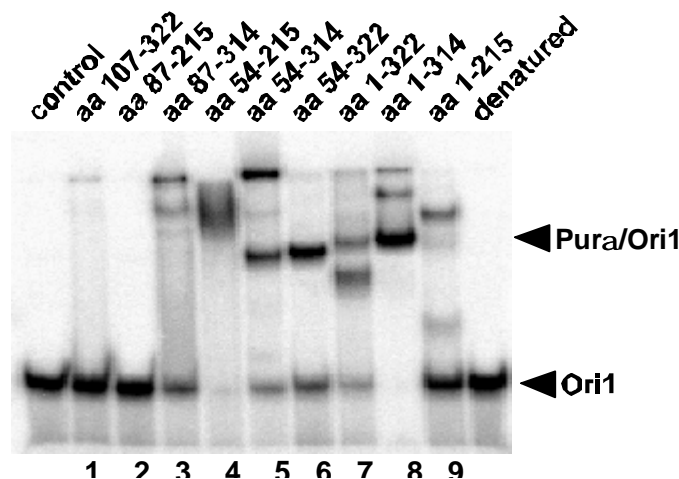


Figure 4-39: Autoradiography of a gel band-shift analysis carried out on an 8% polyacrylamid gel. Purified GST-Pur $\alpha$  mutants were used in DNA binding assays as described in 3.10.7 using  $^{32}\text{P}$  labeled oligonucleotide Ori-1.

As shown in Figure 4-39, deletion of eight C-terminal amino acids (Pur $\alpha$  1-314) led to greatly increased DNA binding activity of Pur $\alpha$  as compared to the full-length protein (Pur $\alpha$  1-322) (Figure 4-39, lanes 7 and 8). Pur $\alpha$  1-215, deleted for 107 C-terminal amino acids, still displayed significant DNA binding activity (Figure 4-39, lane 9). However, the most prominent complex formed by Pur $\alpha$  1-215 and the Pur $\alpha$ /oligonucleotide migrated slower as compared to wild-type, indicating that this deletion protein formed a multimeric complex on the DNA. Deletion of 53 N-terminal amino acids (Pur $\alpha$  54-322) did not affect DNA binding activity of Pur $\alpha$  (Figure 4-39, lane 6), but deletion of these 53 N-terminal aa in the protein missing the eight C-terminal aa (Pur $\alpha$  54-314) seemed to increase tendency to multimeric complexes, since a weak, slower migrating band is visible in this lane (Figure 4-39, lane 5). If the N-terminus was truncated for 86 aa in this context (Pur $\alpha$  87-314), only a very slowly migrating complex was detectable (Figure 4-39, lane 3). Deletion of 106 N-terminal aa of the full-length protein (Pur $\alpha$  107-322) almost completely abolished DNA binding activity (Figure 4-39, lane 1). To define the domain of Pur $\alpha$  essential for DNA binding, we combined N- and C-terminal truncations. While Pur $\alpha$  87-215 displayed no DNA binding activity (Figure 4-39, lane 2), Pur $\alpha$  54-215 showed significant DNA binding (Figure 4-39, lane 4), although the formed complex migrated slowly, indicating formation of a multimeric complex. Some more truncated GST-Pur $\alpha$  proteins (Pur $\alpha$  74-215, Pur $\alpha$  74-322, Pur $\alpha$  74-314, Pur $\alpha$  87-322, Pur $\alpha$  107-314, Pur $\alpha$  107-215, Pur $\alpha$  54-189, Pur $\alpha$  54-203) were also tested in EMSAs (data not

shown) and the results were summarized in Table 4-3. From the data described above it can be concluded that the core domain of Pur $\alpha$  for DNA binding is from aa 54 to 215. Further aa deletion resulted in the complete loss of DNA binding.

#### 4.2.12 dsDNA unwinding activity with different deletion mutants

The same set of truncated GST-Pur $\alpha$  mutants was used in dsDNA unwinding assays. For these unwinding assays the 17-mer/M13 substrate was used and about equal amount of the truncated proteins were added to the unwinding reactions.

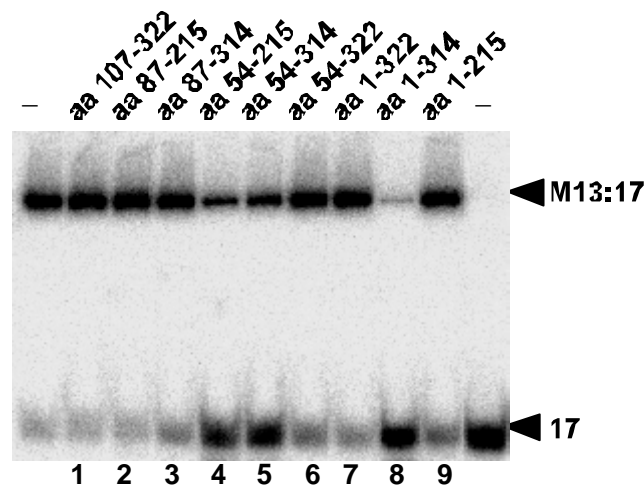


Figure 4-40: Autoradiograph of an unwinding assay carried out on a 12% polyacrylamid gel. Purified GST-Pur $\alpha$  mutants were used in DNA binding assays as described in 3.10.13.2 using 17-mer/M13 substrate.

The results of the DNA unwinding assays are shown in Figure 4-40. Strikingly, it was found that DNA binding and unwinding activity correlated exactly: all truncated Pur $\alpha$  mutants displaying DNA binding activity also unwound the 17-mer/M13 substrate. Increased DNA binding capacity resulted in increased unwinding activity (Figure 4-40). This was most obvious for GST-Pur $\alpha$  1-314 (Figure 4-40, lane 8), that unwind 82% of the substrate while full-length GST-Pur $\alpha$  1-322 (Figure 4-40, lane 7) could only unwind 6.3% of the duplex in this assay. The shortest protein still displaying DNA unwind capacity was GST-Pur $\alpha$  54-215 (Figure 4-40, lane 4). The dsDNA unwinding activity of the different truncated Pur $\alpha$  versions is summarized in Table 4-3. These results suggested that domain 54-215 be essential not only for DNA binding but also for the unwinding activity. Therefore, we concluded that DNA unwinding capacity of Pur $\alpha$  depends on its DNA binding ability.



#### 4.2.13 Self-Association of Pura

It has been described that Pur $\alpha$  is able to self-associate (Gallia *et al.*, 1999; Muralidharan *et al.*, 1997). To investigate if DNA binding/unwinding activity is dependent on the self-association of Pur $\alpha$ , pull-down assays were carried out.

[ $^{35}$ S]-labeled full-length Pur $\alpha$  protein was synthesized *in vitro* using the TNT<sup>®</sup> Quick Coupled Transcription/Translation Systems (Promega) as described in 3.10.10. The plasmid pCDNA3 Pur $\alpha$ .ext containing a T7 promoter and the complete Pur $\alpha$  cDNA was used as template. The synthesized [ $^{35}$ S]-labeled Pur $\alpha$  protein is shown in Figure 4-41 (Figure 4-41, lane 2).

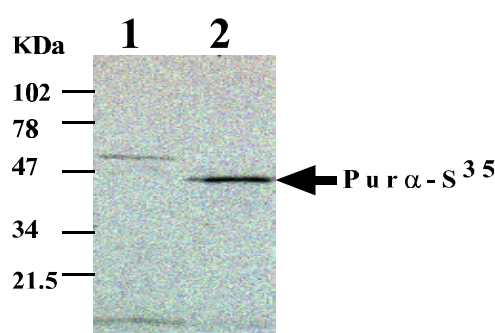


Figure 4-41: SDS-PAGE of *in vitro* transcribed and translated Pur $\alpha$ -S $^{35}$ . Lane 1: no DNA added; Lane 2: 1.0  $\mu$ g of pCDNA3 Pur $\alpha$ .ext added.

In the pull-down assay, [ $^{35}$ S]-labeled full-length Pur $\alpha$  protein was *in vitro* synthesized as described above. Full-length or truncated GST-Pur $\alpha$  proteins were immobilized on glutathione-sepharose and incubated with [ $^{35}$ S]-labeled full-length Pur $\alpha$  protein. After incubation, the glutathione-sepharose beads were washed as described in 3.10.11. The proteins immobilized on glutathione-sepharose were eluted with 2 x SDS gel loading buffer and analyzed by SDS-PAGE and autoradiography. As controls GST alone and GST-Prp<sup>C</sup> fusion protein were used.

Firstly, a pull-down assay was performed using the full-length GST-Pur $\alpha$  protein. As it can be seen in Figure 4-42 (lane 1), full-length Pur $\alpha$  was able to self-associate. The negative controls GST alone or GST-Prp<sup>C</sup> could not associate with the full-length Pur $\alpha$  (Figure 4-42, lane 6, 7, 12 and 13), indicating that interaction of  $^{35}$ S labeled Pur $\alpha$  with GST-Pur $\alpha$  was specific.

Thereafter, to investigate which domain of Pur $\alpha$  is essential for its self-association, the same set of truncated GST-Pur $\alpha$  proteins used in DNA binding and unwinding assays were tested in pull-down assays. The results are shown in Figure 4-42. The smallest protein displaying self-association activity was GST-Pur $\alpha$  54-215. This domain also was essential for DNA binding and unwinding activity. Moreover, all truncated proteins displaying DNA binding and

unwinding activity were able to self-associate. The DNA binding and unwinding activity and self-association ability of various GST-Pur $\alpha$  mutants were summarized in Table 4-3.

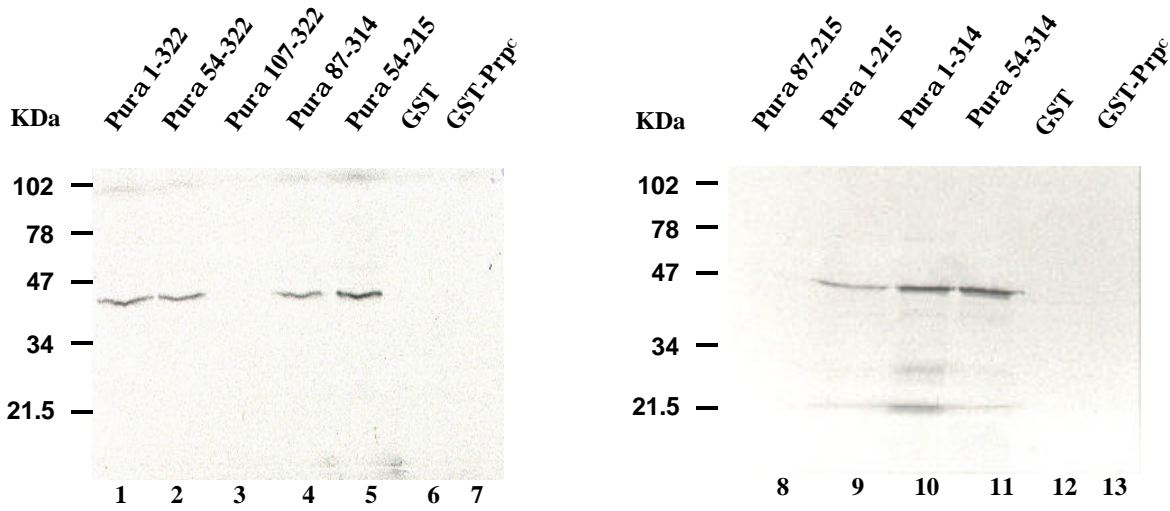
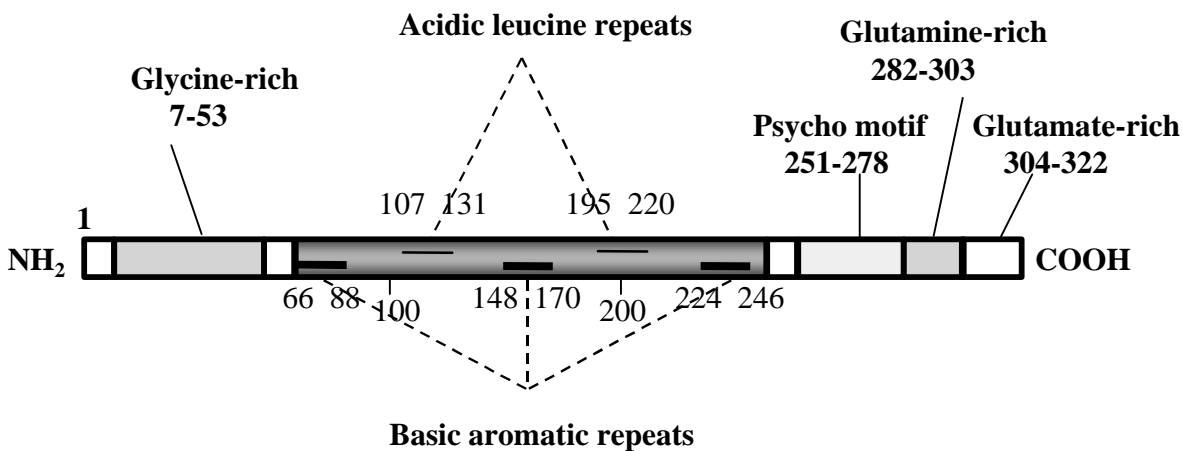


Figure 4-42: Localization of the Pur $\alpha$  self-association region. [<sup>35</sup>S]-labeled Pur $\alpha$  synthesized by *in vitro* transcription and translation was incubated with GST, GST-Prp<sup>C</sup>, GST-Pur $\alpha$ , or various truncated GST-Pur $\alpha$  proteins immobilized on glutathione-sepharose. The bound proteins were fractionated by SDS-PAGE and visualized by autoradiography.

The functional studies of the Pur $\alpha$  deletion mutants clearly indicated that the ability to bind DNA and the DNA unwinding activity of the protein could not be separated. In addition, self-association capacity seem to correlate with DNA-binding and DNA unwinding ability which might suggest that self-association should be an essential feature for DNA binding and unwinding.



<b>Nr.</b>	<b>GST-Purα deletion mutants</b>	<b>DNA binding activity</b>	<b>DNA unwinding activity</b>	<b>Pull-down</b>
1	GST-Purα ( 107-322 )	no	no	no
2	GST-Purα ( 87-215 )	no	no	no
3	GST-Purα ( 87-314 )	+ ( m.a. )	+	yes
4	GST-Purα ( 54-215 )	++ ( m.a. )	+++	yes
5	GST-Purα ( 54-314 )	+++	+++	yes
6	GST-Purα ( 54-322 )	+	++	yes
7	GST-Purα ( 1-322 )	++	++	yes
8	GST-Purα ( 1-314 )	++++	++++	yes
9	GST-Purα ( 1-215 )	++ ( m.a. )	+++	yes
10	GST-Purα ( 74--215 )	no	no	/
11	GST-Purα ( 74--322 )	+ ( m. a )	+	/
12	GST-Purα ( 74--314 )	+ ( m. a )	+	/
13	GST-Purα ( 87--322 )	+ ( m. a )	+	/
14	GST-Purα ( 107-314 )	no	no	/
15	GST-Purα ( 107-215 )	no	no	/
16	GST-Purα ( 54-189 )	no	no	/
17	GST-Purα ( 54-203 )	no	no	/

(m.a. means mutimeric aggregates; “/” means no test)

Table 4-3: Summary of the DNA binding activities, unwinding activities and dimerization ability of various GST-Purα mutants.

## 5 Discussion

As known, Pur $\alpha$  is a 39 kDa sequence specific single-stranded DNA/RNA-binding protein with the ability to modulate transcription of several genes containing the Pur element in their promoter region. Pur $\alpha$  has been implicated in diverse cellular functions, including transcriptional activation, DNA replication and cell growth.

In this study, two independent sets of experiments were carried out to analyze its biological functions: (i) Pur $\alpha$  KO mice were generated and the phenotypes were characterized; (ii) Pur $\alpha$  was at the first time characterized as a dsDNA unwinding enzyme.

### 5.1 The generation of *Pura* knock-out mice

Gene knock-out techniques have been used widely to study the functions of gene products. This procedure replaces a gene with another piece of DNA (usually a selection marker) by homologous recombination in pluripotent embryonic stem cells. Embryonic stem cells in which homologous recombination has occurred are injected into blastocysts or 8-cell stage embryos to produce chimeric mice. Homozygous mice in which the desired gene has been disrupted can be obtained by breeding and interbreeding.

To generate the Pur $\alpha$  knock-out construct, the isolation and characterization of the murine Pur $\alpha$  genomic DNA was firstly performed. A 129/SvJ Mouse Genomic Library in Lambda FIX II vector was used to isolate the Pur $\alpha$  genomic DNA. Two independent phages p5/1 and p14/2 were found. About 25 kb of genomic Pur $\alpha$  sequence were analyzed with different restriction enzymes and sequenced partially. Murine Pur $\alpha$  is composed of two exons and one intron, which is located within the 5'-UTR after bp 388 from the 5'- end of the gene. Exon II contains the remaining 5'-UTR, the translational start site, the ORF and the 3'-UTR. The open reading frame located on the second exon from nucleotides 519 to 1485. Thereafter, in comparison with murine Pur $\alpha$  cDNA sequence, exon/intron junctions were also determined. Figure 4-11 shows the nucleotide composition of the Pur $\alpha$  gene at the junctions of exon I and exon II. A restriction map for murine Pur $\alpha$  genomic structure was generated as shown in Figure 4-10, which was taken as the basis for designing and generating a targeting vector for homologous recombination. These results are in agreement with the Pur $\alpha$  genomic structure published subsequently by Muralidharan (Muralidharan *et al.*, 2000).

On the basis of the known Pur $\alpha$  genomic structure, a replacement vector for homologous recombination was designed. In order to increase the targeting frequency we decided to use the positive-negative selection strategy (Mansour *et al.*, 1988), which enriches for homologous recombination events by simultaneously selection for Neo-resistance and against

a herpes simplex virus thymidine kinase (HSV-TK) gene placed at the 3' end of the targeting sequence. Moreover, it has been shown that the length and sequence of the homologous sequences in the vector will affect the targeting frequency (A.L.Joyner, 1999). The homologous sequences in the vector ranging from 5-8 kb can increase the targeting frequency. Furthermore, the design of such a replacement vector should also consider the screening strategy: The screening by PCR requires the selection marker to be inserted at an asymmetric location near one end of the homologous sequence, creating vectors with one long arm and one short arm. To guarantee sufficient homology for formation of a cross-over, the minimum sequence of homology of the short arm has to be about 0.5-2.0 kb (A.L.Joyner, 1999).

According to the principles outlined above, the replacement vector for deleting Pur $\alpha$  in mice was generated. Its structure is shown in Figure 4-14. This replacement vector consists of two homologous arms, a Neo cassette for positive selection and a TK cassette for negative selection. *In vivo*, exon II containing the whole Pur $\alpha$  open reading frame should be replaced by the neo gene due to homologous recombination. Thus, the Pur $\alpha$  KO mice generated with such a vector will not express a truncated Pur $\alpha$  protein. The left homologous arm is 1.2 kb long, which allows screening of the positive ES clones by PCR. The right arm is 7.0 kb, which is long enough to ensure high targeting rates.

Another key factor for efficient homologous recombination is the use of isogenic DNA to generate the targeting vector. Isogenic DNA results in a four to five times higher recombination rate (Deng and Capecchi, 1992) and a 25-fold higher efficiency at the targeting locus as compared to constructs generated from non-isogenic DNA (van Deursen and Wieringa, 1992). In our laboratory, E14 ES cells derived from mouse strain 129/Ola were used for electroporation. It was reported recently and after the characterization of the genomic Pur $\alpha$  locus that the mouse strain 129/SvJ is a genetically contaminated substrain (Threadgill *et al.*, 1997). Therefore, to ensure the highest possible homologous recombination frequency, the two homologous arms of the targeting vector were amplified by PCR from genomic DNA of E14 ES cells.

Since not all ES cells are transfected and the frequency of homologous recombination is low, it was necessary to enrich for cells with homologous recombination. The neomycin phosphotransferase (*neo*) gene driven by the phosphoglycerate kinase-1 (Pgk-1) promoter can be selected by geneticin (G418) (positive selection) (Mansour *et al.*, 1988), which was applied for cells that had integrated the targeting vector in their genome. In the second step, the herpes simplex virus thymidine kinase (HSV-tk) gene can be used in a selection employing gancyclovir (GNAC) (negative selection). This selection was exerted against cells with a random insertion of the construct (Mansour *et al.*, 1988).

To confirm that the ES cell clones surviving both selections were the results of homologous targeting events and not of random insertion, it is necessary to characterize these cell lines by either PCR or Southern-blot analysis.

Out of 2400 ES cell clones tested, 1900 were screened by PCR. PCR with genomic DNA did not work sometimes, maybe due to the impure genomic DNA obtained from ES cells. Therefore, the PCR products on agarose gel were always blotted onto membranes and then hybridized with a DNA probe for further analysis. The remaining 500 ES clones were screened directly by Southern-blot analysis. One positive ES clone (ES clone 223) was identified by PCR analysis and one positive ES clone (ES clone 248) was identified by Southern-blot analysis. The corresponding two positive ES cell clones were thawed and Southern-blot analysis with the 5'-, 3'- and Neo probes was carried out separately. Both ES clones showed the expected two bands (WT band 13.5 kb and KO band 6.4 kb) with the 5'-probe. In addition, ES clone 248 displayed the correct two bands (WT band 13.5 kb and KO band 7.1 kb) with the 3'- probe while ES clone 223 only displayed the 13.5 kb band corresponding to the wild type allele (Figure 4-16). Moreover, the aberrant ES clone 223 displayed two bands with the Neo probe, indicating two integration events of the targeting vector while the correct positive ES clone 248 displayed only one band with the correct size (data not shown). Thus, ES clone 223 was unsuitable for further use. Analysis of ES clone 223 clearly shows the importance of analyzing both, the 3'- and 5'- aspects of the target locus using external probes from sequences flanking both ends of the vector. An internal Neo probe which hybridized to the selectable marker was used to distinguish between a single gene replacement and multiple integration events of the entire vector.

Mutated ES clones created by gene targeting *in vitro* can be transmitted through the germ-line of a chimera since ES cells correspond closely to the cells of the inner cell mass (ICM) of the blastocysts (Beddington and Robertson, 1989) and differentiate in association with normal mouse embryos, participating in the formation of all tissues of chimeras, including the gametes (Bradley, 1990). There exist several different techniques to introduce ES cells into pre-implantation embryos, such as blastocyst injection, morula injection, morula aggregation, and aggregation with tetraploid cells (A.L.Joyner, 1999). In our laboratory the E14 ES cells, which have the chinchilla ( $Tyr^{c-ch}$ ) alleles at the albino locus were injected routinely into albino BALB/c mice. Eight chimeras (7 female mice and 1 male mouse) with 30-95% chimerism were born. One chimera was found dead after birth. The live born chimeras did not show any abnormality upon eye inspection. The female chimeras were mated with male chimera separately and only the male chimera gave agouti color of pups, which might indicate germ line transmission. 50% of the agouti mice should be heterozygous mice, which were detected by Southern-blot or PCR analysis. Heterozygous mice were then intercrossed to

generate mice homozygous for the targeted allele (KO). Genotype analysis of 132 offspring analyzed at 2 months of age revealed the expected 2:1:1 ration between heterozygous, wild type, and homozygous KO mice, which confirmed to classical Mendelian inheritance (Capecchi, 1989).

As a final proof for the correct targeting of the  $Pur\alpha$  locus, Western-blot analysis for  $Pur\alpha$  expression in wild type, heterozygous and homozygous KO mice was carried out.  $Pur\alpha$  was found to be expressed widely in the mouse brain, especially abundant in the cerebral cortex and cerebellum although it is also found in many other cells and tissues (Osugi *et al.*, 1996). Immunohistochemical studies demonstrated  $Pur\alpha$  protein expression in the Purkinje neurons and granular cells of the mouse cerebellum (Osugi *et al.*, 1996). In addition, in the Purkinje neurons,  $Pur\alpha$  was located in both the nucleus and cytoplasm of the cells. According to its distribution, total protein extractions were prepared from the cerebral cortex of wild type, heterozygous and homozygous mice and analyzed by Western-blot using anti- $Pur\alpha$  monoclonal antibody.  $Pur\alpha$  was not detected in homozygous KO mice while the level of  $Pur\alpha$  in heterozygous mice was approximately 50% as compared to wild type mice (Figure 4-20).

## **5.2 Analysis of the phenotypes of *Pura* knock-out mice**

$Pur\alpha$  KO mice were normal at birth but developed various abnormalities later in life. At postnatal day 12-14 (p12-14) a severe and continuous tremor phenotype was observed in KO mice, while the heterozygous mice did not show this phenotype. The tremor phenotype continued until the mouse was sacrificed or natural death occurred. The brains of  $Pur\alpha$  KO mice were significantly enlarged and the brain weight obviously increased. In addition,  $Pur\alpha$  KO mice possessed more fat layers than wild type mice.

The following sections will introduce and discuss the most notable phenotypes of  $Pur\alpha$  KO mice, namely:

- 1) Why do the  $Pur\alpha$  KO mice display a tremor phenotype?
- 2) Analysis and explanation of the enlarged brains of  $Pur\alpha$  KO mice.

### **5.2.1 Decreased MBP levels in 16-day-old *Pura* KO mice - The explanation of tremor phenotype?**

As mentioned above,  $Pur\alpha$  KO mice display a severe and continuous tremor phenotype. This tremor phenotype is very similar to the *shiverer* (*shi*) mice that lack myelin basic protein (MBP). Significantly, in addition to many other genes,  $Pur\alpha$  is involved in developmental and cell-specific transcriptional control of MBP (Haas *et al.*, 1995). In mice, six isoforms of

MBPs (14kDa, 17.2kDa, 17.3kDa, 18.5kDa, 20.2kDa and 21.5kDa) have been identified (Campagnoni and Skoff, 2001).

MBP is a major component of the myelin sheath in the central nervous system (CNS) (Campagnoni and Macklin, 1988). The primary cell biological function of MBPs is to maintain the structure of the myelin sheath (Campagnoni and Skoff, 2001). The myelin sheath is a multilamellar, spirally wrapped extension of the plasma membrane of oligodendrocytes in the central nervous systems (CNS) and of Schwann cells in the peripheral nervous systems (PNS). The development of the mature myelin structure in both CNS and PNS is fundamentally similar and myelin serves as an insulator to facilitate the conduction of neuronal impulses along the axon. MBPs are considered to be located at the major dense line of myelin. Due to their localization, MBPs are thought to play an important role in the compaction of the myelin sheath. The deletion of the MBP gene in mouse leads to severe dysmyelination and a severe tremor phenotype.

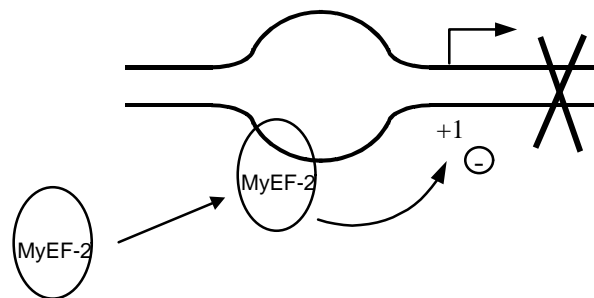
The expression of MBP is controlled both cell- and stage-specific during brain development (Kristensson *et al.*, 1986; Sorg *et al.*, 1987; Verity and Campagnoni, 1988). In the CNS, myelin formation and MBP gene expression occur in oligodendrocytes, whereas in the PNS, Schwann cells are responsible for myelin formation and expression of the MBP gene (Mikoshiha *et al.*, 1991). Myelin formation occurs postnatally in the mouse, such that the MBP mRNA is first detected at the end of the first postnatal week, increases dramatically to peak at 18-21 days, and decreases to about 20% of the peak levels in mature animals (Carson *et al.*, 1983). Earlier studies have indicated that programmed expression of MBP is regulated at the level of transcription (Shiota *et al.*, 1991; Zeller *et al.*, 1984). Functional dissection of the MBP regulatory sequence had led to the identification of a regulatory motif, named MB1, which spans from nucleotide -14 to -50 with respect to the transcription start site (Mukherjee and Chambon, 1990). Analysis of nuclear proteins derived from mouse brain identified a 39 kDa protein that forms a nucleoprotein complex with a DNA fragment containing the MB1 sequence. This protein was identified as Pur $\alpha$ . Pur $\alpha$  was shown to be able to recognize the GGC/GGA rich sequences within MB1 DNA and functionally increase transcription of the MBP promoter both *in vitro* and *in vivo* (Haas *et al.*, 1995).

Pur $\alpha$  interacts also with MyEF-2, which is a single-stranded DNA-binding protein and binds to the MB1 sequence, thereby down-regulating the transcription of MBP (Muralidharan *et al.*, 1997). The interaction between Pur $\alpha$  and MyEF-2 was shown to determine the binding of these proteins to their target DNA sequences within the MB1 motif. There is no evidence for the association of MyEF-2 and Pur $\alpha$ , suggesting that transient communication of these two cellular proteins with each other, or together with their target DNA sequence may determine their interaction with the myelin basic protein promoter element. These observations may



have a functional significance in the programmed expression of the MBP gene during brain development. Of interest, Pur $\alpha$  binding activity to the MB1 sequence occurs in a developmental stage-specific manner that coincides with the pattern of MBP transcription (Haas *et al.*, 1995). It was indicated that at the early stage of brain development (day 3-7, postnatally), the level of Pur $\alpha$  association with MB1 is extremely low, whereas during the phase of myelination (18-20 days) and in adult (day 30), its binding activity to MB1 is increased drastically. It was noted that the levels of Pur $\alpha$  increase at day 10 and remained virtually constant thereafter (Tretiakova *et al.*, 1998). It was also demonstrated that the peak of MyEF-2 expression is detected at the early stages of brain development (7 days postnatal), decreases during the phase of myelination, and remains at low level throughout the animal's life (Muralidharan *et al.*, 1997). Therefore, a model was generated by Muralidharan, in which the association of MyEF-2 with MB1 at the early phase of brain development when the level of Pur $\alpha$  is low suppresses myelin basic protein gene transcription. At a later stage increased level of Pur $\alpha$  then displaces MyEF-2 and results in stimulation of the MBP gene (Figure 5-1).

**Before Myelination:**



**During Myelination:**

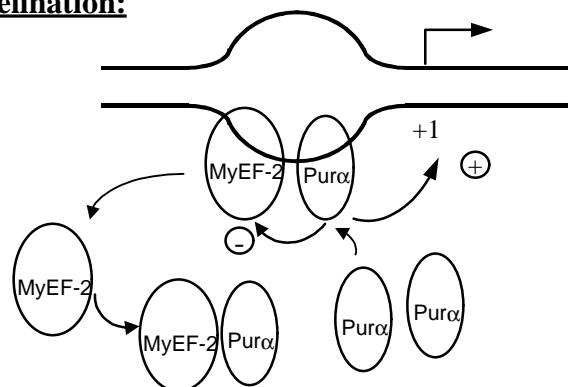


Figure 5-1: Proposed model for involvement of Pur $\alpha$  and MyEF-2 in programmed transcription of the MBP promoter. Before myelination, the binding of MyEF-2 to its target DNA sequence within the MBP promoter exerts negative effects on transcription of the MBP gene. During the phase of myelination, which is concomitant with high level of expression of Pur $\alpha$ , Pur $\alpha$  binding to its motif

within the MB1 dissociates MyEF-2 from the promoter sequence and augments transcription of the MBP gene.

The *shiverer* mouse, a natural formed mutant, lacks MBP completely. Similar to Pur $\alpha$  KO mice *shiverer* mice display a more severe tremor phenotype starting at day 12-15 postnatally. Different from the Pur $\alpha$  KO mice, *shiverer* mice developed convulsions and died between 50-100 days (Chernoff, 1981). However, Pur $\alpha$  KO mice did not have convulsion and was able to live to about 5-6 months. The MLD mouse which is deficient in MBP due to a natural occurred recombination creating an antisense copy of the MBP gene, have a similar phenotype, but live somewhat longer (Mikoshiha *et al.*, 1991). Interestingly, transgenic *shiverer* mice provide an adequate amount of myelin sufficient for a behavioural rescue (Popko *et al.*, 1987; Readhead *et al.*, 1987). Here the transgene is inserted at random therefore only being expressed at about 25% of normal levels, but this was enough to relieve all clinical phenotypes.

According to the above described model, Pur $\alpha$  protein seems to stimulate the transcription of the MBP gene upon binding to the MB1 motif and results in the dissociation of MyEF-2 from the MB1 sequence. Therefore, deletion of Pur $\alpha$  might result in a lack of stimulation of MBP expression and thereby in a decrease in MBP level in the brain of the Pur $\alpha$  KO mice. To analyse whether the tremor phenotype of the Pur $\alpha$  KO mice maybe caused by a dramatic decrease of MBP concentration as described for *shiverer* or MLD mice, we investigated MBP levels in Pur $\alpha$  KO mice brains.

It was shown that MBPs levels in the brain stem of 16-days-old homozygous Pur $\alpha$  KO mice were significantly reduced, but not in heterozygous and wild type mice (Figure 4-25). Both male and female Pur $\alpha$  KO mice displayed the same reduced MBP expression pattern. These results indicate that Pur $\alpha$  affects the expression of MBPs in 16-day-old mice. The mechanism of Pur $\alpha$  regulation of MBP expression remains unclear. We have not yet studied whether the transcripts of MBPs in Pur $\alpha$  KO mice are decreased. According to the model above, it is suggested that the transcription of MBPs may be reduced and thus result in the decreased MBPs expression levels. Surprisingly, there was no difference of MBPs levels between 60-day-old KO mice and wild type mice (Figure 4-26), indicating that the MBP expression was restored between 16-60 days postnatally.

Also correlating with developmentally regulated MBP expression is the synergistic action of Pur $\alpha$  and the ubiquitous DNA binding transcription factor Sp1, which also binds to the MB1 DNA motif at a region partially overlapping the Pur $\alpha$  binding site (Tretiakova *et al.*, 1999). Immunoprecipitation study showed the association of Sp1 and Pur $\alpha$  in nuclear extracts from mouse brain. However, Pur $\alpha$ :Sp1:MB1 complexes have not been detected. In Pur $\alpha$  KO mice,

Sp1 might compensate the function of Pur $\alpha$  and stimulate the expression of MBP in the absence of Pur $\alpha$ .

Although the MBP level in 16-day-old Pur $\alpha$  KO mice was decreased as compared to heterozygous and wild type mice, we cannot conclude that the tremor phenotype of Pur $\alpha$  KO mice is due to the decreased MBP level. In fact, transgenic *shiverer* mice, which express 25% of the normal amount of MBP, provide an adequate amount of myelin sufficient for a behavioural rescue (Popko *et al.*, 1987; Readhead *et al.*, 1987). A comparable result has been obtained with a MBP cDNA construct in transgenic mice, suggesting that one (14K) MBP isoform may be sufficient to serve most of the structural function of the entire protein family (Kimura *et al.*, 1989). Although Pur $\alpha$  KO mice show a comparable tremor phenotype to *shiverer* mice and display reduced MBP level at young age, they still possess 60-70% of wild type amount of MBP. Based on the data described above, this decreased amount of MBP in Pur $\alpha$  KO mice should not lead to tremor phenotype. Our data suggest that the tremor phenotype of Pur $\alpha$  KO mice should not be caused by slightly reduced MBP level but due to some other reasons, which remain unclear.

### 5.2.2 Brain development of Pura knock-out mice

Apart from the tremor phenotype, the most significant difference between Pur $\alpha$  KO and wild type mice is the brain abnormalities: Brains of Pur $\alpha$  KO mice were visibly enlarged and the weight was increased by 30% as compared to wild types. This is mainly due to the enlarged brain stem, whose weight increased by 200% according to the detailed brain analysis of Pur $\alpha$  KO mice. Hippocampus and sensoric cortex of Pur $\alpha$  KO mice were also enlarged but their weights decreased as compared to wild types. The enlargement of the cerebral cortex is accompanied by an increased surface.

A comparable phenotype has not been observed in any dysmyelination mutant mice, including *shiverer* or MLD mice. Moreover, the MLD mice displayed a normal but slightly reduced brain weight compared to wild type (Matthieu *et al.*, 1984). However, such phenotype of enlarged brain is also observed in some other mice models: for example, megencephaly mice, IGF-1 (Insulin-like growth factor I) transgenic mice and the bcl-2 transgenic mice.

The reason for such an enlarged brain can be different, for example, the megencephaly mouse is characterized by an overall hypertrophy of the brain, and not by hyperplasia of particular cell types or by hypertrophy of a singular tissue compartment. Megencephaly also occurs in several acquired and inherited human diseases including Sotos syndrome, Ribinow syndrome, Canavan's diseases, and Alexander disease. This defect can be distinguished from macrocephaly, an enlarged head, which usually occurs as a consequence of congenital

hydrocephalus. Compositional analysis of the brains of the megencephaly mice showed the water as a percentage of brain weight was not different between the two genotypes, excluding edema. Moreover, the ventricles of megencephaly mice were not dilated, ruling out hydrocephalus. Thus, larger brains in the megencephaly mutants are a consequence of increased cell size only. However, the enlarged brains of Pur $\alpha$  knock-out mice are resulted from the increased cell mass as indicated by our new analysis (data not shown). Actually, this enlargement is only a local event, different from the situation in megencephaly mouse.

The IGF-1 transgenic mice have brains that are 55% larger than controls by approximately 2 months of age, with most brain structures affected. However, the increased brain size in transgenic mice results from both increased cell size and increased cell number (Carson *et al.*, 1993). The overexpression of IGF-1 in Pur $\alpha$  KO mice is not possible, since the largement in the brains of Pur $\alpha$  KO mice is not correlated with increased cell number.

The brain size of bcl-2 transgenic mice increased by 50% as compared to wild type animals (Martinou *et al.*, 1994). The bcl-2 gene has a powerful inhibitory action on naturally occurring cell death (NOCD) or apoptosis, which is a prominent feature of the developing nervous system. During this process, the expression of bcl-2 in neurons may determine whether a neuron dies or survives. bcl-2 overexpression reduces neuronal loss during the NOCD period, which leads to increased cell number of the nervous system. For instance, the facial nucleus and the ganglion cell layer of the retina had, respectively, 40% and 50% more neurons than normal. The structures most obviously enlarged are the brain stem and optic nerves (Martinou *et al.*, 1994). These stems in the enlarged brains resemble those in Pur $\alpha$  KO mice where the increased cell number is nonetheless not observed.

Our study shows that a deletion in a single gene, Pur $\alpha$ , can have a dramatic effect on brain size and weight. It was shown that such an enlarged brain is due to the increased cell size but not increased cell number. However, Edema or hydrocephalus cannot be excluded.

The data of fresh wet brain weights showed: (i) The brains of the 60-66 day old Pur $\alpha$  KO mice were significantly heavier than those of wild type; (ii) the brain weight of the heterozygotes resided exactly between the brain weights of the KO and wild type mice. However, the brain weights of 16-day old mice did not differ among the three genotypes. These results indicate that Pur $\alpha$  KO mice demonstrate a significant increase in brain weight beginning from 16 days of age and continuing throughout at least to 66 days of age, while the normal adult brain weight in mice is achieved at approximately 2 weeks of age (Belknap *et al.*, 1992). The further measurement of the brain weight after 66 day postnatally is not carried out and a further continuously increase in brain weight of the KO mice cannot be excluded.

We can also conclude that the tremor phenotype of the Pur $\alpha$  KO mice is not due to the enlarged brain since the onset of tremor begins at postnatal day 12 (p12) while the enlarged brain forms definitively after postnatal day 16 (p16). Moreover, the heterozygotes also have enlarged brains but do not display tremor phenotype. These data suggest that the tremor phenotype might be independent of the enlarged brain and must be due to some other reasons, which are still unclear.

Histological staining of three areas (anterior commissure, facial nerve and pyramidal tract) of the brain of Pur $\alpha$  KO mouse revealed increased lipid staining (Sudan black staining) as compared to wild type. This observation suggests an increased lipid level in the brains of Pur $\alpha$  KO animals. If specific lipids are enriched in brain is unclear. The increased lipid level might be the reason of the brain hypertrophy of the Pur $\alpha$  KO mice. Moreover, histological staining also showed slightly reduced labeling of the myelin sheaths in the brain of KO mouse. Whether it is caused by the reduced level of MBP in the beginning of myelination remains unclear. Altogether, the reduced myelin sheath and increased lipid level in brain suggest an possible changed compositions of the brains and this increased lipid level might affect signal transduction in nervous system, which possibly can lead to the tremor phenotype of the KO mice.

### **5.2.3 Weight development of Pura KO mice**

The weight development significantly differed among the homozygous, heterozygous Pur $\alpha$  KO and wild type mice. The weight loss of the KO animals began with the onset of their tremor phenotype (postnatal day 12-14) and was independent on the sex of the animals. While wild type and heterozygous mice showed continuous weight increase, KO mice showed significant slower weight increase until day 20-25 postnatally (p20-25) (See Figure 4-22). From then on KO mice recovered from weight loss and KO mice reached the same weight as wild type at about p50 (female) or p70 (male). Then homozygous KO males and females started over-proportional weight gain and only lose weight before they died.

Dissection of Pur $\alpha$  KO mice showed that both male and females had increased abdominal and subcutaneous fat layers but interestingly, female mice had much more fat than male mice. Bones and muscle mass of homozygous KO mice were clearly decreased. Moreover, the ration of carcasse to body weight of the KO mice proved also the badly developed muscle as compared to wild type. Thus, overall increased animal weight was apparently due to fat deposits, while they seemed to have weaker musculature (see the ration of carcasse to body weight in Table 4-1). Strikingly, the female KO mice displayed a more significant increase of weight than the males. The KO females were heavier than KO males whereas the wild type male mice were always heavier than females (see Figure 4-22). Heterozygotes, although

showing no tremor phenotype, had amounts of subcutaneous fat and brain weight that lay exactly between homozygous KO and wild type levels (Table 4-1).

There are certain clues that indicate a metabolism disturbance in Pur $\alpha$  KO mice. The clinical chemistry did not display an increased cholesterol level but a decreased triglyceride level. Macroscopically, the blood smear analysis of the Pur $\alpha$  KO mice displayed an increase in fat droplets as compared to the wild type. The degree of such increased fat droplets of the KO females was more severe than that of KO males. The deletion of Pur $\alpha$  in mice might lead to the abnormality of the lipid metabolism in an unknown way, which might also be the reason of the enlarged brain of Pur $\alpha$  KO mice.

Currently available data suggest that Pur $\alpha$  KO mice may have a shorter life span than wild type mice. The two oldest KO mice died between 5-6 months, still shaking persistently. 6 Pur $\alpha$  KO mice died between p20-25 and 3 Pur $\alpha$  KO mice died between p40-65. The shorter life span of Pur $\alpha$  KO mice suggests that Pur $\alpha$  may play a very important role in mouse development.

In summary, the multi-phenotypes of the Pur $\alpha$  KO mice suggest that Pur $\alpha$  should act as a transcription factor that seems to participate in regulating the expression of some genes which are important not only for postnatal brain development but also for basic metabolism.

### **5.3 Helix destabilizing activity of Pura**

Besides the generation of Pur $\alpha$  KO mice, a second important part of this Ph.D thesis was an enzymatic and biochemical characterization of the Pur $\alpha$  protein.

Pur $\alpha$  protein purified from calf thymus was accidentally found to be able to unwind 17-mer/M13 DNA duplex, therefore, the detailed dsDNA unwinding assays were carried out.

In order to obtain large amounts of Pur $\alpha$  protein for functional studies, Pur $\alpha$  cDNA was fused with GST, so that it could be expressed and purified from *E. coli* (Figure 4-27). The GST-Pur $\alpha$  protein displayed identical DNA binding and unwinding activity as compared to native Pur $\alpha$  and therefore could be used for further analysis of Pur $\alpha$  enzymatic activity.

Pur $\alpha$  was able to unwind 17-mer/M13 with high activity but displayed dramatically reduced activity on 25-mer/M13. If the duplex region was increased to 36 bp, no unwinding activity was observed. Moreover, Pur $\alpha$  displayed no preference for fork like structure but was not able to unwind blunt ended 17-mer ds oligonucleotide even at high concentration (see Figure 4-31). Surprisingly, it was found that the DNA unwinding activity of Pur $\alpha$  was independent on nucleoside hydrolysis since Pur $\alpha$  displayed DNA unwinding activity in the presence or in the absence of nucleosides (see Figure 4-33).

Although the majority of proteins with DNA unwinding properties function as helicases, there are some proteins that act as helix destabilizing proteins in an energy independent manner. Many of them are viral proteins like the adenoviral DNA binding protein, DBP (Zijderveld and van der Vliet, 1994) and the Herpes Simplex Virus protein ICP8 (Boehmer and Lehman, 1993). These proteins have been shown to be able to unwind dsDNA without ATP hydrolysis. They miss directionality in their helix destabilizing activity.

Similar to DBP and ICP8, Pur $\alpha$  cannot be described as a helicase since it lacks most of the features common to all helicases (for review see (von Hippel and Delagoutte, 2001)) but can be characterized as helix destabilizing protein (HDP), also called DNA unwinding protein or single-stranded DNA binding protein. All helicases share common biochemical properties, including nucleic acid binding, NTP binding and hydrolysis and NTP hydrolysis-dependent unwinding of duplex nucleic acids (Lohman, 1993). Pur $\alpha$  catalyzed unwinding of dsDNA substrates is energy independent whereas helicase reactions are driven by the hydrolysis of ATP or other nucleosides. Another aspect that distinguishes Pur $\alpha$  from helicases is the lack of directionality. Most helicases have a preferred direction of unwinding. Pur $\alpha$  unwinds substrates containing one blunt and a 3' or 5' overhanging end, respectively. Since Pur $\alpha$  cannot unwind blunt-ended duplex DNA, these data indicate that Pur $\alpha$  displays no directionality of unwinding (Figure 4-32).

Pur $\alpha$  needs single-stranded ends for its function since the protein is not able to unwind a double-stranded 17-mer with no single-stranded overhang (Figure 4-32). The single strand extensions are most likely necessary for binding of the protein to the substrate. Unwinding of the 17-mer/M13 requires binding of Pur $\alpha$  to the substrate since Pur $\alpha$  helix destabilizing activity can be inhibited specifically with an oligonucleotide that binds Pur $\alpha$  with very high affinity (Bergemann *et al.*, 1992; Jurk *et al.*, 1996). Once Pur $\alpha$  has bound to its preferred sequence, it can no longer perform its DNA unwinding activity on nonspecific substrates. DNA unwinding affinity is not affected by the presence of a non-specific competitor oligonucleotide (Mage 11-2).

It has been reported that Pur $\alpha$  can self-associate (Gallia *et al.*, 1999; Muralidharan *et al.*, 1997). Various Pur $\alpha$  deletion mutants, which were generated by PCR and fused with GST, were analyzed to identify the regions responsible for DNA binding, dsDNA unwinding activity and self-association. All the truncated proteins that are able to self-associate still display DNA binding and dsDNA unwinding activity. We could not identify a truncated protein unable to bind DNA but still display DNA unwinding activity. The mapping of the DNA unwinding domain of the Pur $\alpha$  protein showed that this domain cannot be separated from the DNA binding activity (Figure 4-40 and Figure 4-41). As shown in Figure 4-35, the Pur $\alpha$  protein consists of several domains within its 322 amino acids. The N-terminus

contains a glycine-rich region (aa 7-53) followed by a region containing five repeats which can be subdivided into two classes. The C-terminus of the proteins consists of a glutamine rich region (282-303) followed by a glutamate rich domain (304-322) (for review see (Gallia *et al.*, 2000)). Although glycine rich domains have been implicated in RNA binding and helix destabilizing activities (Haynes *et al.*, 1990; Haynes *et al.*, 1987; Steinert *et al.*, 1991), the N-terminal, glycine rich region of the Pur $\alpha$  protein can be removed without affecting DNA binding and unwinding activity of the protein. Deletion of the first 106 amino acids decreases its activity significantly. The deletion mutant GST-Pur $\alpha$  107-322 displays only a very weak DNA binding activity and no detectable DNA unwinding activity (reviewed in Table 4-3). Recently, it has been shown that a Pur $\alpha$  mutant truncated for 166 N-terminal amino acids and fused to GST displays a dramatically reduced but detectable DNA binding activity (Johnson *et al.*, 1995). The fact that the GST-Pur $\alpha$  107-322 binds with even less affinity to DNA may be due to sterical interference within the GST fusion protein.

The C-terminal region of the protein does not seem to be essential for DNA binding and unwinding capacity since deletion of up to 106 amino acids (GST-Pur $\alpha$  1-215) does not interfere with these activities. However, it is interesting to note that deletion of only eight C-terminal aa in GST-Pur $\alpha$  1-314 results in a significant increase in Pur $\alpha$  DNA binding and unwinding efficiency. This is in contrast to data published recently where a similar mutant GST-Pur $\alpha$  protein displays significantly reduced DNA binding activity (Johnson *et al.*, 1995). However, Johnson *et al.* mentioned that eight C-terminal aa had been deleted and 14 other aa had been added. Therefore, the C-terminus may have a regulatory function for Pur $\alpha$  activity. Further experiments are necessary to verify, if the inhibitory effect of the eight C-terminal amino acids is due to the GST fusion context or if they are an intrinsic feature of the Pur $\alpha$  protein.

The three basic features of the Pur $\alpha$  protein, DNA binding, DNA unwinding, and self-association activity are all located in the central region of the protein containing three class I and two class II repeats. Our data indicate that four of these repeats are sufficient for all Pur $\alpha$  function since deletion of one class I repeat (Pur $\alpha$  1-215, Pur $\alpha$  87-322, Pur $\alpha$  54-215) does not abolish any of its activities. However, deletion of two repeats (Pur $\alpha$  87-215) abolishes measurable Pur $\alpha$  activity completely. From these data we conclude that the DNA unwinding activity localizes to the central core domain of Pur $\alpha$  and depends on at least four of the five repeat regions within this domain. DNA binding activity also maps to this part of the protein (Figure 4-41, Figure 4-42) (Chen and Khalili, 1995; Johnson *et al.*, 1995). Considering the inhibitory effect of oligonucleotides specifically bound by Pur $\alpha$  on DNA unwinding activity these results strongly suggest that DNA binding and DNA unwinding are not separable. DNA binding seems to be prerequisite for DNA unwinding.



Pur $\alpha$  efficiently unwinds short dsDNA regions. However, increasing the DNA duplex from 17 to 25 bp results in a dramatically drop of unwinding activity. Moreover, there is no detectable DNA unwinding activity if a 36-mer is annealed to M13 DNA (Figure 4-32). This may be due to missing co-factors not present in the recombinant protein. On the other hand, there may be no need for Pur $\alpha$  to perform extensive unwinding of long double stranded regions in the cell. Pur $\alpha$  could just function to destabilize very short double stranded regions in mainly single stranded DNA, e.g. stem loops or hair pins. This destabilizing activity could then facilitate the access and/or function of other regulatory proteins. This explanation would be in agreement with the notion that Pur $\alpha$  may not only recognize specific sequences but also secondary structures that tend to be present in single stranded DNA and RNA (Jurk *et al.*, 1996) and Marion Jurk, unpublished observation).

Pur $\alpha$  has been shown to bind specifically to sequences found in promoter regions and origins of replication in eukaryotic and viral genomes. Helix-destabilizing proteins serve as accessory factors required for efficient action of replicative enzymes, DNA polymerases, DNA helicases, and also participate in DNA repair and recombination. The binding of Pur $\alpha$  to PUR elements in promoter regions and origins of replication might result in a destabilized and partially unwound DNA duplex, which could be essential for the recruitment of other factors involved in transcription or replication. The finding that Pur $\alpha$  unwinds short regions of double stranded DNA is the first step in understanding the mechanism of how Pur $\alpha$  interferes with many different cellular processes.

#### **5.4 Cellular Pura function**

The ability of Pur $\alpha$  to interact with a GC/GA-rich motif (PUR element) found near the center of a region implicated as an initiation zone for chromosomal DNA replication and the ability of Pur $\alpha$  to unwind short dsDNA suggest a regulatory role of Pur $\alpha$  in the process of DNA replication. However, the data from the Pur $\alpha$  knock-out mice make this speculation improbable. Pur $\alpha$  has also been shown to interact with viral origins of DNA replication, including the JC virus (JCV) and bovine papillomavirus (Chang *et al.*, 1996; Jurk *et al.*, 1996). It has been shown that Pur $\alpha$  can suppress JC viral DNA replication in human glial cells (Chang *et al.*, 1996). The possible explanation is Pur $\alpha$  binds to the PUR element on the replication origins and therefore changes the DNA conformation, which perhaps leads to enhanced or decreased DNA replication.

It has been demonstrated that Pur $\alpha$  binds to the hypophosphorylated form of the pRb protein, which is required for cell differentiation (Johnson *et al.*, 1995). Several results indicate that pRb is involved in the development of the nervous system and indeed high levels of the hypophosphorylated form of pRb are associated with neuronal differentiation. Gene KO

experiments help us to understand the universal role for Rb in the cell cycle control of DNA replication. Homozygous Rb<sup>-/-</sup> fetal mice develop apparently normally until day 12-14 of embryogenesis, at which point they die (Clarke *et al.*, 1992; Lee *et al.*, 1992). At death, defects are found in development of both the hematopoietic system and the hindbrain. Transfer of the human retinoblastoma (Rb) mini-transgene into the mutant mice corrects the developmental defects. Thus, Rb is essential for normal mouse development. However, the Pur $\alpha$  KO mice display normal embryogenesis and early postnatal development, which indicates Pur $\alpha$  is not involved in the embryonic developmental of mice. It can be speculated that the function of Pur $\alpha$  might be redundant due to the presence of other PUR family proteins, Pur $\beta$  and Pur $\gamma$ .

Moreover, the presence of the PUR element near the transcription start sites of several cellular genes (Haas *et al.*, 1995; Thatikunta *et al.*, 1997) and viral genes (Chen *et al.*, 1995; Chen and Khalili, 1995; Chepenik *et al.*, 1998) suggests a regulatory role for Pur $\alpha$  in transcription by altering the DNA duplex structure which facilitates association of transcription factors and the synthesis of RNA. It has been shown that Pur $\alpha$  functionally stimulates transcription of MBP promoter in glial cells (Tretiakova *et al.*, 1998), and the GC/GA motif in the MBP promoter region is necessary for binding of Pur $\alpha$ . In this work, it was also shown that Pur $\alpha$  KO mice, which shows multi-phenotypes, displayed decreased MBP level in the young mice (p16). We can speculate that in the early stage of brain development, the transcription of MBP gene may be decreased because Pur $\alpha$  is not present to unwind dsDNA duplex for the transcription of MBP.

Interestingly, many lines of evidence indicate that Pur $\alpha$  may play an important role in the central nervous system since it can regulate not only the transcription of MBP, but also two other cellular genes related to the nervous system, neuron-specific FE65 gene and neuronal nicotinic acetylcholine (nACh) receptor (Zambrano *et al.*, 1997) (Du *et al.*, 1997).

Rat brain nuclear extracts show three major DNA-protein complexes with the transcriptional control and start site of the neuron specific FE65 gene, which encodes for an adapter protein that interacts with the Alzheimer  $\beta$ -amyloid precursor protein (Zambrano *et al.*, 1997). Two of the DNA-protein complexes contained Pur $\alpha$ , the third the transcription factor YY1. FE65 is almost exclusively expressed in neurons of several regions of the mouse nervous system, mainly in ganglionic structures of somatic, visceral and sense organ systems, and in the brain, particularly in the cortex and hippocampus (Simeone *et al.*, 1994). Regulation of its transcription is a key element in the generation of differentiated phenotypes in both neural and non-neuronal tissues, and this regulation apparently involves either Pur $\alpha$ , or YY1 (Zambrano *et al.*, 1997). It is possible that the loss of Pur $\alpha$  gene affects the expression of FE65. Thus, an investigation of FE65 expression in Pur $\alpha$  KO mice could be quite interesting.

Taken together, the Pur $\alpha$  knock-out mice have opened an important access to the understanding of Pur $\alpha$  function.

## 6 Summary

Pur $\alpha$  is a ubiquitous DNA- and RNA-binding protein that is highly conserved in eukaryotic organisms. Pur $\alpha$  binds preferentially to purine-rich single-stranded DNA. To date, biochemical analyses of Pur $\alpha$  have indicated that this protein might be involved in diverse cellular functions, including DNA replication, transcription, translation and cell growth control (Gallia *et al.*, 2000). However, the function of Pur $\alpha$  *in vivo* remains unclear.

In this study, Pur $\alpha$  knock-out mice (KO) were generated using homologous recombination techniques in ES cells. The Pur $\alpha$  gene locus was isolated from 129/SvJ Mouse Genomic Library and partially sequenced. A targeting vector using positive and negative selection was generated for homologous recombination and was finally electroporated into E14 ES cells for five times. Out of 2400 ES cell clones only one positive ES cell clone (KO 248) was identified by Southern-blot analysis.

Pur $\alpha$  KO mice generated from ES cell clone KO 248 displayed multiple phenotypes. Apparently, they were normal when born, but developed assorted abnormalities. 12-14 days after birth they developed a severe and continuous tremor phenotype similar to *shiverer* mice that lack myelin basic protein (MBP) (Chernoff, 1981). This tremor phenotype continued unabated until natural death occurred. Pur $\alpha$  KO mice seemed to have a shorter life span since none of the Pur $\alpha$  KO mice lived longer than 6 months while the wild type mice lived normally. Pur $\alpha$  has been shown to be involved in developmental and transcriptional control of MBP (Haas *et al.*, 1995), therefore the MBP levels in the brain stems of Pur $\alpha$  KO mice were investigated. It could be shown that MBP levels in 16-day-old Pur $\alpha$  KO mice were decreased by 30-40% as compared to heterozygotes and wild type. However, MBP levels of the 63-day-old Pur $\alpha$  KO, heterozygous and wild type mice did not show significant difference. Although Pur $\alpha$  KO mice showed a tremor phenotype comparable to *shiverer* mice and displayed reduced MBP levels at the beginning of brain myelination, they still possessed 60-70% of normal amounts of MBP, which has been shown to be sufficient to rescue the tremor phenotype in transgenic *shiverer* mice. These data suggest that the tremor phenotype of Pur $\alpha$  KO mice may be due to some other reasons, which are still unclear.

Strikingly, 70-day-old Pur $\alpha$  KO mice displayed a steadily increasing obesity and significantly enlarged brain size with increased lipid content, suggesting aberrant fat metabolism or homeostasis, although the underlying cause(s) are as yet unknown. Brain stems of Pur $\alpha$  KO mice were significantly enlarged and were about three times as heavy as those of the normal mice. The hippocampus and sensoric cortex of Pur $\alpha$  KO mice were also enlarged but had decreased weight. Moreover, more lipids were observed not only in the brain of Pur $\alpha$  KO mice but also in blood according to blood smear analysis. It has also been shown that female

Pur $\alpha$  KO mice had more fat droplets in blood than males. Apart from the phenotypes described above, Pur $\alpha$  KO mice displayed a different weight development curve as compared to normal mice: With the onset of tremor phenotype, Pur $\alpha$  KO mice started to lose their weight; the weight loss of the male KO mice beginning from postnatal day 11-15 was more severe than females and their weight recovery lasted longer than females; the female Pur $\alpha$  KO mice are heavier than males while normal male mice are heavier than females, suggesting that this obesity effect may also be influenced by animal gender. These results indicate that Pur $\alpha$  may influence or regulate the metabolism of fat in an unknown mechanism.

In the second part of this study, a new, yet uncharacterized *in vitro* enzymatic activity of Pur $\alpha$  was investigated. Pur $\alpha$  displayed a helix destabilizing activity by unwinding a labeled 17-mer oligonucleotide annealed to ssM13 DNA. This activity was independent of ATP or any other nucleosides and lacks any directionality, distinguishing it therefore from common helicase activities. 16 truncated GST-Pur $\alpha$  were generated by PCR for mapping of the domain responsible for the DNA unwinding activity. It was revealed that the central part of the protein from amino acids 54-215 was essential for this feature of Pur $\alpha$ . The identical part of Pur $\alpha$  was sufficient and essential for DNA binding activity. Therefore, DNA binding could not be separated from DNA unwinding capacity. In addition, from pull-down assays, it was shown that the same part of the protein was also sufficient and necessary for Pur $\alpha$  self-association. Since Pur $\alpha$  has been shown to influence many important cellular processes, the DNA unwinding activity of the protein may establish a mechanism of how Pur $\alpha$  functions in different cellular processes, such as replication and transcription.

## 7 Literature

A.L.Joyner. (1999) *Gene Targeting*

*A Practical Approach.*

Abdel-Monem, M., Durwald, H. and Hoffmann-Berling, H. (1976) Enzymic unwinding of DNA. 2. Chain separation by an ATP-dependent DNA unwinding enzyme. *Eur J Biochem*, **65**, 441-9.

Amaratunga, M. and Lohman, T.M. (1993) Escherichia coli rep helicase unwinds DNA by an active mechanism. *Biochemistry*, **32**, 6815-20.

Becker, N.A., Kelm, R.J., Jr., Vrana, J.A., Getz, M.J. and Maher, L.J., 3rd. (2000) Altered sensitivity to single-strand-specific reagents associated with the genomic vascular smooth muscle alpha-actin promoter during myofibroblast differentiation. *J Biol Chem*, **275**, 15384-91.

Belknap, J.K., Phillips, T.J. and O'Toole, L.A. (1992) Quantitative trait loci associated with brain weight in the BXD/Ty recombinant inbred mouse strains. *Brain Res Bull*, **29**, 337-44.

Bergemann, A.D., Ma, Z.W. and Johnson, E.M. (1992) Sequence of cDNA comprising the human pur gene and sequence-specific single-stranded-DNA-binding properties of the encoded protein. *Mol Cell Biol*, **12**, 5673-82.

Bergemann, A.D.a.J., E. M. (1992) The Hela Pur Factor Binds Single-Stranded DNA at a Specific Element Conserved in Gene Flanking Regions and Origins of DNA replication. *Mol Cell Bio*, **12**, 1257-1265.

Boehmer, P.E. and Lehman, I.R. (1993) Herpes simplex virus type 1 ICP8: helix-destabilizing properties. *J Virol*, **67**, 711-5.

Bradford, M.M. (1976) A rapid and sensitive method for the quantitation of microgram quantities of protein utilizing the principle of protein-dye binding. *Anal Biochem*, **72**, 248-54.

Bradley, A. (1990) Embryonic stem cells: proliferation and differentiation. *Curr Opin Cell Biol*, **2**, 1013-7.

Bujalowski, W., Klonowska, M.M. and Jezewska, M.J. (1994) Oligomeric structure of Escherichia coli primary replicative helicase DnaB protein. *J Biol Chem*, **269**, 31350-8.

Campagnoni, A.T. and Macklin, W.B. (1988) Cellular and molecular aspects of myelin protein gene expression. *Mol Neurobiol*, **2**, 41-89.

Campagnoni, A.T. and Skoff, R.P. (2001) The pathobiology of myelin mutants reveal novel biological functions of the MBP and PLP genes. *Brain Pathol*, **11**, 74-91.

Capecchi, M.R. (1989) Altering the genome by homologous recombination. *Science*, **244**, 1288-92.

- Carroll, R.B., Neet, K. and Goldthwait, D.A. (1975) Studies of the self-association of bacteriophage T4 gene 32 protein by equilibrium sedimentation. *J Mol Biol*, **91**, 275-91.
- Carson, J.H., Nielson, M.L. and Barbarese, E. (1983) Developmental regulation of myelin basic protein expression in mouse brain. *Dev Biol*, **96**, 485-92.
- Carson, M.J., Behringer, R.R., Brinster, R.L. and McMorris, F.A. (1993) Insulin-like growth factor I increases brain growth and central nervous system myelination in transgenic mice. *Neuron*, **10**, 729-40.
- Chang, C.F., Gallia, G.L., Muralidharan, V., Chen, N.N., Zoltick, P., Johnson, E. and Khalili, K. (1996) Evidence that replication of human neurotropic JC virus DNA in glial cells is regulated by the sequence-specific single-stranded DNA-binding protein Pur alpha. *J Virol*, **70**, 4150-6.
- Chao, K.L. and Lohman, T.M. (1991) DNA-induced dimerization of the *Escherichia coli* Rep helicase. *J Mol Biol*, **221**, 1165-81.
- Chase, J.W. and Williams, K.R. (1986) Single-stranded DNA binding proteins required for DNA replication. *Annu Rev Biochem*, **55**, 103-36.
- Chen, N.N., Chang, C.F., Gallia, G.L., Kerr, D.A., Johnson, E.M., Krachmarov, C.P., Barr, S.M., Frisque, R.J., Bollag, B. and Khalili, K. (1995) Cooperative action of cellular proteins YB-1 and Pur alpha with the tumor antigen of the human JC polyomavirus determines their interaction with the viral lytic control element. *Proc Natl Acad Sci U S A*, **92**, 1087-91.
- Chen, N.N. and Khalili, K. (1995) Transcriptional regulation of human JC polyomavirus promoters by cellular proteins YB-1 and Pur alpha in glial cells. *J Virol*, **69**, 5843-8.
- Cheng, W., Hsieh, J., Brendza, K.M. and Lohman, T.M. (2001) E. coli Rep oligomers are required to initiate DNA unwinding in vitro. *J Mol Biol*, **310**, 327-50.
- Chepenik, L.G., Tretiakova, A.P., Krachmarov, C.P., Johnson, E.M. and Khalili, K. (1998) The single-stranded DNA binding protein, Pur-alpha, binds HIV-1 TAR RNA and activates HIV-1 transcription. *Gene*, **210**, 37-44.
- Chernoff, G.F. (1981) Shiverer: an autosomal recessive mutant mouse with myelin deficiency. *J Hered*, **72**, 128.
- Chowdhury, M., Kundu, M. and Khalili, K. (1993) GA/GC-rich sequence confers Tat responsiveness to human neurotropic virus promoter, JCVL, in cells derived from central nervous system. *Oncogene*, **8**, 887-92.
- Chowdhury, M., Taylor, J.P., Chang, C.F., Rappaport, J. and Khalili, K. (1992) Evidence that a sequence similar to TAR is important for induction of the JC virus late promoter by human immunodeficiency virus type 1 Tat. *J Virol*, **66**, 7355-61.
- Church, G.M. and Gilbert, W. (1984) Genomic sequencing. *Proc Natl Acad Sci U S A*, **81**, 1991-5.

- Clarke, A.R., Maandag, E.R., van Roon, M., van der Lugt, N.M., van der Valk, M., Hooper, M.L., Berns, A. and te Riele, H. (1992) Requirement for a functional Rb-1 gene in murine development. *Nature*, **359**, 328-30.
- Company, M., Arenas, J. and Abelson, J. (1991) Requirement of the RNA helicase-like protein PRP22 for release of messenger RNA from spliceosomes. *Nature*, **349**, 487-93.
- Courey, A.J., Holtzman, D.A., Jackson, S.P. and Tjian, R. (1989) Synergistic activation by the glutamine-rich domains of human transcription factor Sp1. *Cell*, **59**, 827-36.
- Daniele, N., Rajas, F., Payrastra, B., Mauco, G., Zitoun, C. and Mithieux, G. (1999) Phosphatidylinositol 3-kinase translocates onto liver endoplasmic reticulum and may account for the inhibition of glucose-6-phosphatase during refeeding. *J Biol Chem*, **274**, 3597-601.
- Darbinian, N., Gallia, G.L., Kundu, M., Shcherbik, N., Tretiakova, A., Giordano, A. and Khalili, K. (1999) Association of Puralpha and E2F-1 suppresses transcriptional activity of E2F-1. *Oncogene*, **18**, 6398-402.
- de Ferra, F., Engh, H., Hudson, L., Kamholz, J., Puckett, C., Molineaux, S. and Lazzarini, R.A. (1985) Alternative splicing accounts for the four forms of myelin basic protein. *Cell*, **43**, 721-7.
- Dekker, J., Kanellopoulos, P.N., Loonstra, A.K., van Oosterhout, J.A., Leonard, K., Tucker, P.A. and van der Vliet, P.C. (1997) Multimerization of the adenovirus DNA-binding protein is the driving force for ATP-independent DNA unwinding during strand displacement synthesis. *Embo J*, **16**, 1455-63.
- Deng, C. and Capecchi, M.R. (1992) Reexamination of gene targeting frequency as a function of the extent of homology between the targeting vector and the target locus. *Mol Cell Biol*, **12**, 3365-71.
- Donate, L.E., Llorca, O., Barcena, M., Brown, S.E., Dixon, N.E. and Carazo, J.M. (2000) pH-controlled quaternary states of hexameric DnaB helicase. *J Mol Biol*, **303**, 383-93.
- Du, Q., Tomkinson, A.E. and Gardner, P.D. (1997) Transcriptional regulation of neuronal nicotinic acetylcholine receptor genes. A possible role for the DNA-binding protein Puralpha. *J Biol Chem*, **272**, 14990-5.
- Egelman, E.H. (1998) Bacterial helicases. *J Struct Biol*, **124**, 123-8.
- Fried, M. and Crothers, D.M. (1981) Equilibria and kinetics of lac repressor-operator interactions by polyacrylamide gel electrophoresis. *Nucleic Acids Res*, **9**, 6505-25.
- Gallia, G.L., Darbinian, N., Johnson, E.M. and Khalili, K. (1999) Self-association of Puralpha is mediated by RNA. *J Cell Biochem*, **74**, 334-48.
- Gallia, G.L., Johnson, E.M. and Khalili, K. (2000) Puralpha: a multifunctional single-stranded DNA- and RNA-binding protein. *Nucleic Acids Res*, **28**, 3197-205.
- Ganesan, S. and Smith, G.R. (1993) Strand-specific binding to duplex DNA ends by the subunits of the Escherichia coli RecBCD enzyme. *J Mol Biol*, **229**, 67-78.



- Gorbalenya AE, K.E. (1993) *Curr. Opin. Struct. Biol.*, **3**, 419.
- Gray, M.D., Shen, J.C., Kamath-Loeb, A.S., Blank, A., Sopher, B.L., Martin, G.M., Oshima, J. and Loeb, L.A. (1997) The Werner syndrome protein is a DNA helicase. *Nat Genet*, **17**, 100-3.
- Haas, S., Thatikunta, P., Steplewski, A., Johnson, E.M., Khalili, K. and Amini, S. (1995) A 39-kD DNA-binding protein from mouse brain stimulates transcription of myelin basic protein gene in oligodendrocytic cells. *J Cell Biol*, **130**, 1171-9.
- Hall, M.C. and Matson, S.W. (1999) Helicase motifs: the engine that powers DNA unwinding. *Mol Microbiol*, **34**, 867-77.
- Hanawalt, P.C. (1994) Transcription-coupled repair and human disease. *Science*, **266**, 1957-8.
- Haynes, S.R., Raychaudhuri, G. and Beyer, A.L. (1990) The *Drosophila* Hrb98DE locus encodes four protein isoforms homologous to the A1 protein of mammalian heterogeneous nuclear ribonucleoprotein complexes. *Mol Cell Biol*, **10**, 316-23.
- Haynes, S.R., Rebbert, M.L., Mozer, B.A., Forquignon, F. and Dawid, I.B. (1987) pen repeat sequences are GGN clusters and encode a glycine-rich domain in a *Drosophila* cDNA homologous to the rat helix destabilizing protein. *Proc Natl Acad Sci U S A*, **84**, 1819-23.
- Hill, T.L. and Tsuchiya, T. (1981) Theoretical aspects of translocation on DNA: adenosine triphosphatases and treadmilling binding proteins. *Proc Natl Acad Sci U S A*, **78**, 4796-800.
- Hodgman, T.C. (1988) A new superfamily of replicative proteins. *Nature*, **333**, 22-3.
- Itoh, H., Wortman, M.J., Kanovsky, M., Uson, R.R., Gordon, R.E., Alfano, N. and Johnson, E.M. (1998) Alterations in Pur(alpha) levels and intracellular localization in the CV-1 cell cycle. *Cell Growth Differ*, **9**, 651-65.
- Johnson, E.M., Chen, P.L., Krachmarov, C.P., Barr, S.M., Kanovsky, M., Ma, Z.W. and Lee, W.H. (1995) Association of human Pur alpha with the retinoblastoma protein, Rb, regulates binding to the single-stranded DNA Pur alpha recognition element. *J Biol Chem*, **270**, 24352-60.
- Jones, K.A. (1997) Taking a new TAK on tat transactivation. *Genes Dev*, **11**, 2593-9.
- Jurk, M., Weissinger, F., Lottspeich, F., Schwarz, U. and Winnacker, E.L. (1996) Characterization of the single-strand-specific BPV-1 origin binding protein, SPSF I, as the HeLa Pur alpha factor. *Nucleic Acids Res*, **24**, 2799-806.
- Kamholz, J., de Ferra, F., Puckett, C. and Lazzarini, R. (1986) Identification of three forms of human myelin basic protein by cDNA cloning. *Proc Natl Acad Sci U S A*, **83**, 4962-6.
- Kawasaki, E.S. (1990) *PCR protocols: a guide to methods and applications*. , 146-152.
- Kim, C. and Wold, M.S. (1995) Recombinant human replication protein A binds to polynucleotides with low cooperativity. *Biochemistry*, **34**, 2058-64.
- Kimura, M., Sato, M., Akatsuka, A., Nozawa-Kimura, S., Takahashi, R., Yokoyama, M., Nomura, T. and Katsuki, M. (1989) Restoration of myelin formation by a single type

of myelin basic protein in transgenic shiverer mice. *Proc Natl Acad Sci U S A*, **86**, 5661-5.

Kowalczykowski, S.C., Lonberg, N., Newport, J.W. and von Hippel, P.H. (1981) Interactions of bacteriophage T4-coded gene 32 protein with nucleic acids. I. Characterization of the binding interactions. *J Mol Biol*, **145**, 75-104.

Krachmarov, C.P., Chepenik, L.G., Barr-Vagell, S., Khalili, K. and Johnson, E.M. (1996) Activation of the JC virus Tat-responsive transcriptional control element by association of the Tat protein of human immunodeficiency virus 1 with cellular protein Pur alpha. *Proc Natl Acad Sci U S A*, **93**, 14112-7.

Kristensson, K., Zeller, N.K., Dubois-Dalcq, M.E. and Lazzarini, R.A. (1986) Expression of myelin basic protein gene in the developing rat brain as revealed by in situ hybridization. *J Histochem Cytochem*, **34**, 467-73.

Kristie, T.M. and Roizman, B. (1986a) Alpha 4, the major regulatory protein of herpes simplex virus type 1, is stably and specifically associated with promoter-regulatory domains of alpha genes and of selected other viral genes. *Proc Natl Acad Sci U S A*, **83**, 3218-22.

Kristie, T.M. and Roizman, B. (1986b) DNA-binding site of major regulatory protein alpha 4 specifically associated with promoter-regulatory domains of alpha genes of herpes simplex virus type 1. *Proc Natl Acad Sci U S A*, **83**, 4700-4.

Laemmli, U.K. (1970) Cleavage of structural proteins during the assembly of the head of bacteriophage T4. *Nature*, **227**, 680-5.

Lahue, E.E. and Matson, S.W. (1988) Escherichia coli DNA helicase I catalyzes a unidirectional and highly processive unwinding reaction. *J Biol Chem*, **263**, 3208-15.

Laird, P.W., Zijderveld, A., Linders, K., Rudnicki, M.A., Jaenisch, R. and Berns, A. (1991) Simplified mammalian DNA isolation procedure. *Nucleic Acids Res*, **19**, 4293.

Le Beau, M.M., Espinosa, R., 3rd, Neuman, W.L., Stock, W., Roulston, D., Larson, R.A., Keinanen, M. and Westbrook, C.A. (1993) Cytogenetic and molecular delineation of the smallest commonly deleted region of chromosome 5 in malignant myeloid diseases. *Proc Natl Acad Sci U S A*, **90**, 5484-8.

Lee, E.Y., Chang, C.Y., Hu, N., Wang, Y.C., Lai, C.C., Herrup, K., Lee, W.H. and Bradley, A. (1992) Mice deficient for Rb are nonviable and show defects in neurogenesis and haematopoiesis. *Nature*, **359**, 288-94.

Lezon-Geyda, K.A., Najfeld, V., and Johnson, E.M. (1997) The PURA gene, encoding the single-stranded DNA binding protein Puro $\alpha$ , as a marker for 5q31 alteration in myeloproliferative disorders, a potentially early step in induction of AML. *FASEB J*, **11**, A100.

Lezon-Geyda, K., Najfeld, V. and Johnson, E.M. (2001) Deletions of PURA, at 5q31, and PURB, at 7p13, in myelodysplastic syndrome and progression to acute myelogenous leukemia. *Leukemia*, **15**, 954-62.

Li, X., Yoder, B.L. and Burgers, P.M. (1992) Three new DNA helicases from *Saccharomyces cerevisiae*. *Chromosoma*, **102**, S93-9.

- Lohman, T.M. (1992) Escherichia coli DNA helicases: mechanisms of DNA unwinding. *Mol Microbiol*, **6**, 5-14.
- Lohman, T.M. (1993) Helicase-catalyzed DNA unwinding. *J Biol Chem*, **268**, 2269-72.
- Lohman, T.M. and Bjornson, K.P. (1996) Mechanisms of helicase-catalyzed DNA unwinding. *Annu Rev Biochem*, **65**, 169-214.
- Lohman, T.M., Bujalowski, W. and Overman, L.B. (1988) E. coli single strand binding protein: a new look at helix- destabilizing proteins. *Trends Biochem Sci*, **13**, 250-5.
- Ma, Z.W., Bergemann, A.D. and Johnson, E.M. (1994) Conservation in human and mouse Pur alpha of a motif common to several proteins involved in initiation of DNA replication. *Gene*, **149**, 311-4.
- Ma, Z.W., Pejovic, T., Najfeld, V., Ward, D.C. and Johnson, E.M. (1995) Localization of PURA, the gene encoding the sequence-specific single- stranded-DNA-binding protein Pur alpha, to chromosome band 5q31. *Cytogenet Cell Genet*, **71**, 64-7.
- Manitatis, T., Fritsch, E. F. and Sambrook, J. (1982) Molecular cloning. A laboratory manual.
- Mansour, S.L., Thomas, K.R. and Capecchi, M.R. (1988) Disruption of the proto-oncogene int-2 in mouse embryo-derived stem cells: a general strategy for targeting mutations to non-selectable genes. *Nature*, **336**, 348-52.
- Martinou, J.C., Dubois-Dauphin, M., Staple, J.K., Rodriguez, I., Frankowski, H., Missotten, M., Albertini, P., Talabot, D., Catsicas, S., Pietra, C. and et al. (1994) Overexpression of BCL-2 in transgenic mice protects neurons from naturally occurring cell death and experimental ischemia. *Neuron*, **13**, 1017-30.
- Mastrangelo, I.A., Hough, P.V., Wall, J.S., Dodson, M., Dean, F.B. and Hurwitz, J. (1989) ATP-dependent assembly of double hexamers of SV40 T antigen at the viral origin of DNA replication. *Nature*, **338**, 658-62.
- Matise, M.P., Auerbach, W., and Joyner, A. L. (2000) Production of targeted embryonic stem cell clones. *Gene Targeting, a Practical Approach. second edition*.
- Matson, S.W., Bean, D.W. and George, J.W. (1994) DNA helicases: enzymes with essential roles in all aspects of DNA metabolism. *Bioessays*, **16**, 13-22.
- Matson, S.W. and George, J.W. (1987) DNA helicase II of Escherichia coli. Characterization of the single- stranded DNA-dependent NTPase and helicase activities. *J Biol Chem*, **262**, 2066-76.
- Matthieu, J.M., Omlin, F.X., Ginalski-Winkelmann, H. and Cooper, B.J. (1984) Myelination in the CNS of mld mutant mice: comparison between composition and structure. *Brain Res*, **315**, 149-58.
- McDougal, V.V. and Guarino, L.A. (1999) Autographa californica nuclear polyhedrosis virus DNA polymerase: measurements of processivity and strand displacement. *J Virol*, **73**, 4908-18.
- Mewes, H.W., Hani, J., Pfeiffer, F. and Frishman, D. (1998) MIPS: a database for protein sequences and complete genomes. *Nucleic Acids Res*, **26**, 33-7.

- Mikhailov, V.S. (2000) Helix-destabilizing properties of the baculovirus single-stranded DNA-binding protein (LEF-3). *Virology*, **270**, 180-9.
- Mikoshiba, K., Aruga, J. and Okano, H. (1991) Molecular biology of myelin basic protein: gene rearrangement and expression of anti-sense RNA in myelin-deficient mutants. *Comp Biochem Physiol C*, **98**, 51-61.
- Monaghan, A., Webster, A., and Hay, R. T. (1994) Adenovirus DNA binding protein: Helix destabilizing properties. *Nucleic Acids Res.*, **22**, 742-748.
- Monuki, E.S., Kuhn, R., Weinmaster, G., Trapp, B.D. and Lemke, G. (1990) Expression and activity of the POU transcription factor SCIP. *Science*, **249**, 1300-3.
- Mukherjee, R. and Chambon, P. (1990) A single-stranded DNA-binding protein promotes the binding of the purified oestrogen receptor to its responsive element. *Nucleic Acids Res*, **18**, 5713-6.
- Muralidharan, V., Cort, L., Meier, E., Blankenhorn, E.P. and Khalili, K. (2000) Molecular characterization and chromosomal localization of mouse Puralpha gene. *J Cell Biochem*, **77**, 1-5.
- Muralidharan, V., Tretiakova, A., Steplewski, A., Haas, S., Amini, S., Johnson, E. and Khalili, K. (1997) Evidence for inhibition of MyEF-2 binding to MBP promoter by MEF-1/Pur alpha. *J Cell Biochem*, **66**, 524-31.
- Nakura, J., Ye, L., Morishima, A., Kohara, K. and Miki, T. (2000) Helicases and aging. *Cell Mol Life Sci*, **57**, 716-30.
- Neumann, E., Schaefer-Ridder, M., Wang, Y. and Hofschneider, P.H. (1982) Gene transfer into mouse lyoma cells by electroporation in high electric fields. *Embo J*, **1**, 841-5.
- Newman, S., Kitamura, K. and Campagnoni, A.T. (1987) Identification of a cDNA coding for a fifth form of myelin basic protein in mouse. *Proc Natl Acad Sci U S A*, **84**, 886-90.
- O'Donnell, M.E., Elias, P., Funnell, B.E. and Lehman, I.R. (1987) Interaction between the DNA polymerase and single-stranded DNA-binding protein (infected cell protein 8) of herpes simplex virus 1. *J Biol Chem*, **262**, 4260-6.
- Osugi, T., Ding, Y., Tanaka, H., Kuo, C.H., Do, E., Irie, Y. and Miki, N. (1996) Involvement of a single-stranded DNA binding protein, ssCRE-BP/Pur alpha, in morphine dependence. *FEBS Lett*, **391**, 11-6.
- Pedersen, B. (1993) 5q-: pathogenetic importance of the common deleted region and clinical consequences of the entire deleted segment. *Anticancer Res*, **13**, 1913-6.
- Popko, B., Puckett, C., Lai, E., Shine, H.D., Readhead, C., Takahashi, N., Hunt, S.W., 3rd, Sidman, R.L. and Hood, L. (1987) Myelin deficient mice: expression of myelin basic protein and generation of mice with varying levels of myelin. *Cell*, **48**, 713-21.
- Potter, H., Weir, L. and Leder, P. (1984) Enhancer-dependent expression of human kappa immunoglobulin genes introduced into mouse pre-B lymphocytes by electroporation. *Proc Natl Acad Sci U S A*, **81**, 7161-5.

- Ramirez-Solis, R., Rivera-Perez, J., Wallace, J.D., Wims, M., Zheng, H. and Bradley, A. (1992) Genomic DNA microextraction: a method to screen numerous samples. *Anal Biochem*, **201**, 331-5.
- Ray, B.K., Lawson, T.G., Kramer, J.C., Cladaras, M.H., Grifo, J.A., Abramson, R.D., Merrick, W.C. and Thach, R.E. (1985) ATP-dependent unwinding of messenger RNA structure by eukaryotic initiation factors. *J Biol Chem*, **260**, 7651-8.
- Readhead, C., Popko, B., Takahashi, N., Shine, H.D., Saavedra, R.A., Sidman, R.L. and Hood, L. (1987) Expression of a myelin basic protein gene in transgenic shiverer mice: correction of the dysmyelinating phenotype. *Cell*, **48**, 703-12.
- Robertson, E.J. (1986) Embryo-derived stem cell lines. *Tetracarciomas and Embryonic stem Cells, a practical Approach*. .
- Roth, H.J., Kronquist, K., Pretorius, P.J., Crandall, B.F. and Campagnoni, A.T. (1986) Isolation and characterization of a cDNA coding for a novel human 17.3K myelin basic protein (MBP) variant. *J Neurosci Res*, **16**, 227-38.
- Roth, H.J., Kronquist, K.E., Kerlero de Rosbo, N., Crandall, B.F. and Campagnoni, A.T. (1987) Evidence for the expression of four myelin basic protein variants in the developing human spinal cord through cDNA cloning. *J Neurosci Res*, **17**, 321-8.
- Runyon, G.T., Bear, D.G. and Lohman, T.M. (1990) Escherichia coli helicase II (UvrD) protein initiates DNA unwinding at nicks and blunt ends. *Proc Natl Acad Sci U S A*, **87**, 6383-7.
- Sancar, A. (1994) Mechanisms of DNA excision repair. *Science*, **266**, 1954-6.
- Schneider, C., Weisshart, K., Guarino, L.A., Dornreiter, I. and Fanning, E. (1994) Species-specific functional interactions of DNA polymerase alpha- primase with simian virus 40 (SV40) T antigen require SV40 origin DNA. *Mol Cell Biol*, **14**, 3176-85.
- Shiota, C., Ikenaka, K. and Mikoshiba, K. (1991) Developmental expression of myelin protein genes in dysmyelinating mutant mice: analysis by nuclear run-off transcription assay, in situ hybridization, and immunohistochemistry. *J Neurochem*, **56**, 818-26.
- Simeone, A., Duilio, A., Fiore, F., Acampora, D., De Felice, C., Faraonio, R., Paolocci, F., Cimino, F. and Russo, T. (1994) Expression of the neuron-specific FE65 gene marks the development of embryo ganglionic derivatives. *Dev Neurosci*, **16**, 53-60.
- Smith, D.B., Davern, K.M., Board, P.G., Tiu, W.U., Garcia, E.G. and Mitchell, G.F. (1986) Mr 26,000 antigen of Schistosoma japonicum recognized by resistant WEHI 129/J mice is a parasite glutathione S-transferase. *Proc Natl Acad Sci U S A*, **83**, 8703-7.
- Soengas, M.S., Gutierrez, C. and Salas, M. (1995) Helix-destabilizing activity of phi 29 single-stranded DNA binding protein: effect on the elongation rate during strand displacement DNA replication. *J Mol Biol*, **253**, 517-29.
- Sorg, B.A., Smith, M.M. and Campagnoni, A.T. (1987) Developmental expression of the myelin proteolipid protein and basic protein mRNAs in normal and dysmyelinating mutant mice. *J Neurochem*, **49**, 1146-54.

- Stacey, D.W., Hitomi, M., Kanovsky, M., Gan, L. and Johnson, E.M. (1999) Cell cycle arrest and morphological alterations following microinjection of NIH3T3 cells with Puralpha. *Oncogene*, **18**, 4254-61.
- Steinert, P.M., Mack, J.W., Korge, B.P., Gan, S.Q., Haynes, S.R. and Steven, A.C. (1991) Glycine loops in proteins: their occurrence in certain intermediate filament chains, loricrins and single-stranded RNA binding proteins. *Int J Biol Macromol*, **13**, 130-9.
- Steinmetz, E.J., Brennan, C.A. and Platt, T. (1990) A short intervening structure can block rho factor helicase action at a distance. *J Biol Chem*, **265**, 18408-13.
- Takahashi, N., Roach, A., Teplow, D.B., Prusiner, S.B. and Hood, L. (1985) Cloning and characterization of the myelin basic protein gene from mouse: one gene can encode both 14 kd and 18.5 kd MBPs by alternate use of exons. *Cell*, **42**, 139-48.
- Thatikunta, P., Sawaya, B.E., Denisova, L., Cole, C., Yusibova, G., Johnson, E.M., Khalili, K. and Amini, S. (1997) Identification of a cellular protein that binds to Tat-responsive element of TGF beta-1 promoter in glial cells. *J Cell Biochem*, **67**, 466-77.
- Thomas, K.R. and Capecchi, M.R. (1987) Site-directed mutagenesis by gene targeting in mouse embryo-derived stem cells. *Cell*, **51**, 503-12.
- Thommes, P. and Hubscher, U. (1990) Eukaryotic DNA helicases. *FEBS Lett*, **268**, 325-8.
- Thommes, P. and Hubscher, U. (1992) Eukaryotic DNA helicases: essential enzymes for DNA transactions. *Chromosoma*, **101**, 467-73.
- Threadgill, D.W., Yee, D., Matin, A., Nadeau, J.H. and Magnuson, T. (1997) Genealogy of the 129 inbred strains: 129/SvJ is a contaminated inbred strain. *Mamm Genome*, **8**, 390-3.
- Tretiakova, A., Gallia, G.L., Shcherbik, N., Jameson, B., Johnson, E.M., Amini, S. and Khalili, K. (1998) Association of Puralpha with RNAs homologous to 7 SL determines its binding ability to the myelin basic protein promoter DNA sequence. *J Biol Chem*, **273**, 22241-7.
- Tretiakova, A., Stepkowski, A., Johnson, E.M., Khalili, K. and Amini, S. (1999) Regulation of myelin basic protein gene transcription by Sp1 and Puralpha: evidence for association of Sp1 and Puralpha in brain. *J Cell Physiol*, **181**, 160-8.
- Tuteja, N., Tuteja, R., Ochem, A., Taneja, P., Huang, N.W., Simoncsits, A., Susic, S., Rahman, K., Marusic, L., Chen, J. and et al. (1994) Human DNA helicase II: a novel DNA unwinding enzyme identified as the Ku autoantigen. *Embo J*, **13**, 4991-5001.
- Tuteja, N., Tuteja, R., Rahman, K., Kang, L.Y. and Falaschi, A. (1990) A DNA helicase from human cells. *Nucleic Acids Res*, **18**, 6785-92.
- van Deursen, J. and Wieringa, B. (1992) Targeting of the creatine kinase M gene in embryonic stem cells using isogenic and nonisogenic vectors. *Nucleic Acids Res*, **20**, 3815-20.
- Verity, A.N. and Campagnoni, A.T. (1988) Regional expression of myelin protein genes in the developing mouse brain: in situ hybridization studies. *J Neurosci Res*, **21**, 238-48.

- von Hippel, P.H. and Delagoutte, E. (2001) A general model for nucleic acid helicases and their "coupling" within macromolecular machines. *Cell*, **104**, 177-90.
- Wong, I., Chao, K.L., Bujalowski, W. and Lohman, T.M. (1992) DNA-induced dimerization of the Escherichia coli rep helicase. Allosteric effects of single-stranded and duplex DNA. *J Biol Chem*, **267**, 7596-610.
- Wong, I. and Lohman, T.M. (1992) Allosteric effects of nucleotide cofactors on Escherichia coli Rep helicase-DNA binding. *Science*, **256**, 350-5.
- Woods, D.E., Markham, A.F., Ricker, A.T., Goldberger, G. and Colten, H.R. (1982) Isolation of cDNA clones for the human complement protein factor B, a class III major histocompatibility complex gene product. *Proc Natl Acad Sci U S A*, **79**, 5661-5.
- Yarranton, G.T. and Gefter, M.L. (1979) Enzyme-catalyzed DNA unwinding: studies on Escherichia coli rep protein. *Proc Natl Acad Sci U S A*, **76**, 1658-62.
- Yu, C.E., Oshima, J., Fu, Y.H., Wijsman, E.M., Hisama, F., Alisch, R., Matthews, S., Nakura, J., Miki, T., Ouais, S., Martin, G.M., Mulligan, J. and Schellenberg, G.D. (1996) Positional cloning of the Werner's syndrome gene. *Science*, **272**, 258-62.
- Zambrano, N., De Renzis, S., Minopoli, G., Faraonio, R., Donini, V., Scaloni, A., Cimino, F. and Russo, T. (1997) DNA-binding protein Pur alpha and transcription factor YY1 function as transcription activators of the neuron-specific FE65 gene promoter. *Biochem J*, **328**, 293-300.
- Zeller, N.K., Hunkeler, M.J., Campagnoni, A.T., Sprague, J. and Lazzarini, R.A. (1984) Characterization of mouse myelin basic protein messenger RNAs with a myelin basic protein cDNA clone. *Proc Natl Acad Sci U S A*, **81**, 18-22.
- Zijderveld, D.C. and van der Vliet, P.C. (1994) Helix-destabilizing properties of the adenovirus DNA-binding protein. *J Virol*, **68**, 1158-64.
- Zimmermann, U. and Vienken, J. (1982) Electric field-induced cell-to-cell fusion. *J Membr Biol*, **67**, 165-82.

## 8 Appendix

### 8.1 Southern-blot of p5/1 and p14/2

p5/1 Blot:

Nr	Enzyme	<i>Hind</i> III 450 bp	<i>Pst</i> I 450bp
1	<i>Not</i> I/ <i>Hind</i> III	450 bp	2.1 kb
2	<i>Not</i> I/ <i>Pst</i> I	4.5 kb	450 bp
3	<i>Not</i> I/ <i>Eco</i> RI	>>7.0 kb	2.1 kb
4	<i>Not</i> I/ <i>Xba</i> I	4.5 kb	2.1 kb
5	<i>Not</i> I/ <i>Sma</i> I	>>7.0 kb	1.7 kb
6	<i>Not</i> I/ <i>Bam</i> HI	7.0 kb	2.1 kb
7	<i>Not</i> I/ <i>Eco</i> RV	6.0 kb	2.1 kb
8	<i>Not</i> I/ <i>Bgl</i> II	2.4 kb	1.3 kb
9	<i>Not</i> I/ <i>Sal</i> I	>>7.0 kb	2.1 kb
10	<i>Not</i> I	>>7.0 kb	2.1 kb

Table 8-1: Size of DNA fragments got from blot p5/1 hybridized with *Hind*III 450 bp fragment or *Pst*I 450bp fragment.

P14/2 Blot:

Nr	Enzyme	<i>Hind</i> III 450 bp	<i>Pst</i> I 450bp
1	<i>Not</i> I/ <i>Hind</i> III	450 bp	5.8 kb
2	<i>Not</i> I/ <i>Pst</i> I	4.5 kb	450 bp
3	<i>Not</i> I/ <i>Eco</i> RI	3.0 kb	4.2 kb
4	<i>Not</i> I/ <i>Xba</i> I	4.2 kb	2.8 kb
5	<i>Not</i> I/ <i>Sma</i> I	5.0 kb	7.0 kb
6	<i>Not</i> I/ <i>Bam</i> HI	>5.0 kb	>7.0 kb
7	<i>Not</i> I/ <i>Eco</i> RV	3.5 kb	2.6 kb
8	<i>Not</i> I/ <i>Bgl</i> II	2.3 kb	1.3 kb
9	<i>Not</i> I/ <i>Sal</i> I	2.5 kb	6.0 kb
10	<i>Not</i> I	>>5.0 kb	>7.0 kb

Table 8-2: The size of DNA fragments got from blot p14/2 hybridized with *Hind*III 450 bp fragment or *Pst*I 450bp fragment.



P14/2 Blot:

Nr	Enzyme	P2M1	P2M2
1	<i>NotI/HindIII</i>	2.5 kb	1.2 kb
2	<i>NotI/PstI</i>	1.1 kb	4.2 kb
3	<i>NotI/EcoRI</i>	1.3 kb	1.8 kb
4	<i>NotI/XbaI</i>	2.5 kb	3.3 kb
5	<i>NotI/SmaI</i>	/	/
6	<i>NotI/BamHI</i>	300 bp	7.0 kb
7	<i>NotI/EcoRV</i>	/	4.0 kb
8	<i>NotI/BglII</i>	1.1 kb	4.5 kb
9	<i>NotI/SalI</i>	2.5 kb	950 bp
10	<i>NotI</i>	2.5 kb	7.0 kb

Table 8-3: The size of DNA fragments got from blot p14/2 hybridized with P2M1 and P2M2.

## 8.2 The oligonucleotides used in this study

### 8.2.1 Oligonucleotides used for generation of Pura knock-out mice

The oligonucleotides p11M1 to p10M2 are from murine Puro $\alpha$  genomic DNA sequence.

#### p11M1

5'- CGTACGCCCCGGGGCTCTCATTGATACTTGCTAATTTTCTGGG -3'

#### p11M2

5'- CGTACGCCCCGGGGTAAAGGGGTAAGTGAACCTGGTTTAATG -3'

#### P7M1E

5'- GATCGCCCCGGGCAGACGAGACCCGGTAACAGG -3'

#### P10M1A

5'- CGTACGCTCGAGACAATGTAAATATGAGGTGACCG -3'

#### P10M1B

5'- CGTACGCTCGAGTGTGCATTTTCCATTGTTCC -3'

#### P10M2

5'- CGCTAGCTCGAGGCTCATATTTATAAAGAATTTTATGGGC -3'

#### Neo.primer

5'- GGATGCGGTGGGCTCTATGGCTTCTGAGG -3'

#### Neo2a

5'- GATCTCCTGTCATCTCACCTTGC -3'

**Neo2b**

5'- TGGCAACTAGAAGGCACAGTCG -3'

**8.2.2 Oligonucleotides used for the generation of truncated Pura mutants**

The oligonucleotides HeM1-A to HeM10 are derived from Hela Pur $\alpha$  cDNA. The letters written in small are the linker sequence containing a restriction site and the following sequence in capital letters is derived from Hela Pur $\alpha$  cDNA.

Nr.	GST-Pur $\alpha$ deletion mutants	Primers for PCR		Annealing Temp (°C)	Size of PCR fragment (bp)
		sense-primer	antisense-primer		
1	GST-Pur $\alpha$ ( 107-322 )	HeM5	HeM1-C1	54°C	756 bp
2	GST-Pur $\alpha$ ( 87-215 )	HeM7	HeM4	54°C	411 bp
3	GST-Pur $\alpha$ ( 87-314 )	HeM7	HeM2-C2	54°C	716 bp
4	GST-Pur $\alpha$ ( 54-215 )	HeM1-A	HeM4	54°C	512 bp
5	GST-Pur $\alpha$ ( 54-314 )	HeM1-A	HeM2-C2	54°C	815 bp
6	GST-Pur $\alpha$ ( 54-322 )	HeM1-A	HeM1-C1	54°C	855 bp
7	GST-Pur $\alpha$ ( 1-322 )	HeM2-A	HeM1-C1	54°C	1011 bp
8	GST-Pur $\alpha$ ( 1-314 )	HeM2-A	HeM2-C2	54°C	971 bp
9	GST-Pur $\alpha$ ( 1-215 )	HeM2-A	HeM4	54°C	668 bp
10	GST-Pur $\alpha$ ( 74--215 )	HeM6	HeM4	54°C	449 bp
11	GST-Pur $\alpha$ ( 74--322 )	HeM6	HeM1-C	54°C	794 bp
12	GST-Pur $\alpha$ ( 74--314 )	HeM6	HeM2-C2	54°C	754 bp
13	GST-Pur $\alpha$ ( 87--322 )	HeM7	HeM1-C1	54°C	756 bp
14	GST-Pur $\alpha$ ( 107-314 )	HeM5	HeM2-C2	54°C	652 bp
15	GST-Pur $\alpha$ ( 107-215 )	HeM5	HeM4	54°C	349 bp
16	GST-Pur $\alpha$ ( 54-189 )	HeM1-A	HeM8	50°C	478 bp
17	GST-Pur $\alpha$ ( 54-203 )	HeM1-A	HeM9	50°C	439 bp

Table 8-4: Various truncated Pur $\alpha$  cDNA generated fragments with different primer pairs.**heM1-A**

5'- tacggaattcatGCTGCAGCACGAGACG -3'

**heM2-A**

5'- tacggaattcATGGCGGACCGAGAC -3'

**heM1-C1**

5'- ctaggtcgacGGGGGTTTCATTCTGTTTGA -3'

**heM2-C2**

5'- ctaggtcgactcaACCCTGCAGTAGCAGAG -3'

**heM3**

5'- tacggaattcatGTGGAGTCCGCGAC -3'

**heM4**

5'- ctaggtcgacCGGCTCCTCCTCCAC -3'

**heM5**

5'- tacggaattcatgGTGGAGTCCGCGAC -3'

**heM6**

5'- tacggaattcatgCTGGACGTGAAGCAGAAC -3'

**heM7**

5'- tacggaattcatgATCGCCGAGGTGGGCG -3'

**heM8**

5'- ctaggtcgactcaCAGCGCAATGGTCTGG -3'

**heM9**

5'- ctaggtcgactcaGGCCAGAGCGTCACG -3'

**heM10**

5'- tacggaattcATGGCGGACCGAGACAG -3'

**pGEX-4T1 Primer (antisense)**

5'- GCGACATCGTATAACGTTAC -3'

**8.2.3 Oligonucleotids used for the DNA binding assay****Ori-1**

5'-AGCTCACCGAAACCGGTAAGTAAAGACTATGTATTTTTTCCCAGTGAATAATT  
GTTGTTAACAATAATCACACCATCACCGTTTTTTCAAGCGGGAAAAAA -3'

**PUR1**

5'- GGAGGTGGTGGAGGGAGAGAAAAG -3'

**Mage 11-2**

5'- GGGAAAAGGACTCAGGGTCTATC -3'

## 9 Appendix of Color Figures

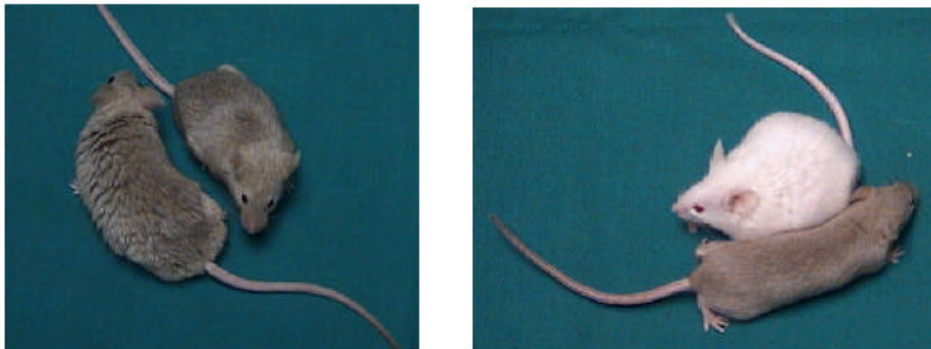


Figure 4-21: Pur $\alpha$  KO mice are bigger than their wild type littermates from postnatal day 70 because of obesity.

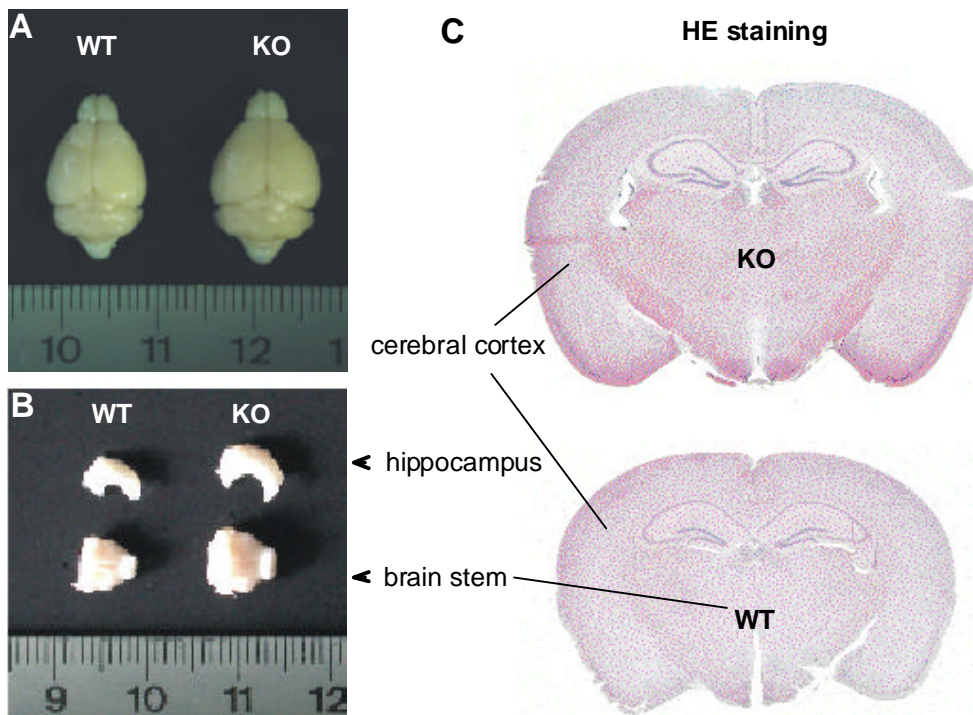
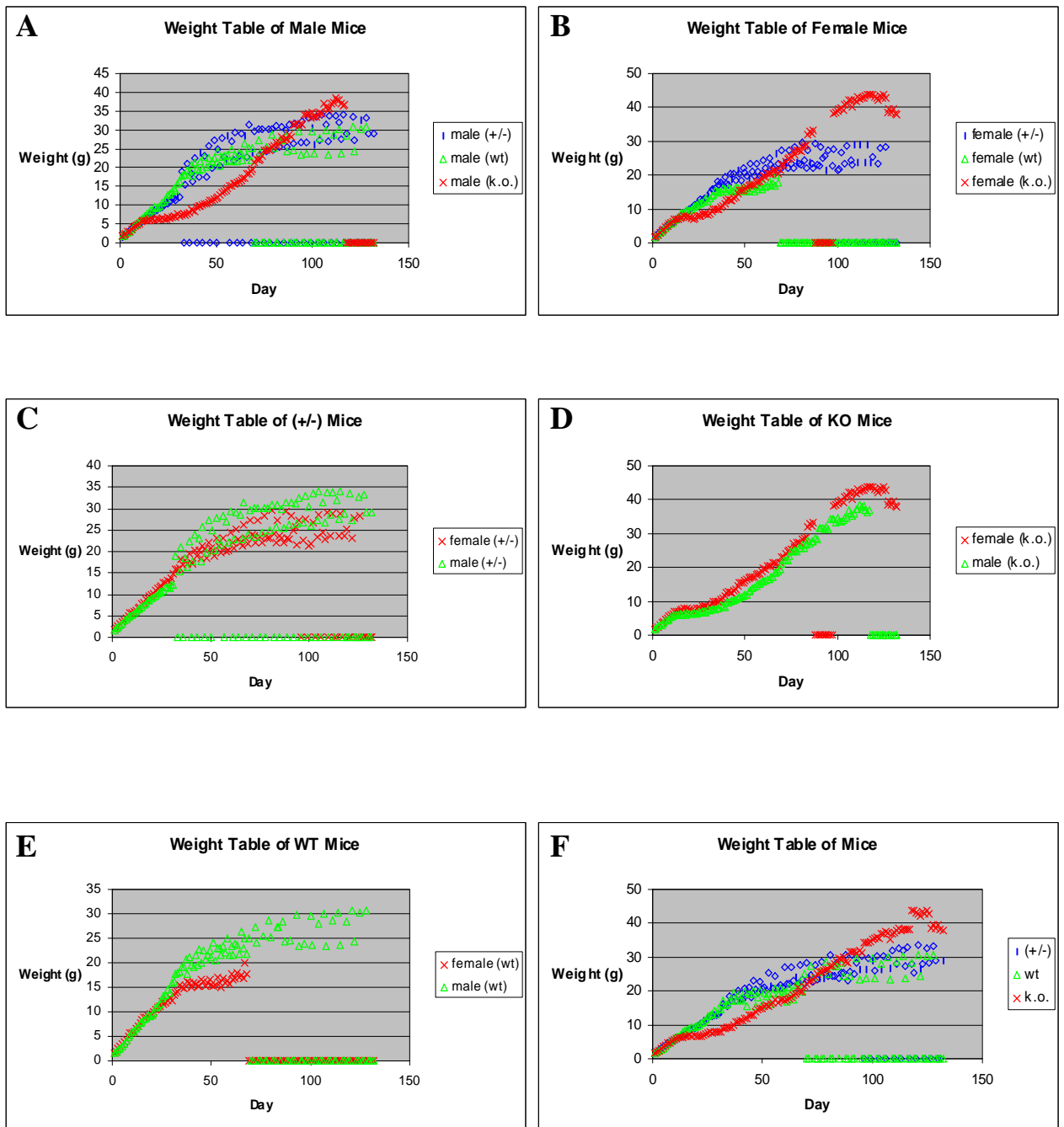


Figure 4-23: (A) The whole brain of Pur $\alpha$  KO and wild type mice (p48). (B) The brain stem and hippocampus prepared from the brains of the KO and wild type mice. (C) HE staining of the brains of the KO and wild type mice.

Figure 4-22: Weight tables of the  $Pur\alpha$  KO, heterozygous and wild type mice.

anterior commissure

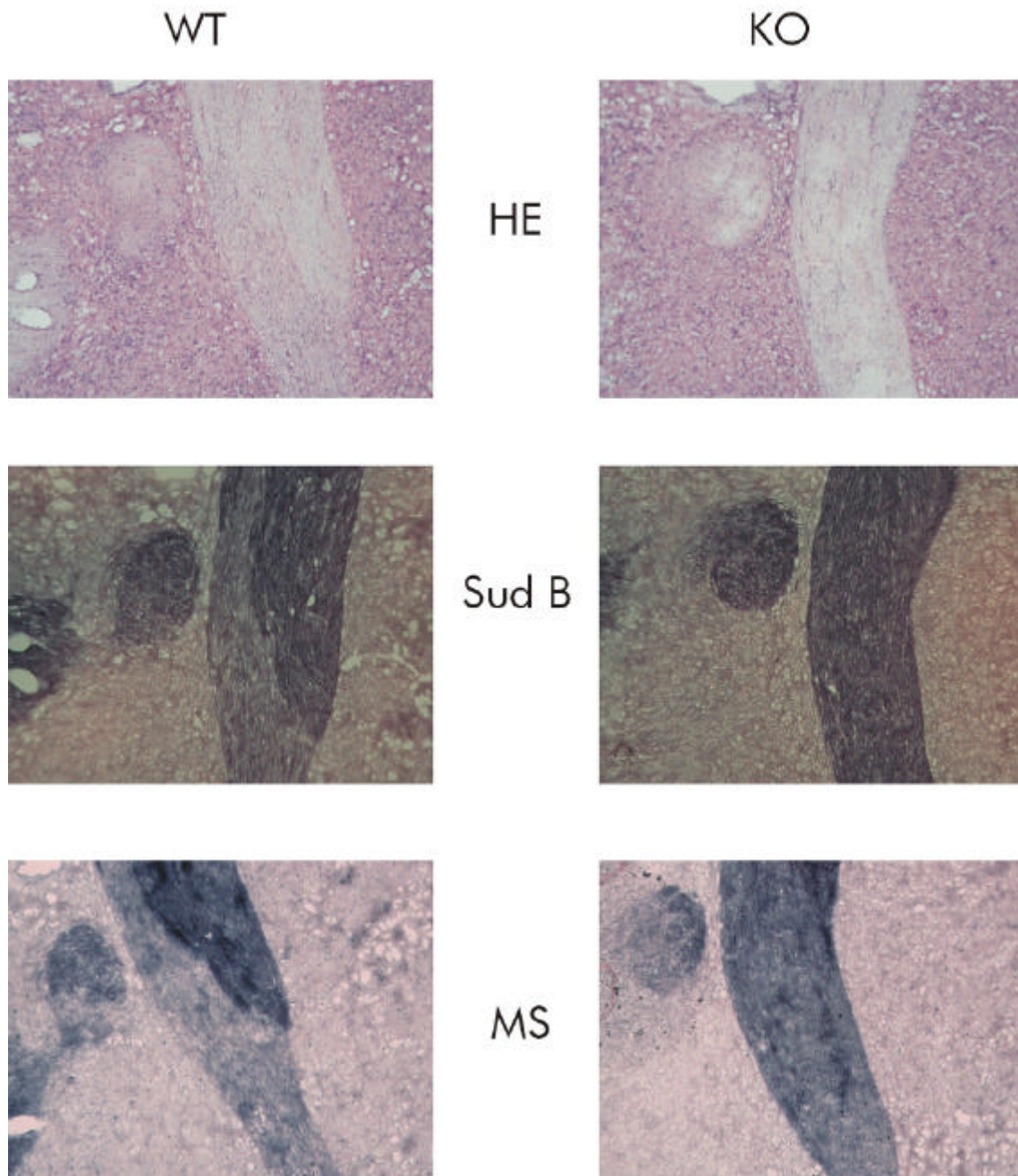


Figure 4-24: A) Histological staining of the anterior commissure of the mice brains: Brains from a Pur $\alpha$  KO and a wild type mouse were analyzed using three different histological stanings: HE staining (labels nuclei and plasma), Sudan black (lipid staining), and myelin sheaths staining.

## facial nerve

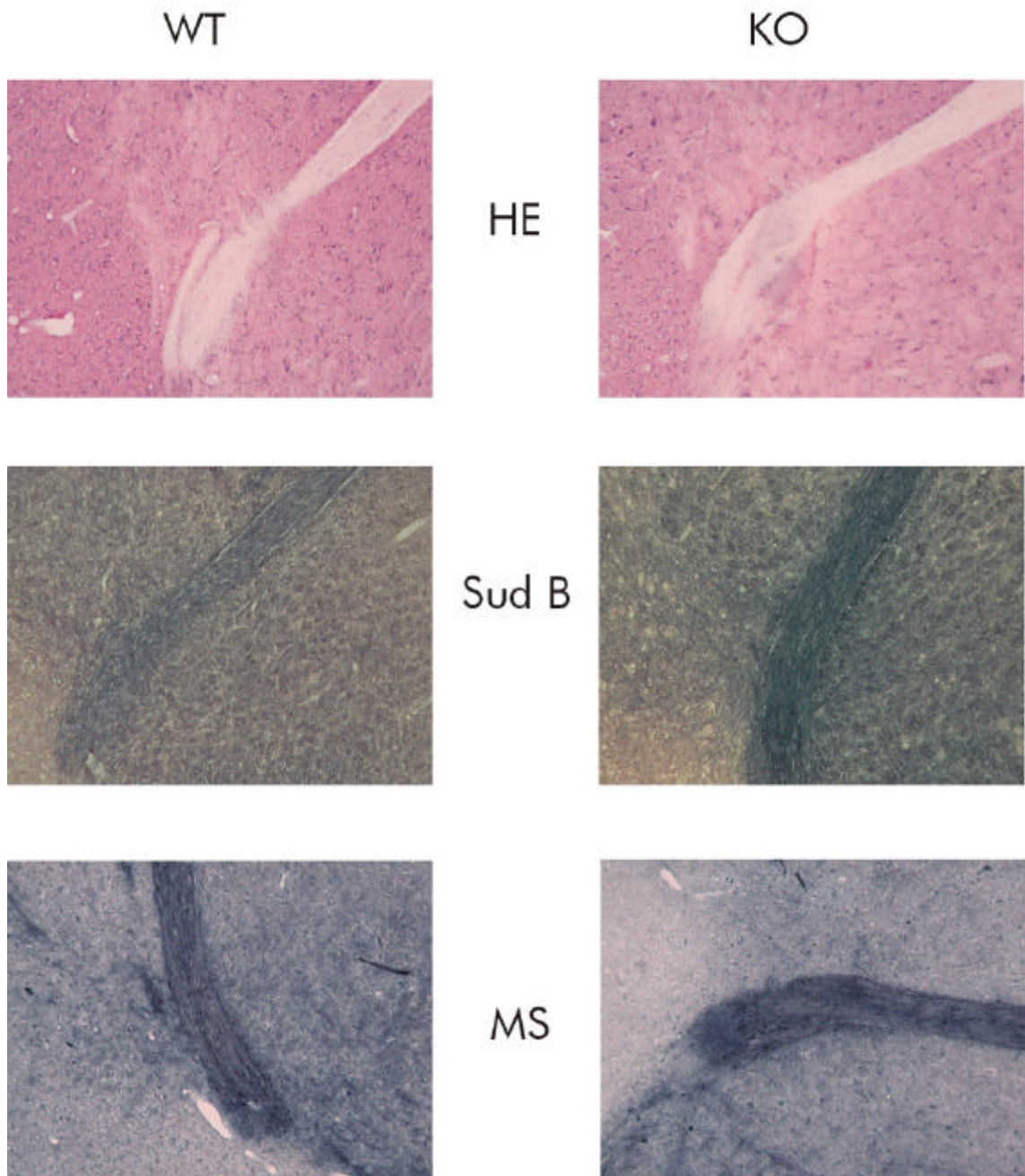
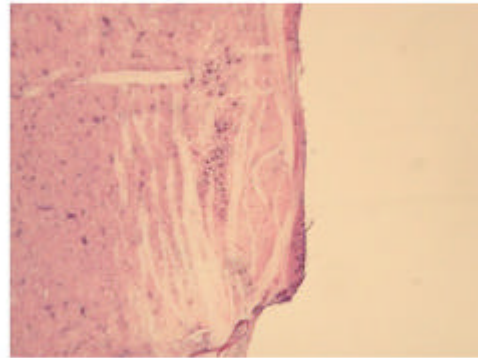
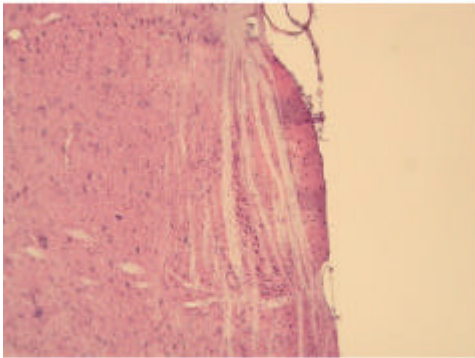


Figure 4-24: B) Histological staining of the facial nerve of the mice brains: Brains from a  $Pur\alpha$  KO and a wild type mouse were analyzed using three different histological stainings: HE staining (labels nuclei and plasma), Sudan black (lipid staining), and myelin sheaths staining.

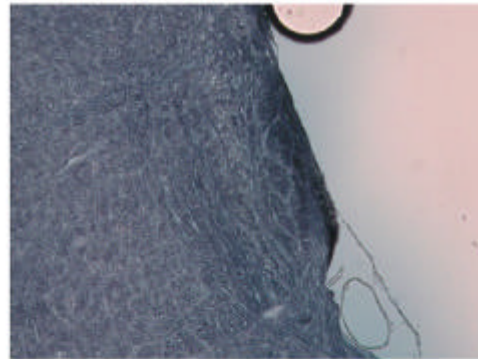
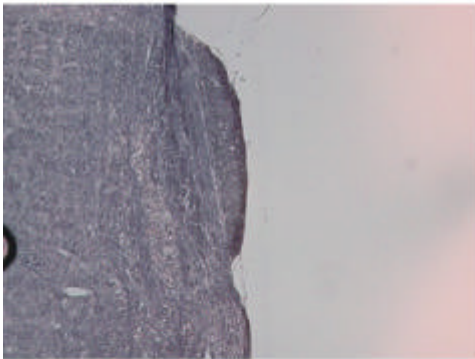
pyramidal tract

WT

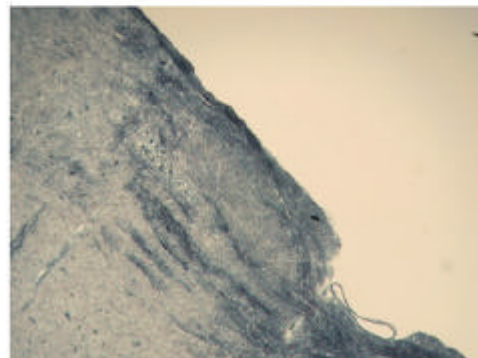
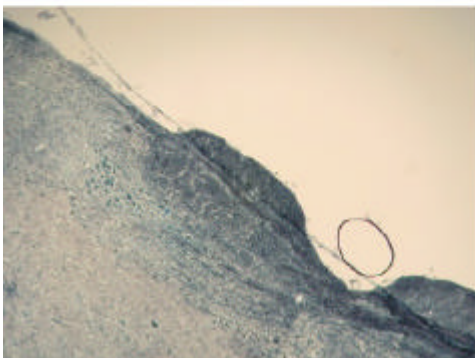
KO



HE



Sud B



MS

Figure 4-24: C) Histological staining of the pyramidal tract of the mice brains: Brains from a Pur $\alpha$  KO and a wild type mouse were analyzed using three different histological stainings: HE staining (labels nuclei and plasma), Sudan black (lipid staining), and myelin sheaths staining.



## Lebenslauf

Name: Haiyan Ding  
Geburtsdatum: 27. 06. 1968  
Geburtsort: Hangzhou, VR China  
Eltern: Guangshu Jiang und Xiaoling Ding

### **Schulbildung:**

1975-1980                    Grundschule in Hangzhou, VR China  
1980-1986                    Mittelschule in Hangzhou, VR China

### **Studium:**

9/1986-7/1990                Studium der Pharmazie  
   Zhejiang Medizinische Universität, VR China  
1990                            Bachelor of Science  
9/1994-9/1995                Magister-Studium der pharmazeutisch-analytischen Chemie  
   Zhejiang Medizinische Universität, VR China  
  
11/1996 –12/2001            Doktorarbeit am Institut für Biochemie der LMU München  
   unter der Anleitung von Prof. Dr. E.-L. Winnacker  
  
   "Functional characterization of Pur $\alpha$  in vivo and in vitro  
   Pur $\alpha$  knock-out mice and Pur $\alpha$  DNA unwinding activity "

### **Berufstätigkeiten:**

10/1990 –10/1995            Wissenschaftliche Mitarbeiterin  
   Fakultät für Pharmazie  
   Zhejiang Medizinische Universität, VR China